Earthquake Response of Stationary and Deteriorating Hysteretic Structures(Dissertation_全文)

AUTHOR(S):

Iemura, Hirokazu

EARTHQUAKE RESPONSE OF STATIONARY AND DETERIORATING HYSTERETIC STRUCTURES

By

Hirokazu IEMURA

Department of Civil Engineering
Kyoto University
Kyoto, Japan
May, 1977

EARTHQUAKE RESPONSE OF STATIONARY AND DETERIORATING HYSTERETIC STRUCTURES

By

Hirokazu IEMURA

Department of Civil Engineering
Kyoto University
Kyoto, Japan
May, 1977

SUMMARY

This dissertation is devoted to investigations of earthquake response of stationary and deteriorating simple hysteretic structures through numerical simulations, theoretical analyses and examinations of earthquake accelerograms.

Plastic deformation of simple structures with bilinear and curved hysteresis loops subjected to artificial earthquakes is simulated on a digital computer as a moving average of the displacement time history, eliminating elastic component of vibration. Shapes of the hysteresis loops are found to have significant effects on the plastic deformation of relatively short period structures.

Plastic deformation of the one-way yielding perfectly elasto-plastic structures for each yielding is estimated analytically through replacing the kinetic energy at yielding point by the equivalent plastic deformation.The analytical results are compared with simulated results to check the applicability of the technique, from which it is found that estimation of the plastic deformation in random response is satisfactory. Further application of the technique to equivalently linearized vibrational system is tried to find the expected amount of the accumulated plastic deformation subjected to stationary white noise excitation.

Two different types of equivalent linearization techniques are adopted for theoretical discussions and statistical prediction of earthquake hysteretic response. The relation between the two techniques is examined to conclude that they have the same expression of equivalent linear parameters. Stationary and nonstationary rms response of bilinear hysteretic structures are analytically predicted with application of linearization techniques. Using the results, probability distribution of the maximum hysteretic response is also predicted through pure-birth and envelope methods. Monte Carlo simulation performed on a digital computer verifies the applicability of the techniques within admissible ranges of error.

The strong motion earthquake accelerograms are investigated to find deteriorating hysteretic properties of restoring force of a reinforced concrete structure. Equivalently linearized and hysteretic models for the fundamental mode of the structure are examined to see if they can describe the observed response. Models with time-depending parameters are found to match the response with suggestions of degrading stiffness and energy dissipation capacity of the structure. A new simple model of which equivalent structural parameters are controlled to degrade with decreasing residual strength is proposed to represent general deteriorating hysteretic structures. Response analysis of the proposed model points out the significant effects of time-depending structural capacities to the earthquake response both in amplitude and frequency components.

ACKNOWLEDGEMENTS

The author wishes to express his sincere gratitude to Professor Hisao Goto of Kyoto University for constant encouragement during the course of studies and also for critical reading of the manuscript. His special gratitude is extended to Professor Yoshikazu Yamada of Kyoto University for his valuable suggestions in completing the dissertation. He is further indebted to Professor Hiroyuki Kameda, Dr. Masaru Kitaura and his colleagues of Professor Goto's laboratory for their profitable discussions and constructive criticisms in the course of daily research activities. He is also thankful for hearty encouragement from Professor Kenzo Toki of the Disaster Prevention Research Institute.

The author is deeply grateful to Professor Paul C. Jennings of the California Institute of Technology for his advice and assistance in carrying out the main part of Chapter 5. He is pleased to acknowledge the award from the Rotary Foundation which enabled him to study at Cal Tech.

It is suitable at this time for the author to appreciate his parents' understanding and support throughout his course of studies. Typing of the manuscript by his wife Etsuko requires special acknowledgement.

Table of Contents

1. INTRODUCTION

1-1 General Remarks

Relatively recent development in the field of earthquake engineering especially since the tragic Kanto Earthquake in 1923 in Japan reveals the great endeavours that have been made by many research workers and engineers. Current earthquake resistant designing codes for civil engineering structures could be considered as one of the great fruits of the studies in the early stage of this field as described below.

Development of the instrument for measurement of ground acceleration since the early 1930's by U.S. Coast and Geodetic Survey made investigators possible to use recorded seismograms as excitations to idealized mechanical, electronical and mathematical models of different types of structures.

The idea of response spectrum first suggested by M.A.Biot[1] was improved and generalized by G.W.Housner et al[2] to propose that the structural codes should be based on the frequency-dependent maximum response of one-degree-of-freedom (simple) linear structures not on the maximum value of ground acceleration. D.E.Hudson[3] showed the technique to combine the response spectrum and the modal analysis to estimate the maximum linear response of more complicated structures having many degree-of-freedom.

The structural codes for aseismic design have been improved by these investigations and have been used widely even today because of relatively simple procedure of predicting the maximum linear response of structures and also because of the current elastic-designing codes to let the maximum stress of each structural member within the allowable elastic limit.

In this way of designing, however, it was completely out of the question how dynamic behaviour of structures beyond linear elastic limit would be explained, mainly due to the lack of powerful techniques and tools available to solve nonlinear equation of motion.

Inevitable necessities of nonlinear response analyses have been

proposed since the First World Conference on Earthquake Engineering (WCEE) for the following reasons.

1) Ductile structures with less strength than that required by building codes have withstood strong earthquakes with only moderate damages. The hysteretic energy absorbing capacity of ductile structural members in the plastic range was considered favourable to structures during earthquakes to suppress their dynamic response.
2) Observed dynamic properties of structures during strong earthquakes such as natural periods of them sometimes showed quite different from those of small amplitude vibration tests.
   Nonlinear relations between displacement and restoring force of structures and ground were pointed out as one of main reasons of the difference.
3) Recent severe damages of R.C. buildings due to strong ground motion have needed extensive studies on the restoring force characteristics of brittle structural members and also structural response characteristics in the plastic range up to failure.
4) Possibly general understandings of response properties of hysteretic structures through theoretical and numerical investigations would achieve new limit-designing codes which will estimate more accurate reliability of structures during strong earthquakes than the current elastic-designing codes.

Numerious studies have been made on these problems according as analog and digital computers and also experimental facilities have made tremendous developments, which will be discussed in the next section. However these nonlinear problems are so complicated because of incapability of the principle of linear superposition, that there still exist many problems to be investigated. Among these problems, following four topics are the contents of this dissertation to grasp possibly general understandings of earthquake response properties of stationary and deteriorating hysteretic structures.

(1) Simulation techniques to estimate the plastic deformation from the time history of hysteretic response of structures with various

shapes of hysteresis loops.

(2) Analytical methods to predict the plastic deformation in random response through replacing the kinetic energy by the equivalent plastic deformation.

(3) Theoretical discussions and statistical prediction of earthquake response of hysteretic structures by means of linearization techniques.

(4) Examination of seismograms recorded at an existing building to propose general deteriorating hysteretic models of which structural capacities degrade during earthquake motion.

1-2 Reviews of Studies on Nonlinear Hysteretic Response to Earthquake Motion

It is quite interesting to note that investigations of nonlinear hysteretic response initiated with elementary techniques almost at the same time when the First World Conference on Earthquake Engineering (WCEE) was held in 1956 and since then remarkable developments of analog and digital computers and experimental facilities have contributed toward the significant steps to open the wide varieties of this field.

Hence it would be worthwhile in the first part of this section to take a brief review of papers which appeared at the proceedings of WCEE from the first to the latest sixth in 1977.

At the First WCEE, G.W.Housner[4] proposed a method of limit-design which expects the hysteretic energy absorption capacity to let the velocity response spectrum of yielding structures less than linear response spectrum which D.E.Hudson et al[5] calculated. Although the time history of nonlinear response was not estimated in his paper, it was a first step in earthquake engineering field that significance of nonlinear hysteretic effects to structural response during severe ground shaking was pointed out.

R.Tanabashi[6] calculated the hysteretic response subjected to a few pulse-type excitation with an improved Phase-Plane-Delta method and

proposed almost the same idea as G.W.Housner had shown.

At the Second WCEE, 9 studies about earthquake response of hysteretic structures were brought out to show the remarkable advances made in this field after the First WCEE supported by development of analog and digital computers.

Response Analyzer Committee[7] in Japan developed the analog computer RAC III to enable engineers to calculate the nonlinear response of elasto-plastic structures subjected to any types of random excitation. Displacement response spectrum of simple structures with bilinear hysteresis loops for recorded seismograms during the Imperial Valley (1940) and the Saitama (1956) earthquakes was calculated.

R.Tanabashi[8] also calculated the hysteretic response of multi-degree-of-freedom structures subjected to a few pulse-type excitation through an analog computers. Phase-Plane-Delta method was still used by T.Kobori and R.Minai[9]. Response time history curves obtained by the Phase-Plane-Delta method and by an analog computer were compared by H.Goto and K.Kaneta[10]. Stability of nonlinear hysteretic structures subjected to a stationary sinusoidal excitation was theoretically discussed by N.Ando[11].

Digital computers developed mainly in the U.S.A. at that time played significant roles in the earthquake response analyses of hysteretic structures. J.Penzien[12] calculated the elasto-plastic response of multi-story buildings to suggest that there exists optimum yielding level which minimizes the displacement response. A.S.Veletsos and N.M.Newmark[13] pointed out that lateral force coefficient (Spectral Acceleration/Acceleration of gravity) decreased significantly for the larger values of ductility factor. The energy absorption capacity of yeilding structures was especially investigated by J.A.Blume[14].

At the Third WCEE, 16 papers were presented in this field which reflected the remarkable development in computational speed and memory capacity of digital computers. In these papers, new trials for general understandings of nonliner hysteretic response characteristics of

relatively simple structures and for practical applications of elasto-plastic response analyses of structures with multi-degree-of-freedom to designings of high-rise buildings seem to have initiated. Following papers are devoted to investigations of one-degree-of-freedom (simple) hysteretic structures.

An exact solution for the steady state response of bilinear hysteretic systems was presented by W.D.Iwan[15] and general yielding structures with curved hysteretic loops were proposed by P.C.Jennings[16].

Statistically generated random processes were used as excitations for hysteretic structures by P.C.Jennings[16] and mathematical discussion of nonlinear response statistics was made by J.M.J.Pereira[17] by means of Fokker-Planck equation.

T.Odaka and F.Horie[18] pointed out the existence of the optimum seismic coefficient which minimizes the maximum displacement response of bilinear structures.

A.S.Veletsos, N.M.Newmark and C.V.Chelapati[19] presented the deformation spectra subjected to pulse-type ground shock, from which the effects of hysteretic characteristics was found quite different between short period and long period structures. Similar tendency which seems due to nonlinear vibration with longer natural period than that of linear systems was reported by G.R.Walker[20].

D.E.Hudson[21] discussed the equivalent viscous damping for hysteretic systems and found relatively low values that correspond to earthquake-type excitation with suggestions that hysteretic systems might be equally linearized.

Six papers were devoted to hysteretic response analyses of multi-degree-of-freedom systems for the purpose of practical designing of high-rise buildings. Some of them reported the maximum displacement response of elasto-plastic structures to be significantly greater than that of the corresponding linear structures, contrary to the findings for simple oscillators.

Fifteen papers were presented at the Fourth WCEE in the field of

nonlinear hysteretic response analysis. Although no remarkable developments of analyzing tools and methods could be observed since the Third WCEE, response spectra of simple hysteretic structures and reliability of high-rise buildings during strong earthquakes were more intensively investigated.

A.S.Veletsos[22] and A.Poceski[23] discussed the displacement response spectra of simple linear and hysteretic structures to show that the difference between them depends on their natural period. J.Penzien and S.-C.Liu[24] presented the probability distribution of maximum displacement response of simple linear, elasto-plastic and stiffness-degrading structures by simulating large number of artificial earthquakes on a digital computer.

W.D.Iwan[25] proposed the conbination of sliders and springs to express a new type of curved hysteretic loops. R.Husid[26] discussed the effects of gravity to the rocking motion of structures especially in the plastic range of restoring force.

Rotarional and torsional vibration of relatively simple elasto-plastic structures subjected to three components of excitation was investigated by N.C.Nigam and G.W.Housner[27] to show significant drift of response displacement from the zero base line. This drift is considered to be the structural plastic deformation which will be further discussed in Chapter 2 and 3. A.Shibata et al[28] also discussed hysteretic torsional response of unsymmetrical building models with analytical and experimental methods.

Eight papers were devoted to estimation of reliability of steel framed and reinforced concrete high-rise buildings during strong earthquakes through hysteretic response analyses of multi-degree-of-freedom systems. In some of these papers, experimentally obtained displacement and restoring-force relations of structural members were taken into account for step-by-step integration of time history of response.

At the fifth WCEE held in Rome in 1973, found is the trememdous increase in number of papers. Ninety-five out of 439 papers in total

were presented in the session of "Response of Structures to Ground Shaking" to show not only research worker's but also engineer's strong interests and urgent needs for earthquake engineering. Most papers were devoted to precise and practical investigations of earthquake response of specific structures such as buildings, bridges, dams, tunnels, pipe-lines, towers, water tanks and so on, through mathematical modeling by means of discrete multi-degree-of-freedom systems and finite elements representation.

Nonlinearities in force-deflection relations of structures which were taken into account in almost half of these papers have become no more especially interesting parts of papers to be noted but necessary and inevitable topics for accurate estimation of structural reliablility during strong earthquakes. Recent developments mainly in software of digital computers has made it possible and relatively easy to calculate nonlinear hysteretic response of complex structures when force-deflection relations of structural members are available.

From these view points, about 30 papers were devoted to studies on experimental dynamic loading of structural members such as columns, beams, frames, bracings, walls and so on in the session of "Dynamic Behavior of Structural Elements". In most of these papers, dynamic behavior of R.C. elements were tested up to failure to show significant deterioration of dynamic load-bearing capacities in the plastic range, in search of the severe damages of R.C. buildings during the Tokachioki in 1968 and the San Fernando in 1971 earthquakes. Theoretical models for deteriorating force-deflection relation were proposed for R.C. structures and analysis of recorded response of R.C. building also resulted in nonstationary deteriorating characteristics of structural parameters. Further discussions of structural deterioration under severe earthquake loading will be made in Chapter 5.

Remaining several papers dealt with steel elements to show in most cases stable energy absorbing capacity in the plastic range which would be of significant favour for structural safety against severe dynamic loading.

Results of experiments on structural members instead of conventional

hysteretic modelings such as bilinear loops were taken into account for computation of structural response for more accurate prediction of structural reliability during strong earthquakes. In some of these papers[29], nonlinear response analyses were applied to precise and sophisticated designing procedures of buildings to avoid structural collapse without increasing the yielding level of structural members.

In most numerical calculations, force-deflection relation was mathematically modeled in computers to simulate the experimental results, however it is interesting to note that on-line connection of a dynamic loading machine to an analog computer for direct use of restoring force to response estimation was proposed[30].

In the preprints of the latest sixth WCEE held at New Delhi in 1977, 611 papers in total were found. Among them 191 papers contributed to the sessions of "Response of Structures to Ground Shaking", "Dynamic Test on Structures" and "Dynamic Behavior of Structural Elements". Nonlinearity effects of structures to earthquake response were investigated in about half of the papers. The latest development of research works in the sessions is now being studied.

Besides above mentioned papers which appeared in the proceedings of WCEE, theoretical and numerical investigations of statistical response of hysteretic systems were made mainly in the field of applied mechanics. Both randomness in accelerograms of ground motion and nonlinearity in structural members are quite important features to be simultaneously investigated in earthquake response analyses.

T.K.Caughey[31),32)] for the first time discussed the stationary random response of simple bilinear hysteretic systems through linearization techniques and the Fokker-Planck equation to open this field. T.Kobori and R.Minai[33)] extended the linearization techniques for nonstationary response. W.D.Iwan[34)], L.D.Lutes[35)] and H.Takemiya[36)] discussed the applicability of linearization techniques for prediction of stationary hysteretic response through investigations of deficiencies between analytical and experimental response statistics. Further discussions of

linearization techniques will be made in Chapter 4.

1-3 Outline of the Dissertation

In this dissertation, earthquake response properties of simple hysteretic structures are investigated with special interests on how the differences between hysteretic and linear response could be explained in general terms through numerical simulations on digital computers, theoretical analysis with approximate linearization techniques and examination of strong motion earthquake accelerograms.

In Chapter 2, the plastic deformation of elasto-plastic structures in strong earthquakes is investigated by means of numerical simulation on a digital computer, since accumulation of the plastic deformation is considered to have direct connection with the process of structural collapse due to severe ground shaking. The plastic deformation is defined as a moving average on the time axis of the displacement response, by which the elastic component of the vibration is eliminated. Discussions are made as to what cases will make the plastic deformation grow large by reference to nondimensional parameters showing the intensity and duration of exitation, rate of nonlinearity of hysteresis loops and natural frequency of structures.

An analytical method is adopted in Chapter 3, to predict the amount of the plastic deformation in random response of the perfectly elasto-plastic structures. In this method, the plastic deformation at each yielding is estimated by equating the kinetic energy at the yielding point to the dissipated energy during the plastic drifting and the accumulated value in certain interval is calculated from the response statistics of an artificially linearized vibrational system. The predicted plastic deformation is compared with simulated results to check the applicability of this method for earthquake-type excitation.

Chapter 4 is devoted to the discussion of applicability of two

equivalent linearization techniques for the investigation of general properties of earthquake response statistics of nonlinear hysteretic structures. One is the least mean-square error method and the other is the energy balance method. The relation between linearization criteria of the two techniques is examined to conclude that they have the same expression of equivalent linear parameters for any types of hysteresis loops. Stationary and nonstationary root-mean-square (r.m.s.) response of bilinear hysteretic structures are theoretically predicted by an iterative and a step-by-step linearization techniques, respectively. Using the results, probability distribution of the maximum hysteretic response is also predicted through pure-birth and envelope methods. Monte Carlo simulations are performed on a digital computer to check the applicability of the techniques used in this chapter.

In Chapter 5, examined are the strong motion earthquake accelerograms recorded at the Millikan Library on the campus of the California Institute of Technology during the San Fernando earthquake of February 9, 1971. The time-dependence of the hysteretic behavior of the library is studied by plotting the measured values of acceleration against the calculated values of relative displacement. The equivalent natural frequency and the equivalent damping factor for each full cycle of the response are estimated from the experimental hysteresis loops to show that they are significantly time-dependent suggesting degradation of the stiffness and energy dissipation capacities of the building. Four simple linear and hysteretic models for the fundamental mode of the building, two stationary and two with changing parameters are examined to see if they could describe the observed response.

Another new simple model is proposed to represent dynamic properties of general deteriorating hysteretic structures. The equivalent structural capacities of the model are controlled to degrade with the decreasing residual strength defined from the theory of low-cycle fatigue. From response analyses of the proposed models, it is also

investigated how significant the effects of time-depending structural capacities to the earthquake response both in amplitude and frequency components are.

Main results of these chapters are reviewed comprehensively in Chapter 6 to derive conclusions with proposals for earthquake engineers at the present time and also in relation to the prospects for the future studies to be continued.

References for Chapter 1

1) M.A. Biot: Analytical and Experimental Methods in Engineering Seismology, Proc. of American Society of Civil Engineers (ASCE), Vol. 108, 1943, pp. 365-408.
2) G.W. Housner, R.R. Martel and J.L. Alford: Spectrum Analysis of Strong Motion Earthquakes, Bulletin of Seismological Society of America (SSA), Vol. 43, 1953.
3) D.E. Hudson: Response Spectrum Techniques in Engineering Sesimology, Proc. of the first World Conference on Earthquake Engineering (WCEE), 1956, pp. 4-1∿4-12.
4) G.W. Housner: Limit Design of Structures to Resist Earthquakes, Proc. of the first WCEE, 1956, pp. 5-1∿5-13.
5) D.E. Husdon and G.W. Housner: Structural Vibrations Produced by Ground Motion, Proc. of ASCE, Vol. 81, Paper 816, October, 1955.
6) R. Tanabashi: Studies on the Nonlinear Vibrations of Structures Subjected to Destructive Earthquakes, Proc. of the first WCEE, 1956, pp. 6-1∿6-16.
7) Response Analyzer Committee: Non-linear Response Analyzers and Application to Earthquake Resistant Design, Proc. of the second WCEE, Vol. II , July, 1960, pp. 649-668.
8) R. Tanabashi: Nonlinear Transient Vibration of Structures, Proc. of the second WCEE, Vol. II , July, 1960, pp. 1223-1238.
9) T. Kobori and R. Minai: Study on Unstationary Vibration of Building Structure with Plastic Deformation of Substructure, Proc. of the second WCEE, Vol. II , July, 1960, pp. 1085-1104.
10) H. Goto and K. Kaneta: Analysis with an Application to Aseismic Design of Bridge Piers, Proc. of the second WCEE, Vol. II , July, 1960, pp. 1449-1466.
11) N. Ando: Nonlinear Vibrations of Building Structures, Proc. of the second WCEE, Vol. II , July, 1960, pp. 1045-1060.

12) J. Penzien: Elasto-Plastic Response of Idealized Multi-Story Structures Subjected to a Strong Motion Earthquake, Proc. of the second WCEE, Vol. II , 1960, pp. 739-760.

13) A.S. Veletsos and N.M. Newmark: Effect of Inelastic Behavior on the Response of Simple Systems to Earthquake Motions, Proc. of the second WCEE, Vol. II , July, 1960, pp. 895-912.

14) J.A. Blume: A Reserve Enegy Technique for the Earthquake Design and Rating of Structures in the Inelastic Range, Proc. of the second WCEE, Vol. II , July, 1960, pp. 1061-1084.

15) W.D. Iwan: The Dynamic Response of the One Degree of Freedom Bilinear Hysteretic System, Proc. of the third WCEE, Vol. II , January, 1965, pp. II -783∿796.

16) P.C. Jennings: Response of Yielding Structures to Statistically Generated Ground Motion, Proc. of the third WCEE, Vol. II , January, 1965, pp. II -237∿259.

17) J.M.J. Pereira: Behavior of an Elasto-Plastic Oscillator Acted by Random Vibration, Proc. of the third WCEE, Vol. II , January, 1965, pp. II -491∿501.

18) T. Odaka and F. Horie: A Study on the Optimum Value of a Seismic Coefficient, Proc. of the third WCEE, Vol. II , January, 1965, pp. II -399∿420.

19) A.S. Veletsos, N.M. Newmark and C.V. Chelapati: Deformation Spectra for Elastic and Elasto-Plastic Systems Subjected to Ground Shock and Earthquake Motions, Proc. of the third WCEE, Vol. II , January, 1965, pp.II -663∿682.

20) G.R. Walker: Earthquake Resistant Design-The Pulse Method, Proc. of the third WCEE, Col. II , January, 1965, pp. II -683∿694.

21) D.E. Husdon: Equivalent Viscous Friction for Hysteretic Systems with Earthquake-like Excitaions, Proc. of the third WCEE, Vol. II , January, 1965, pp. II -185∿206.

22) A.S. Veletsos: Maximum Deformations of Certain Nonlinear Systems, Proc. of the fourth WCEE. Vol. II , January, 1969, pp. A4-155∿170.

23) A. Poceski: Response Spectra for Elastic and Elastoplastic Systems Subjected to Earthquakes of Short Duration, Proc. of the fourth WCEE, Vol. II , January, 1969, pp. A4-171∿178.

24) J. Penzien and S.-C. Liu: Nondeterministic Analysis of Nonlinear Structures Subjected to Earthquake Excitations, Proc. of the fourth WCEE, Vol. I, January, 1969, pp. AI-114∿129.

25) W.D. Iwan: The Distributed-Element Concept of Hysteretic Modeling and Its Application to Transient Response Problems, Proc. of the fourth WCEE, Vol. II , January, 1969, pp. A4-45∿58.

26) R. Husid: The Effect of Gravity on the Collapse of Yielding Structures with Earthquake Excitation, Proc. of the fourth WCEE, Vol. II , January, 1969, pp. A4-31∿44.

27) N.C. Nigam and G.W. Housner: Elastic and Inelastic Response of Framed Structures During Earthquakes, Proc. of the fourth WCEE, Vol. II , January, 1969, pp. A4-89∿104.

28) A. Shibata, J. Onose and T. Shiga: Torsional Response of Buildings to Strong Earthquake Motions, Proc. of the fourth WCEE, Vol. II , January, 1969, pp. A4-123∿138.

29) H.Umemura, H. Aoyama and H. Takizawa: Analysis of the Behavior of Reinforced Concrete Structures During Strong Earthquakes Based on Empirical Estimation of Inelastic Restoring Force Characteristic of Members, Proc. of the fifth WCEE, Vol. 2, June, 1973, pp. 2201-2210.

30) M. Hakuno: Hybrid Failure Test on a Structural Member, Proc. of the fifth WCEE, Vol. 1, June, 1973, pp. 799-802.

31) T.K. Caughey: Random Excitation of a System with Bilinear Hysteresis, Journal of Applied Mechanics, American Society of Mechanical Engineers (ASME), Vol. 27, December, 1960, pp. 649-652.

32) T.K. Caughey: Deviation and Application of the Fokker-Planck Equation to Discrete Nonlinear Dynamic Systems Subjected to White Random Excitation, Journal of the Acoustical Society of America (ASA), Vol. 35, 1963, November 1963, pp. 1683-1692.

33) T. Kobori and R. Minai: Linearization Technique for Evaluating the Elasto-Plastic Response of a Structural System to Non-stationary Random Excitations, Annual Report of the Disaster Prevention Research Institute (DPRI), Kyoto Univ., No. 10A, 1967, pp. 235-260, (in Japanese).

34) W.D. Iwan and L.D. Lutes: Response of the Bilinear Hysteretic System to Stationary Random Excitation, The Journal of the ASA, Vol. 43, Number 3, 1968, pp. 545-552.

35) L.D. Lutes: Equivalent Linearization for Random Response, Journal of the Engineering Mechanics (EM) Division, Proc. of the ASCE, EM2, June, 1970, pp. 227-242.

36) H. Takemiya: Equivalent Linearization for Randomly Excited Bilinear Oscillator, Proc. of Japan Society of Civil Engineers (JSCE), No. 219, November, 1973, pp. 1-14, (in Japanese).

2. SIMULATED PLASTIC DEFORMATION OF SIMPLE HYSTERETIC STRUCTURES

2-1 General Remarks

Earthquake response analyses of structures with hysteretic restoring force (hysteretic structures) could be distinguished into two categories by their analyzing techniques as briefly explained in the previous chapter.

First technique for response analyses of hysteretic structures corresponds to earthquake excitation with quite severe size of intensity. In this technique, every ideally modeled hysteretic loop has been taken into account for step-by-step integration of nonlinear equations of motion.

The other technique for hysteretic analyses deals with earthquake excitations with relatively moderate size of intensity. This technique replaces hysteretic properties of restoring forces by equivalently determined linear stiffness and linear viscous damping to let nonlinear problems easy to solve and also to compare the difference between linear and nonlinear hysteretic response.

These two types of analyzing techniques have been used for research and designing purposes according to the case of investigation with consideration of intensity of excitations and types of structures. However next two issues which seem to be interesting subjects of study have not yet been discussed precisely.

Calculated response of hysteretic structures with the first technique sometimes shows quite different features from those of linear structures, which is the notable drift of displacement from zero base line. The cause of the drift has not been studies intensively but seems due to growth of plastic deformation of hysteretic structures, although it is quite difficult to estimate the amount of plastic deformation on the time history of response extinguishing the elastic component of fluctuation.

In the application of second technique, stable dynamic behavior of hysteretic loops should be guaranteed for the proper and accurate equivalent linearization of the loops. But admissible conditions of excitations and hysteretic structures for linearization techniques have not yet been examined nor clarified except limiting the technique for

"week" nonlinear structures.

This chapter is aimed to deal with the above mentioned two issues through investigation of numerically simulated plastic deformation on a digital computer

P.C.Jennings[1] proposed the curved hysteretic loops which can cover wide range of shapes to make force-deflection relations of structures more similar to observed results than idealistic and conventional modelings such as bilinear hysteresis. Not only stationary response of the simple hysteretic structures subjected to a sinusoidal excitation but also nonstationary response excited by artificially generated earthquakes was calculated through theoretical analysis and numerical simulation respectively. The plastic deformation only at the end of an excitation was examined for different parameters of hysteresis and excitation, remaining the problem how to pick out the plastic component from the total displacement response during structural vibration.

J.Penzien and S.-C.Liu[2] performed numerous simulations on response statistics of simple structures with elasto-plastic and stiffness-degrading hysteresis subjected to artificial earthquakes. The probability distribution functions of maximum response of linear and hysteretic structures were especially examined to show the significantly different characteristics according to the natural period of structures in small vibration. However general understanding of hysteretic response is not easy from this paper because of no analytical treatments of the problem and also of no discussions about the plastic deformation. S.-C.Liu[3] made an additional study on the amount of the plastic deformation for limitted sets of parameters to remain further discussions in future studies.

N.C.Nigam and G.W.Housner[4] also noticed the drift of displacement and pointed out plastic deformation during rotational and torsional vibration of a relatively simple hysteretic structure. However hysteretic loops were limitted only for elasto-plastic shapes and the amount of the plastic deformation was not specifically investigated.

D.Karnopp and T.D.Scharton[5] proposed theoretical methods to predict

the accumulated plastic deformation of elasto-plastic structures in random vibration. Although the methods to convert the kinetic energy at the yielding level into the potential energy of plastic deformation is promissing for further studies, stationary and monotonous accumulation of plastic deformation was assumed to limit the investigation for specified problems.

M.Hakuno and M.Shidawara[6),7)] adopted the force-deflection relation of a small piece of steel for hysteretic response analysis. They connected a dynamic loading machine and an analog computer to find the restoring force characteristics directly from the testing piece and then to calculate the displacement response on the real time, feeding back the relative displacement response to the loading machine. Some of the simulated hysteretic response showed the significant drift of displacement from the zero base line, which seems as the consequence of accumulation of plastic deformation. However it is not made clear what range of parameters would make the drift grow large.

This chapter is devoted to the discussions of the simulated plastic deformation of the structures with various shapes of hysteretic loops subjected to artificial earthquakes.

First to make the analysis as general as possible, every term of the equation of motion with arbitrary types of restoring force is made dimensionless. A stationary artificial earthquake of which intensity and frequency properties are clearly defined is used as the excitation.

Then the step-by-step integration of the equation of motion is performed on a digital computer with relatively precise explanation of computing procedures and a moving average method is proposed to pick out the plastic deformation from the total displacement, extinguishing the elastic component of vibration.

Discussions are made as to what cases would make the plastic deformation grow large by reference to dimensionless parameters showing the intensity and duration of excitation, rate of nonlinearity of two different types of hysteresis loops and the natural frequency of structures in small vibration.

2-2 Dimensionless Representation of Hysteretic Restoring Force

2-2-1 Dimensionless Equation of Motion

It is desirable for general discussions about numerical results of nonlinear response to try dimensionless representation of equation of motion with any types of hysteresis loops.

Let structures be expressed by single-degree-of-freedom systems (simple structures) with hysteretic restoring force $P(\alpha,\beta,x,t)$ and also with viscous damping proportional to relative velocity. Then the equation of motion of simple hysteretic structures subjected to ground acceleration $\ddot{Z}(t)$ is written as

$$M\frac{d^2x}{dt^2} + C_d\frac{dx}{dt} + P(\alpha,\beta,x,t) = -M\cdot\ddot{Z}(t) \qquad (2\text{-}1)$$

where M : mass of a simple structure, C_d : viscous damping constant, x : relative displacement, α and β : parameters which show characteristics of hysteresis loops, t : time, respectively.

Let x_y be yielding displacement of hysteresis, P_y be yielding restoring force and ground acceleration $\ddot{Z}(t)$ be expressed by the product of a constant F_o which has dimension of acceleration and dimensionless stationary random process $N(t)$ of which average and root-mean-square (r.m.s.) values are zero and unity, respectively and of which predominant frequency is ω_f, i.e., $\ddot{Z}(t)=F_oN(t)$. Then dimensionless parameters h_o, r_s, τ, μ, q, η will be introduced as

$$\left.\begin{aligned} &\omega_o^2 = P_y/(M\cdot x_y), \quad C_p = C_d/M, \quad h_o = C_p/(2\omega_o) \\ &r_s = MF_o/P_y, \quad \tau = \omega_o t, \quad \mu = x/x_y, \quad \eta = \omega_f/\omega_o \\ &q(\alpha,\beta,\mu,\tau) = P(\alpha,\beta,\mu,\tau)/P_y \end{aligned}\right\} \qquad (2\text{-}2)$$

In these equations, intensity F_o and predominant frequency ω_f of excitation are made dimensionless by yielding force of hysteresis P_y and natural frequency of hysteretic structures ω_o in elastic range, respectively.

Dimensionless time τ is proportional to the ratio of real time and the natural period of structures. Relative displacement and restoring force of hysteresis are divided by yielding displacement and yielding restoring force.

Using these parameters in Eq.(2-1), the dimensionless equation of motion is written as

$$\frac{d^2\mu}{d\tau^2} + 2h_o \frac{d\mu}{d\tau} + q(\alpha,\beta,\mu,\tau) = -r_s N(\eta\tau/\omega_f) \qquad (2\text{-}3)$$

In this study, response characteristics of dimensionless displacement (ductility factor) will be simulated on a digital computer, for different sets of parameters r_s, η, α and β which represent relative intensity of excitation, relative natural period of structures and types and shapes of hysteresis loops, respectively.

2-2-2 Bilinear Hysteresis Loops

In this study, force-deflection relations will be discussed on the dimensionless coordinate which consists of dimensionless displacement μ and restoring force q shown in Fig.2.1 (a). On this coordinate, yielding occurs at the points where $\mu=q=1$ or -1 and the stiffness before yielding is unity. In many studies, hysteresis loops have been modeled on the conventional coordinate shown in Fig.2.1 (b), then dimensionless representation has been tried. However, modelings of hysteresis loops on the dimensionless coordinate adopted in this study would give more convinience to compare effects of different types of hysteresis loops to their random response, because less parameters are needed for representation of hysteresis loops than for modelings on the conventional coordinate.

As one of two different types of hysteresis loops, typical and commonly used bilinear hysteresis has been adopted. The stiffness of bilinear hysteresis after yielding is represented by $(1-n)$ shown in Fig.2.1 (a), where n represents the nonlinearity of the second slope of bilinear hysteresis loops. Various shapes of bilinear hysteresis loops

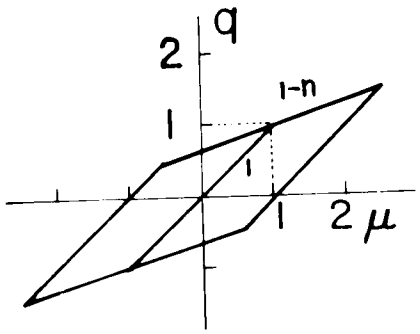

(a) Bilinear Hysteresis on Dimensionless Coordinate

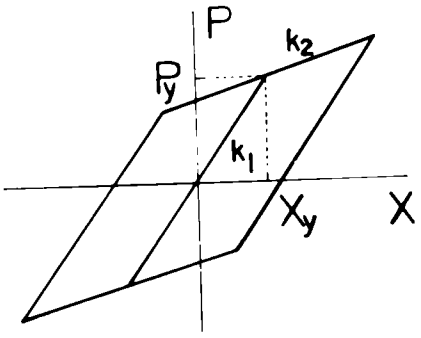

(b) Bilinear Hysteresis on Conventional Coordinate

Fig.2.1 Dimensionless Representation of Bilinear Hysteretic Restoring Force

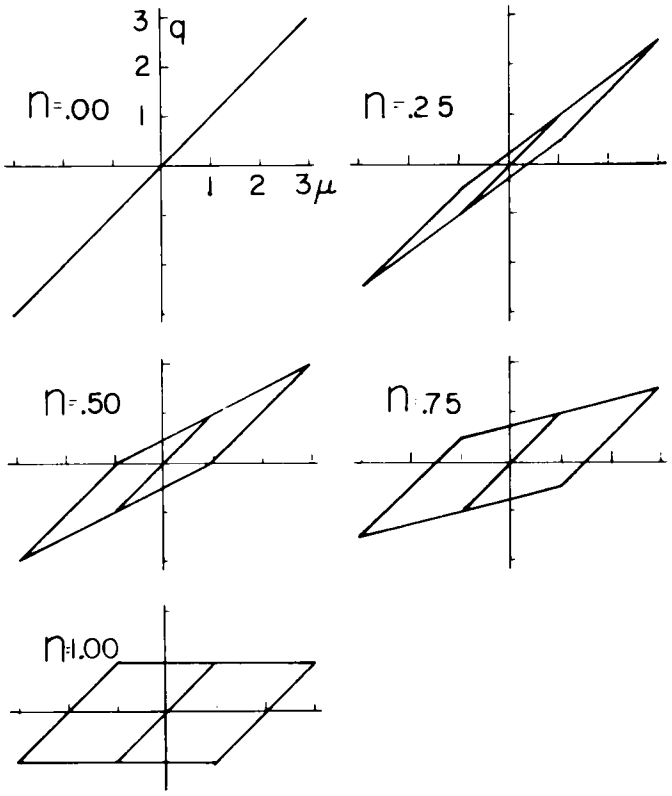

Fig.2.2 Various Shapes of Bilinear Hysteresis Loops with a Parameter n

for different values of n are shown in Fig.2.2, where the perfect elasto-plastic hysteresis is represented when n=1 and linear structures are represented when n=0. This bilinear representation of hysteresis has commonly been used for earthquake response analyses of hysteretic structures by many engineers and investigators mainly because of the simplicity not only for representation of a shape itself but also for procedures of step-by-step numerical calculation.

2-2-3 Modified Jennings Hysteresis loops

Smooth and curved restoring force characteristic has been adopted as the other type of hysteresis loops in this study. P.C.Jennings[8] proposed curved and smooth hysteresis loops for representation of general yielding structures. Although mathematical expression of force-deflection relation of the loops by him is complicated, continuously decreasing stiffness of them seems much more close to real structures consisting of many structural yielding elements than that of bilinear hysteresis. When the representation of curved hysteresis by him is tried directly on the dimensionless coordinate, however, the skeleton curve of the hysteresis which is the force-deflection relation in virgin loading does not come across the previously defined yielding point ($\mu=q=\pm 1$).

H.Goto et al[9] made a little modification to the curved hysteresis by P.C.Jennings to come across the yielding point. Typical shape of modified Jennings hysteresis is shown in Fig.2.3 and the equations of the skeleton and each branch are expressed as follows:

$$\left.\begin{aligned} &\text{Skeleton} : \quad \mu = \frac{1}{1+\alpha}\{q + \alpha q^r\} \\ &\text{Branches} : \quad \frac{\mu-\mu_o}{2} = \frac{1}{1+\alpha}\left\{\frac{q-q_o}{2} + \alpha\left(\frac{q-q_o}{2}\right)^r\right\} \end{aligned}\right\} \qquad (2\text{-}4)$$

where α: positive constant, r: positive odd integer, (μ_o, q_o) is the point where relative velocity $d\mu/d\tau$ changes its sign.

Various shapes of the hysteresis for α=0.1 and different values of r are shown in Fig.2.4. It is easily known that the larger values of r

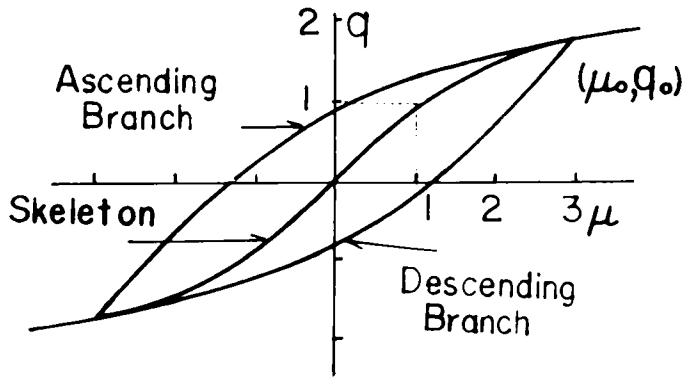

Fig.2.3 Modified Jennings Hysteresis Loop

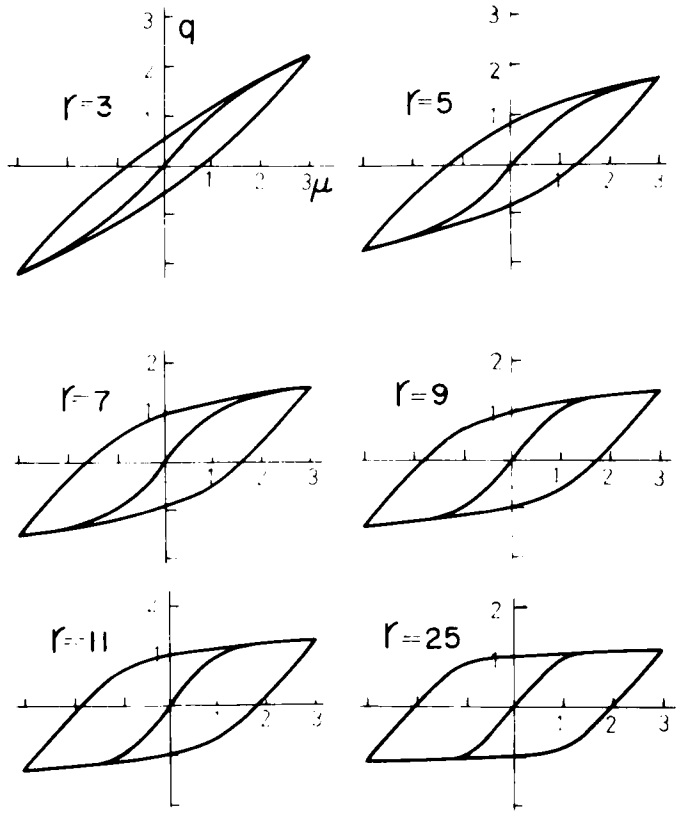

Fig.2.4 Various Shapes of Modified Jennings Hysteresis Loops with a Parameter r (α=0.1)

give the stronger nonlinearity and also the larger area of the hysteresis loops. This curved and smooth modeling can represent quite wide range of hysteretic shapes using two parameters α and r. When $\alpha=0$ or $r=1$, the hysteresis becomes linear systems. On the other hand $r=\infty(\alpha=0)$ gives the perfect elast-plastic hysteresis. Although different values of α give different shapes of hysteresis, α was set exclusively 0.1 to make the natural frequency of the hysteretic structures in small vibration constant.

It is easily understood that the stiffness of the hysteresis of small amplitude will be given as a function of α as

$$\left.\frac{dq}{d\mu}\right|_{\mu=0} = \left.\frac{1+\alpha}{(1+\alpha r q^{r-1})}\right|_{\mu=0} = 1 + \alpha \tag{2-5}$$

Then the natural frequency of the structure is

$$\omega_o = \sqrt{1 + \alpha} \tag{2-6}$$

2-3 Simulational Techniques

2-3-1 Generation of Artificial Earthquakes

The difference between artificial earthquakes and real strong motion accelerograms has often been discussed by many researchers, when random excitation is needed for response analyses of linear and nonlinear structures.

Records of strong earthquake ground motion have been used not only for practical purposes of structural designing to estimate the maximum response of structures, but also for research purposes to investigate dynamic characteristics of mathematically modeled structures, because strong motion accelerograms can be used among many engineers and reseachers on the common bases of their reality of being recorded. However, nonstationality and frequency characteristics of records

differ from one to another and such full of variety of accelerograms is not always suitable for investigation of foundamental characteristics of dynamic response of especially nonlinear structures.

On the contrary, artificial earthquakes which are usually generated from imitation of averaged characteristics of recorded earthquake accelerograms have the merit of being mathematically well-defined both in amplitude and on frequency domain. For example, white noise random process which consists of equally distributed frequency components is often used to investigate the dynamic characteristics of linear and nonlinear structures because of its mathematical simplicity.

As mentioned above, artificially generated accelerograms and real strong motion accelerograms have their own merits and demerits. Therefore, it seems preferable to use both of them in common for practical and research purposes.

However, from the purpose of this chapter to investigate the fundamental characteristics of plastic deformation of hysteretic structures with possibly general discussions, a stationary artificial earthquake which has relatively simple amplitude and frequency characteristics is exclusively generated and used following the work done by M.Shinozuka and Y.Sato[10]. It is the same as the stationary velocity response of simple linear oscillator with damping factor h_f and natural frequency ω_f subjected to white noise excitation. The power spectral density of this artificial earthquake $S_f(\omega)$ is obtained as the product of the constant power spectral density of white noise random process D and the receptance of simple oscillator in the case of acceleration excitation and velocity response; i.e.,

$$S_f(\omega) = D \cdot |H(h_f, \omega_f)|^2 = \frac{D\,\omega^2}{(\omega_f^2-\omega^2)^2 + 4h_f^2\omega_f^2\omega^2} \qquad (2\text{-}7)$$

The corresponding autocorrelation function $R_f(\tau)$ is obtained by the inverse Fourier transform of $S_f(\omega)$ from the well-known Wiener-Khinchin[11] relation.

$$R_f(\tau) = \frac{1}{2\pi}\int_{-\infty}^{\infty} S_N(\omega)\cdot e^{i\omega\tau}\, d\omega$$
$$= \frac{D\, e^{-h_f\omega_f\tau}}{4h_f\omega_f\sqrt{1-h_f^2}}\{-h_f\omega_f\sin(\omega_f\sqrt{1-h_f^2}\tau)+\omega_f\sqrt{1-h_f^2}\cos(\omega_f\sqrt{1-h_f^2}\tau)\} \quad (2\text{-}8)$$

The same autocorrelation function will also be estimated from the direct calculation of the definition of the function as

$$R_f(\tau) = E[\ddot{Z}(t)\ddot{Z}(t+\tau)] = E[\int_{-\infty}^{t}\dot{h}_o(t-\tau_1)n(\tau_1)d\tau_1\int_{-\infty}^{t+\tau}\dot{h}_o(t+\tau-\tau_2)n(\tau_2)d\tau_2]$$
$$= \int_{-\infty}^{t}\int_{-\infty}^{t+\tau}\dot{h}_o(t-\tau_1)\dot{h}_o(t+\tau-\tau_2)E[n(\tau_1)n(\tau_2)]d\tau_1 d\tau_2$$
$$= \int_{-\infty}^{t}\int_{-\infty}^{t+\tau}\dot{h}_o(t-\tau_1)\dot{h}_o(t+\tau-\tau_2)D\delta(\tau_1-\tau_2)d\tau_1 d\tau_2$$
$$= D\cdot\int_{-\infty}^{t+\tau}\dot{h}_o(t-\tau_1)\dot{h}_o(t+\tau-\tau_1)d\tau_1 \quad (2\text{-}9)$$

where $\ddot{Z}(t)$ is the random process considered as the acceleration of the artificial earthquakes, $n(t)$ is white noise random process, $\dot{h}_o(t)$ is a unit impulse response function of velocity given as

$$\dot{h}_o(t) = e^{-h_f\omega_f t}\{\frac{h_f}{\sqrt{1-h_f^2}}\sin(\sqrt{1-h_f^2}\omega_f t) - \cos(\sqrt{1-h_f^2}\omega_f t)\} \quad (2\text{-}10)$$

Then the mean square value of the artificial earthquake is given from random theory as shown below.

$$E[\ddot{Z}^2(t)] = R_f(\tau)\big|_{\tau=0} = \frac{1}{2\pi}\int_{-\infty}^{\infty} S_f(\omega)d\omega = D/(4\omega_f h_f) \quad (2\text{-}11)$$

In this chapter, the damping factor h_f is determined as 30% of critical to let the power spectral density of the artificial earthquake have relatively sharp peak around the predominant frequency ω_f. The parameter of frequency ratio $\eta=\omega_f/\omega_o$ determines long or short period structures relative to the predominant period of the artificial earthquake.

The way of generating the artificial earthquake on a digital computer is as follows.

Firstly white noise random process $n(t)$ is generated by the summation of cosine time functions which have uniform distribution of frequency and phase angle as it was done by H.Goto, K.Toki and T.Akiyoshi[12], that is,

$$n(t) = \frac{a}{\sqrt{L}} \sum_{r=1}^{L} \cos(2\pi f_r t + \phi_r) \tag{2-12}$$

where a is a constant value which determines the intensity of the process, L is a number of the summation, f_r and ϕ_r are random values of frequency and phase angle respectively. K.Toki[13] showed that the Fourier transform of the autocorrelation function of the above equation gives the relation between the power spectral density $S_f(f)$ of this process and the function of probability density $p(f_r)$ of random frequency component f_r as

$$S_f(f) = a^2/2 \; p(f_r) \tag{2-13}$$

Thus, the random frequency and phase angle of which probability density functions $p(f_r)$ and $p(\phi_r)$ are shown in Fig.2.5 (a) and (b) are generated using RADOM(0) in the Scientific Subroutine[14] at the Kyoto University Computer Center. In the Fig.2.5 (a), Δt represents the time interval of generated random variables. The autocorrelation function of the generated white noise random process shown in Fig.2.6 looks almost like Dirac's delta function even though there is a little correlation for large value of τ.

Secondly, the velocity response of simple linear oscillator with natural frequency ω_f and damping factor h_f subjected the the generated white noise is calculated by the linear acceleration method to make the artificial earthquake. To take only the stationary part of the velocity response, the transient part of the response due to initial conditions of zero-displacement and zero-velocity is thrown out. The duration which is ten times as long as the natural period of the filtering

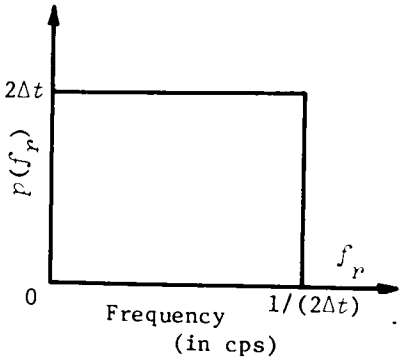

(a) Probability Density of Frequency

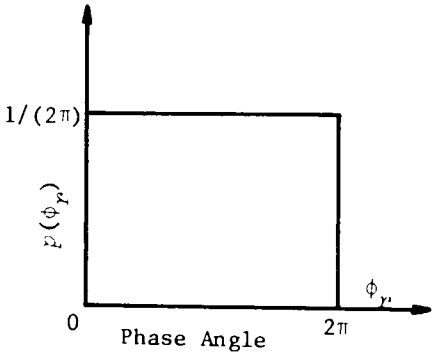

(b) Probability Density of Phase Angle

Fig.2.5 Random Frequency and Phase Angle for the White Noise

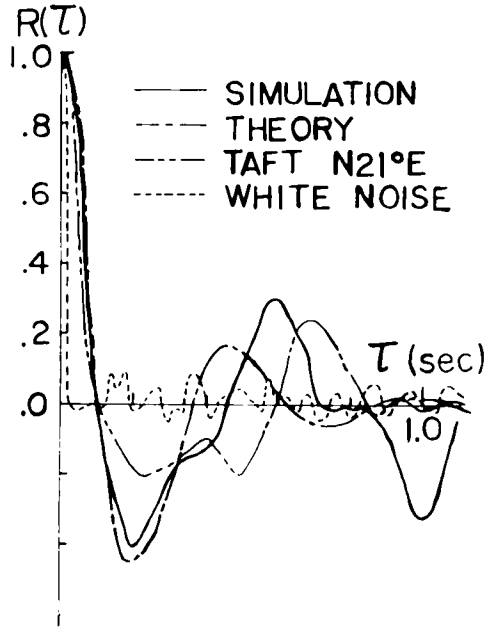

Fig.2.6 Autocorrelation Functions of Accelerograms

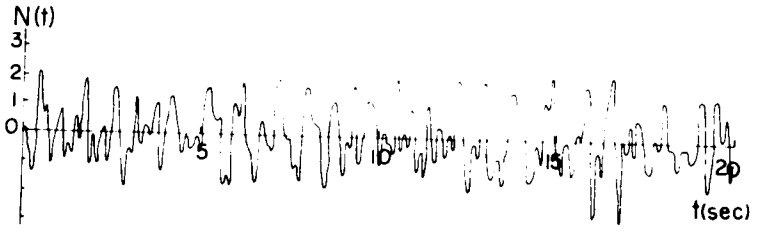

Fig.2.7 A Part of Artificial Earthquake Accelerograms

oscillator is considered as the transient part with the reference of the theoretical results by T.K.Caughey[15]. A typical example of time history of the generated artificial earthquake is shown in Fig.2.7. The autocorrelation function of the generated earthquake shows good agreement with the theoretical results given by Eq.(2-8) at their first peaks. A little time lag at their second peaks does not seem to make the generated result considerablely differ from the theoretical one. The autocorrelation function of the recorded accelerogram of the N21°E component at Taft during the Kern County earthquake is also shown in Fig.2.6.

2-3-2 Control of Time History of Bilinear Hysteresis Loops

(a) Control due to change of velocity sign

At the point B and E shown in Fig.2.8, relative velocity of hysteretic structures $d\mu/d\tau$ shall be zero. Hence when relative velocity changes its sign during step-by-step calculation with time interval of $\Delta t'$, an approximate time when relative velocity is zero will be estimated by the Taylor expansion as

$$\Delta t' = (\dot{\mu}_{i+1} - \dot{\mu}_i)/\ddot{\mu}_i \qquad (2\text{-}14)$$

where $\dot{\mu}_{i+1}$ is the calculated relative velocity at the next step under the initial conditions of $\dot{\mu}_i$ and μ_i, without changing the previous stiffness. Then an approximate coordinate when $\dot{\mu}$ is zero will be determined on g or l line which have the stiffness of plastic region to continue the calculation toward B-C or E-F line which have the stiffness of elastic region.

(b) Control due to change of stiffness

At the points A,C,D,F shwon in Fig.2.8, the stiffness of elastic region reduces its value to that of the plastic region. The displacement of these alteration points can be predicted by adding the width of elastic region to or reducing it from the displacement at the previous points where relative velocity $\dot{\mu}$ is zero. Hence, when the response of relative displacement during step-by-step calculation goes beyond this alteration

point, an approximate time when stiffness change shall occur will also be estimated by the Taylor expansion as

$$\Delta t'' = (\mu_{i+1} - \mu_i)/\dot{\mu}_i \tag{2-15}$$

Then an approximate velocity at these alteration points will be determined to continue the further calculation for g or l line.

In this way, the control due to the change of the stiffness can be done by defining the displacement of alteration points. So this way of controlling method of bilinear hysteresis loops would be considered as though it were depending exclusively on the displacement.

From the phisical view points of dynamic characterisitcs of structural materials, however, it seems desirable to take a different way of the controlling method by which the restoring force is limitted by two parallel straight lines; g which limits the upper boundary and l which limits the lower boundary of the restoring force. Because it is natural to consider that restoring force of structures is not restricted by displacement but the level of restoring force which makes structural elements yield.

This view point that the hysteresis is controlled by the limitted level of restoring force gives an easy way to control more complex hysteresis loops like modified Jennings hysteresis to be discussed in the next section.

To check the accuracy of the controlling method above mentioned, the calculated response of the elasto-plastic structure with no viscous damping subjected to sinusoidal excitation which has the same intensity as the yielding level of the restoring force is compared with the theoretical frequency response curve which was firstly obtained by T.K.Caughy[16] using slowly varying parameter method (Appendix 2-A). Both results are plotted in Fig.2.9 to show fairly good agreement, which would allow one to use both numerical and theoretical techniques for investigations of nonlinear hysteretic response.

It is also pointed out that the frequency response curve of the

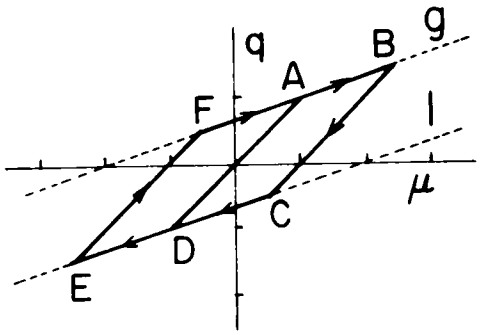

Fig.2.8 Control of Bilinear Hysteresis Loop

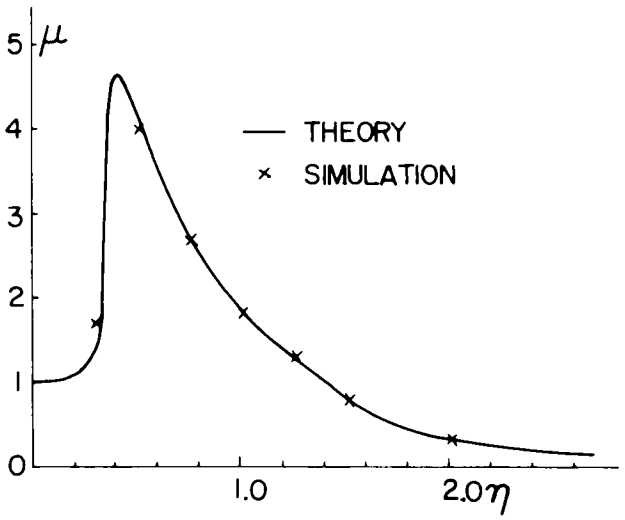

Fig.2.9 Predicted and Simulated Frequency Response Curve of the Elasto-Plastic Structure (h_o=0.0)

elasto-plastic structure with no viscous damping has its limitted peak around η=0.4, which is due to energy dissipation by the hysteresis loops and softening type of restoring force, respectively. It is noted that frequency response curves of linear structures with no viscous damping shall show infinite value at η=1.0.

2-3-3 Control of Time History of Modified Jennings Hysteresis Loops

A more complex and skillful technique is needed for the step-by-step control of random time history of modified Jennings hysteresis loops, because transition of restoring force from one curve to another can not be controlled exclusively by the displacement as was done for the control of bilinear hysteresis loops, but shall be controlled by the restoring force curves appropriately defined from the previous time history.

P.C.Jennings[17] proposed the two restoring force curves which define the upper and the lower boundary of time history to calculate earthquake response of structures with the curved hysteresis loops he presented. The way of controlling technique which seems to be applicable for any types of hysteresis loops will be explained briefly to adopt it also for this study.

(a) Control due to change of velocity sign

At the points A and C shown in Fig.2.10, relative velocity of hysteretic structures shall change its sign. The same technique as used for the control of bilinear hysteresis loops is adopted at these points to change the restoring force curve from one skeleton or one branch to another branch. The equation of the ascending or descending branch represented by Eq.(2-4) will be defined exclusively from the previous point where relative velocity is zero unless each branch cuts across the previously defined upper or lower boundary of the restoring force.

(b) Control of branches by the restoring force curve

On the ascending branch (C→D→A) or on the descending branch (A→B→C) in Fig.2.10, it should be checked whether each branch cuts across the

upper or lower boundary curves which are defined from the previous time history.

The upper boundary curves as shown in Fig.2.11 consists of one of ascending branches which has the minimum value of the intercept on μ-axis during the previous random time history and also of the skeleton except A-B section.

The lower boundary curve as shown in Fig.2.12 consists of one of descending branches which has the maximum value of the intercept on μ-axis at B-A section and also of the skeleton except B-A section.

When the ascending branch goes beyond the upper boundary curve during the step-by-step calculation of response, the transition of the restoring force from the branch to the upper boundary curve should be performed to avoid the higher level of restoring force than that of previous time history at the same displacement. Similarly when the descending branch goes below the lower boundary curve, the transition of the restoring force from the branch to lower boundary curve should be performed to avoid the lower level of restoring force than that of previous time history at the same displacement.

Approximate time and the coordinate of the transition point of the restoring force can also be determined by using the same techniques as it was used for the reduction of stiffness of bilinear hysteresis loops.

This method to control time history of hysteresis loops by two boundary curves seems applicable for any types and shapes of hysteresis loops, because appropriately defined upper and lower boundary curves could control complex restoring force characteristics, even the rotation of hysteresis loops as S.Yoshihara[18] adopted.

The frequency response curves of the modified Jennings hysteresis loops (α=0.1, r=9) obtained from the theoretical analysis using the slowly varying parameter method (Appendix 2-A) and also from the simulation using above mentioned controlling technique are plotted in Fig.2.13 to show good agreement between them, from which accuracy of both methods could be considered satisfactory for practical usage

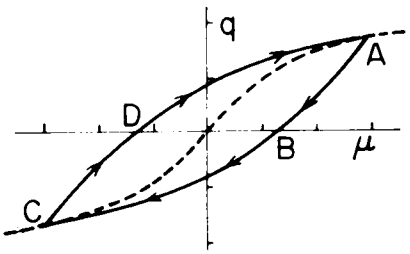

Fig.2.10 Control due to Change of Velocity Sign

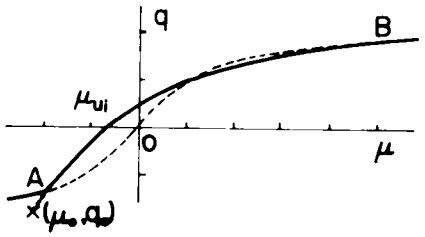

Fig.2.11 The Upper Boundary Curve

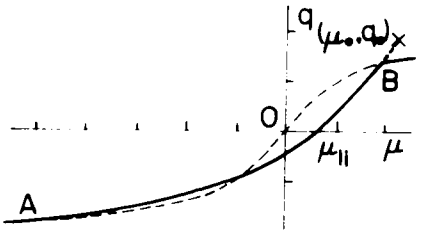

Fig.2.12 The Lower Boundary Curve

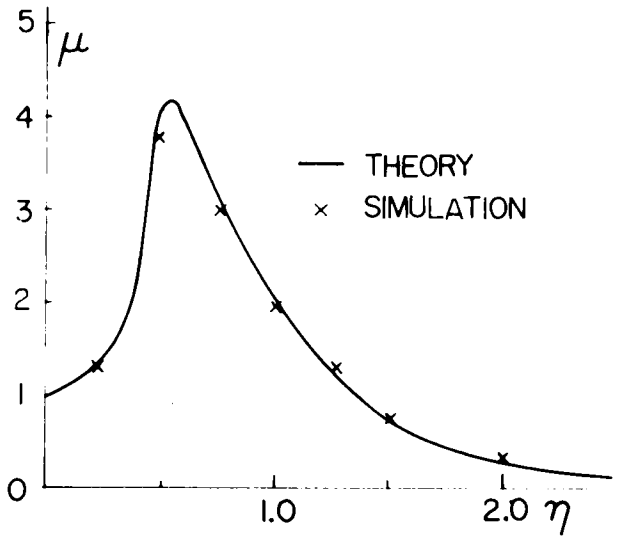

Fig.2.13 Predicted and Simulated Frequency Response Curve of the Modified Jennings Hysteresis Loop (h_o=0.0, α=0.1, r=9)

like the simulation in this study.

A typical example of calculated random response of a structure with modified Jennings hysteresis loop (α=0.1, r=11) subjected to the generated artificial earthquake is shown in Fig.2.14 (a) and (b).

The drift of displacement from zero base line which seems due to growth of plastic deformation is apparent along the computed displacement shown in Fig.2.14 (a).

The limitted part of the time history of the hysteresis loops plotted in Fig.2.14 (b) indicates satisfactorily smooth control of the hysteresis loops with strong nonlinearity.

2-4 Simulated Plastic Deformation

2-4-1 Estimation of Plastic Deformation by Moving Average Method

As shown in Fig.2.14 (a), time history of displacement response of structures with strong nonlinearity of hysteresis loops subjected to strong earthquake excitation often shows plastic drift from zero base line, which is also reported by P.C.Jennings[17], N.C.Nigam[3], M.Hakuno[6] and others. Such complex features of nonlinear hysteretic response which consists of elastic component of vibration and also of plastic drift are quite different from those of linear elastic response.

It seems not sufficient enough for discussions of structural damages or process of failure due to strong earthquakes to calculate only maximum response of structures over the yielding limit. Because the values of ductility factor and plastic deformation seems to concern strongly with structural damages such as cracks of walls, columns and beams.

In this section, a technique to estimate the amount of local plastic drift from zero base line during earthquake-type random excitation is proposed. The amount of plastic drift could be estimated by taking an average of displacement response over limitted section where drift seems constant. The component of elastic vibration over there would be

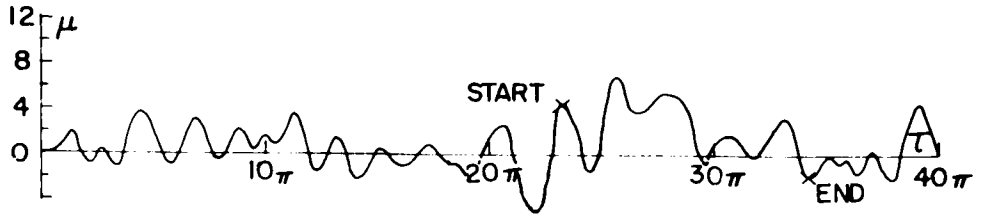

(a) Ductility Factor Response

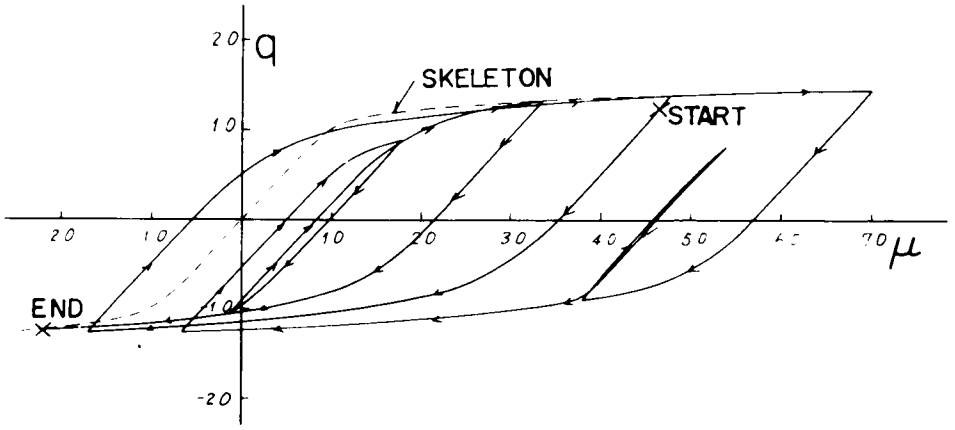

(b) Response of Hysteretic Restoring Force

Fig.2.14 A Part of Random Response of Modified Jennings Hysteresis Loops Subjected to Artificial Accelerograms (h_o=0.05, α=0.1, r=11, r_s=1.0, η=1.0)

eliminated by averaging process.

A moving average technique which is one kind of filters to eliminate small period fluctuations along relatively long period drift of displacement is adopted to estimate the amount of local plastic drift.

Let define the moving average as

$$\mu_{av}(\tau, T_l) = \begin{cases} \frac{1}{T_l}\int_0^{\tau+T_l/2} \mu(\tau)d\tau & ; \ \tau \le T_l/2 \\ \frac{1}{T_l}\int_{\tau-T_l/2}^{\tau+T_l/2} \mu(\tau)d\tau & ; \ T_l/2 \le \tau \le T_m - T_l/2 \\ \frac{1}{T_m-\tau-T_l/2}\int_{\tau-T_l/2}^{T_m} \mu(\tau)d\tau & ; \ T_m - T_l/2 \le \tau \le T_m \end{cases} \quad (2\text{-}16)$$

where T_l is the time interval of the averaging section and T_m is the total duration of the calculated response. In this study T_m is set as 60π which is 30 times as long as the natural period 2π of hysteretic structures in small oscillation.

The time interval of the averaging section T_l would be the most important parameter of this technique to estimate the plastic drift. That is, too much short T_l could not eliminate the elastic vibration component. In this case, the value of plastic drift might be estimated much bigger than real one. On the contrary, too long T_l could not point out the local value of plastic drift due to the local strong pulse of excitation. Therefore T_l should be set as the shortest interval by which the most of elastic vibration component could be eliminated.

In Fig.2.15, the time history of displacement response of a linear structure (h_o=0.05, η=1.0) subjected to the artificial earthquake (r_s=1.0) and the moving average of it for the set of parameters $T_l=2\pi$, 4π, 8π, 12π which correspond to 1, 2, 4, 6 times as long as the natural period of the structure 2π. This figure indicates that the most of elastic vibration components is eliminated and the moving average becomes almost zero when T_l is set larger than 8π.

The displacement response of a structure with elasto-plastic hysteresis loop (h_o=0.05, n=1.0, η=1.0) subjected to the same excitation in Fig.2.15 and the moving average of it are plotted in Fig.2.16. The time history of the displacement response shows large amount of the plastic drift which seems due to strong nonlinearity of the hysteresis and also short period fluctuations with relatively small amplitude which seems due to large amount of energy dissipation by hysteresis loops. The moving average with similar set of parameters of T_l as in Fig.2.15 shows that the large value of T_l gives the smoother time variation of the average as could be expected. It is noted that the initial value of the moving average at τ=0 for T_l which is less than 4π shows non-zero value because the small fluctuation can not be eliminated for such small averaging interval.

Similar results of a structure with modified Jennings hysteresis loops (α=0.1, r=11, h_o=0.05, η=1.0) are shown in Fig.2.17. Although the small period fluctuation of displacement response is almost same as that of a structure with elasto-plastic hysteresis loops, much less amount of plastic drift is found. This difference seems due to the different type of hysteresis loops.

From the numerical results shown in Figs.2.15, 16, 17 and above discussions, T_l is set as 8π which is 4 times as long as the natural period of hysteretic structures in small oscillation to estimate the local variation of plastic drift eliminating the small period elastic fluctuation.

$$\mu_p(\tau) = \mu_{av}(\tau, 8\pi) \tag{2-17}$$

It is of great interest for designing of structures to resist strong earthquake to know the direction and the amount of the plastic deformation for different parameters of structures and also of excitations. As symmetric shapes of hysteresis loops are assumed in this study, however, the direction of the plastic drift would be affected exclusively

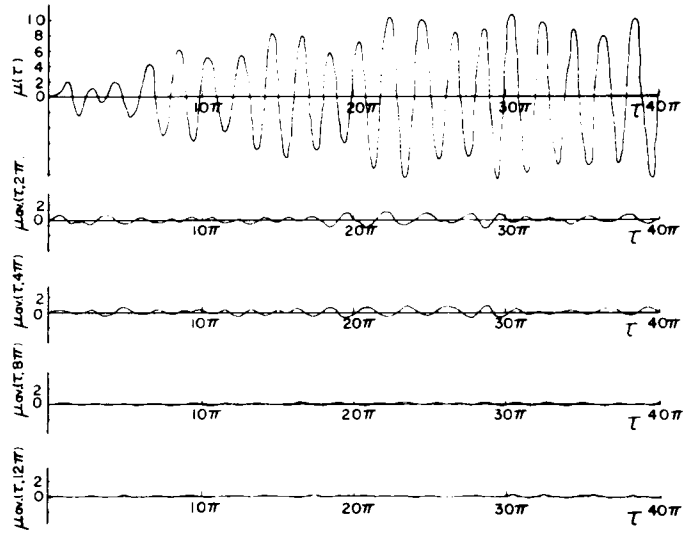

Fig.2.15 Response of Linear Structure and its Moving Average (h_o=0.05, r_s=1.0, η=1.0)

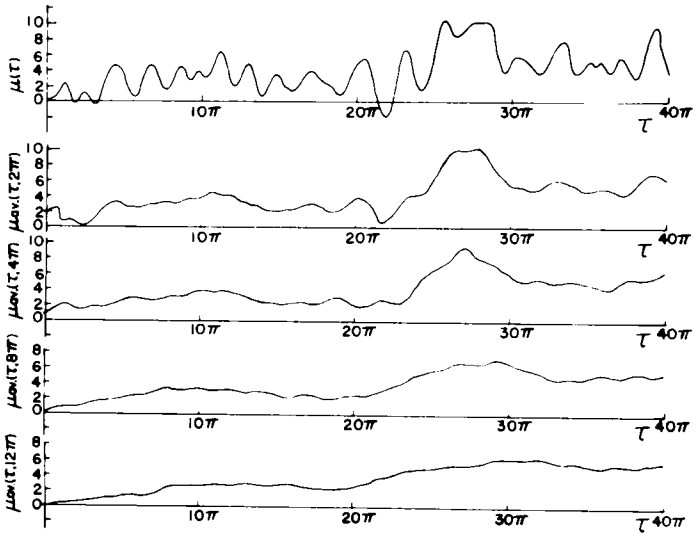

Fig.2.16 Response of Elasto-Plastic Hysteretic Structures and its Moving Average (h_o=0.05, n=1.0, r_s=1.0, η=1.0)

by the characteristics of exciting accelerograms. Hence the direction will not be discussed herein but only the absolute value of plastic drift will be investigated with relative to the absolute value of displacement response.

It is one of the purposes of this study to find how the local absolute maximum displacement grows and how the plastic deformation accumulates with the duration of excitation. Hence the absolute maximum value $\mu_{max}(\tau)$ is defined as shown in Fig.2.18. In this figure, the absolute value of $\mu(\tau)$ is plotted for the first step, then the envelope of the peaks which are bigger than any other previous ones is taken.

The absolute maximum values defined in this way would be convenient to examine the nonstationary characteristics of hysteretic structures especially the duration effects more in detail. Discussions about the simulated results will be made in following sections as to the effects of types and shapes of hysteresis loops, intensity of excitation and frequency ratio between natural frequency of hysteretic structures and predominant frequency of excitation.

2-4-2 Effects of Shapes of Hysteresis Loops

The parameters which determine the shapes of restoring force are n for bilinear hysteresis and r for modified Jennings hysteresis. Another parameter α for modified Jennings hysteresis is set constant as 0.1. The larger values of n and r show the stronger nonlinearity of restoring force.

In Fig.2.19 (a) and (b), shown are the absolute maximum value of the response displacement $\mu_{max}(\tau)$ and also the absolute maximum value of the plastic drift $\mu_{p,max}(\tau)$ of a structure with bilinear hysteresis (h_o=0.05, η=1.0) subjected to the artificial earthquake (r_s=1.0), respectively.

This set of parameters is supposed to express the situation that structures are subjected to very strong random ground motion of which predominant frequency is the same as the natural frequency of structures in small oscillation for relatively long duration.

It is not easy to find any clear difference among $\mu_{max}(\tau)$ shown in

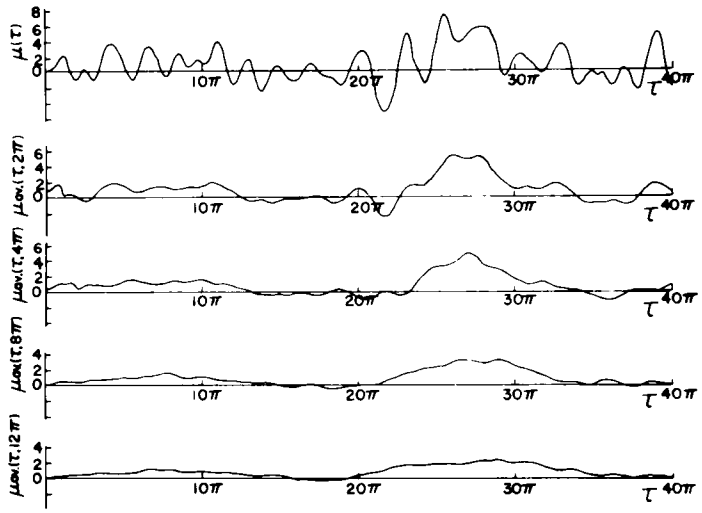

Fig.2.17 Response of Modified Jennings Hysteretic Structures and its Moving Average (α=0.1, r=11, h_o=0.05, r_s=1.0, η=1.0)

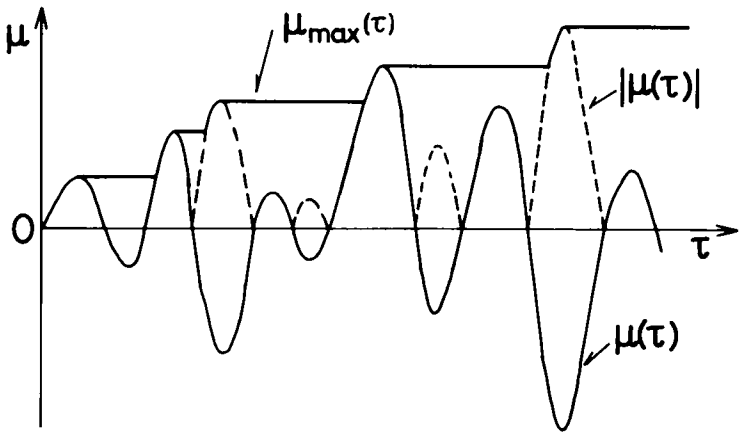

Fig.2.18 Definition of the Absolute Maximum Value $\mu_{max}(\tau)$ of Ductility Factor Response $\mu(\tau)$

Fig.2.19 (a) for different values of n. However displacement response of hysteretic structures seems to show larger value than that of the linear structure at the time-section $\tau \geq 25\pi$ except for the case of n=0.75.

The effect of the duration of excitation to hysteretic response is significant up to about $\tau=30\pi$ which is 15 times as long as the natural period of structures in small oscillation.

On the results of the improved Phase-Plane-Delta method, R.Tanabashi[19] and T.Kobori suggested that a few strong pulses would be sufficient enough for estimation of hysteretic response at the early stage of this field. Mainly because energy dissipation due to hysteretic behavior of restoring force would add so much damping to structures that preceding small pulses before the strong pulses would not have any significant effects to the total response.

The necessity of nonlinear hysteretic response analyses has been highly appreciated by many research workers since then as mentioned in the previous chapter. However the effect of duration of excitation shown in Fig.2.19 (a) does not seem small enough to be neglected. Similar results are also reported by J.Penzien and S.-C.Liu[2].

D.E.Hudson[20] reported that the order of hysteretic energy dissipation in random response is about several percent of critical damping.

These results point out the importance of further intensive investigations of the duration effects of excitations on hysteretic response for different sets of parameters.

The absolute maximum value of the plastic drift $\mu_{p,max}(\tau)$ shown in Fig.2.19 has significantly different character with respect to the parameter of n. It is found that a structure with elasto-plastic hysteresis loop (n=1.0) which has no stiffness in the plastic range shows considerable amount of plastic drift than any other structures with bilinear hysteresis loops, even though $\mu_{max}(\tau)$ does not change so much among them.

This result suggests that features of displacement response of elasto-plastic structures would be quite different from those of bilinear or

linear structures. That is, the part of plastic drift in the total displacement response is significantly large for elasto-plastic structures and little for bilinear or linear structures. These different features of response should especially be noticed when estimation of response statistics of hysteretic structures is tried using linearization technique such as those which will be discussed in the next chapter.

Effects of different shapes of modified Jennings hysteresis loops to μ_{max} and $\mu_{p,max}$ are also plotted in Fig.2.20 (a) and (b) for different values of the paramter r. Plotted μ_{max} does not have significant difference within the range of r from 3 to 11 used hearein. It is interesting to note that the corresponding linear structure shows larger response than almost all of modified Jennings hysteresis, contrary to the results of bilinear hysteresis. Values of μ_{max} keeps growing up to 30π as that of bilinear hysteresis to suggest the effect of duration of excitation is not negligibly small.

Plotted $\mu_{p,max}$ in Fig.2.20 (b) shows the larger value for the bigger r. The large plastic deformation seems due to strong nonlinearity after yielding for large value of r as is known from the shapes of modified Jennings hysteresis loops shown in Fig.2.4. There is no significant step-wise increase of $\mu_{p,max}$ with respect to the parameter r. None of specified r determines which hysteresis loop is stable or nonstable with relative to plastic deformation. Even the hysteresis loop with the weakest nonlinearity (r=3) shows noticeable plastic deforamtion ($\mu_{p,max}$= 1.0 for μ_{max}=8.0) This value of plastic deformation is bigger than that of the bilinear hysteresis of n=0.75 which shows realtively strong nonlinearity. Therefore modified Jennings hysteresis representation is considered as models of restoring force which let the plastic deformation grow easier than bilinear hysteresis representation.

This consequence could be explained from the difference of stiffness after yielding of two hysteresis loops. Bilinear hysteresis loops show constant stiffness after yielding as

$$\frac{dq}{d\mu} = 1-n \qquad \text{for } 1.0<\mu<\infty \tag{2-18}$$

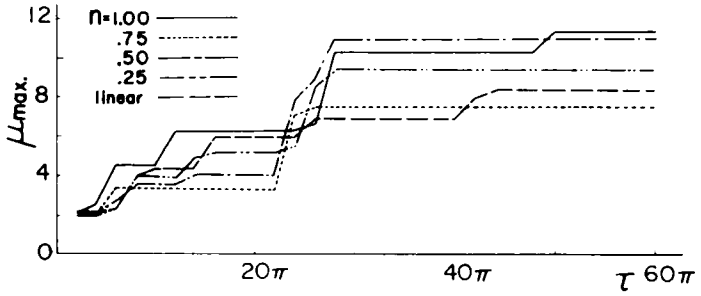

(a) The Absolute Maximum Ductility Factor Response

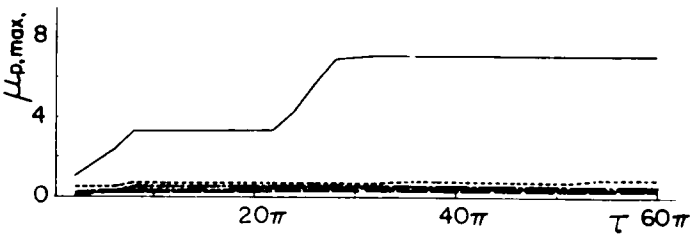

(b) The Absolute Maximum Plastic Deformation

Fig.2.19 Effects of A Parameter n of Bilinear Hysteresis Loops
(h_o=0.05, r_s=1.0, η=1.0)

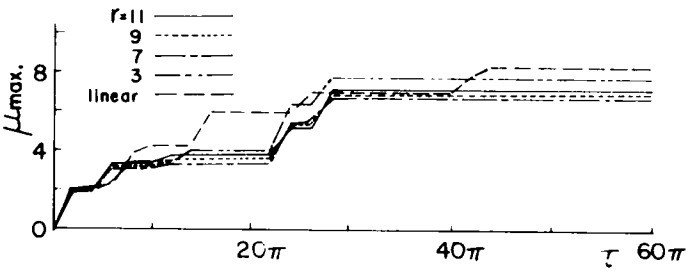

(a) The Absolute Maximum Ductility Factor Response

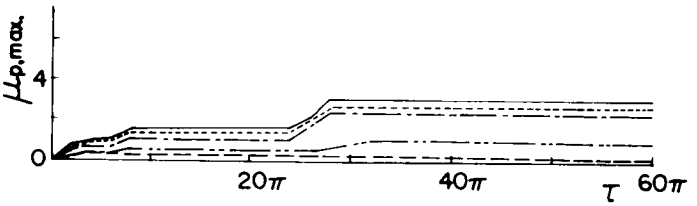

(b) The Absolute Maximum Plastic Deformation

Fig.2.20 Effects of A Parameter r of Modified Jennings Hysteresis Loops
(h_o=0.05, α=0.1, r_s=1.0, η=1.0)

On the contrary, the stiffness of modified Jennings hysteresis loops after yielding gradually decreases and it is asymptotic to zero when amplitude increases infinitely as

$$\frac{dq}{d\mu}\Big|_{\mu=\infty} = \frac{1+\alpha}{\{1+\alpha r q^{r-1}\}}\Big|_{q=\infty} = 0 \qquad (2\text{-}19)$$

Hence, higher ductility of modified Jennings hysteresis loops lets the plastic deformation occur easily due to the significant loss of the stiffness even for small value of r.

2-4-3 Effects of Intensity of Excitation

Effects of intensity of the excitation to the absolute maximum displacement μ_{max} and the plastic deformation $\mu_{p,max}$ are investigated in this section for specified bilinear hysteresis and modified Jennings hysteresis by changing the intensity parameter r_s. It is again noted that r_s represents the ratio of r.m.s. intensity of excitation to the yielding level of a structure.

In Fig.2.21 (a) and (b), shown is the response of a structure with the elasto-plastic hysteresis loop (n=1.0, h_o=0.05, η=1.0) subjected to the stationary artificial earthquake of which intensity parameter r_s varies from 0.25 to 1.0.

Plotted μ_{max} in Fig.2.21 (a) shows unusually large response for r_s=0.75 and 1.0. That is, μ_{max} of r_s=0.75 is almost two times as large as that of r_s=0.50, and also μ_{max} of r_s=1.0 is about two times as large as that of r_s=0.75. For linear structures, μ_{max} should be proportional to the intensity parameter r_s from the principle of linear superposition. When the intensity of the excitation is small (r_s=0.25 and 0.50), the linear principle seems applicable, since μ_{max} of r_s=0.5 is about twice of that of r_s=0.25.

These nonlinear characteristics of the elasto-plastic hysteresis loops would clearly be understood by examining the $\mu_{p,max}$ shown in Fig.2.21 (b). Plotted $\mu_{p,max}$ shows small value for low level of the excitation (r_s=0.25 and 0.50), because ductility response itself is

still small. However when r_s becomes larger than 0.50, $\mu_{p,max}$ grows remarkably to let μ_{max} out of the linear principle.

The results obtained in Fig.2.19 and here suggest that the plastic deformation grows almost exclusively for the elasto-plastic hysteresis loop subjected to relatively strong excitation ($r_s \geq 0.75$) to show the strong nonlinearity of μ_{max}.

Similar examination of effects of the intensity of the excitation to modified Jennings hysteresis loops (h_o=0.05, α=0.1, r=9) is done by plotting μ_{max} and $\mu_{p,max}$ in Fig.2.22 (a) and (b). The values of μ_{max} and $\mu_{p,max}$ are almost proportional to r_s at any point of their time history. This result suggests that the response of the modified Jennings hysteresis which keeps the positive stiffness even decreasing strongly after yielding, follows linear principle better than that of the elasto-plastic hysteresis which loses stiffness completely after yeilding. So it is hard to find the critical value of r_s which lets $\mu_{p,max}$ of the modified Jennings hysteresis grow significantly.

The results obtained in Fig.2.20 and here conclude that the amount of plastic deformation $\mu_{p,max}$ of modified Jennings hysteresis is not so large as that of the elasto-plastic hysteresis and also that the $\mu_{p,max}$ of modified Jennings hysteresis would grow, even a little, for structures with relatively weak nonlinearity of hysteresis loops subjected to relatively low level of the excitation.

2-4-4 Effects of Natural Period of Structures

Effects of natural period of hysteretic structures in infinitesimal vibration to the response of μ_{max} and $\mu_{p,max}$ are investigated in this section.

In Fig.2.23 (a) and (b), response of the elasto-plastic hysteresis loops (h_o=0.05, n=1.0, r_s=1.0) is plotted with the frequency parameter η which shows the ratio of the natural period of the structure T_o and the predominant period of the excitation T_f (i.e., $\eta = T_o/T_f$). Fig.2.23 (a) shows that the μ_{max} of the elasto-plastic hysteresis is larger for

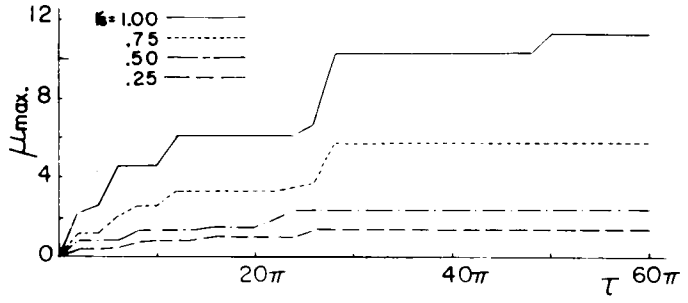

(a) The Absolute Maximum Ductility Factor Response

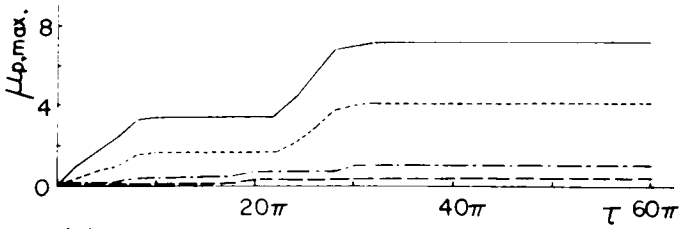

(b) The Absolute Maximum Plastic Deformation

Fig.2.21 Effects of Intensity Parameter r_s to Elasto-Plastic Hysteretic Structures (h_o=0.05, n=1.0, η=1.0)

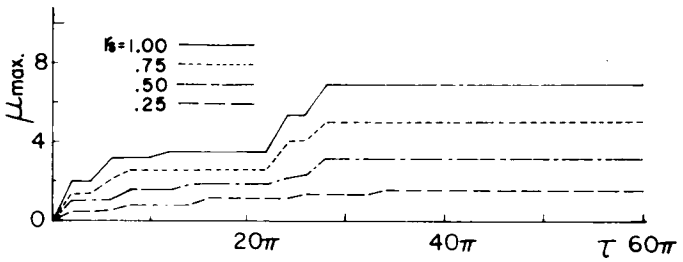

(a) The Absolute Maximum Ductility Factor Response

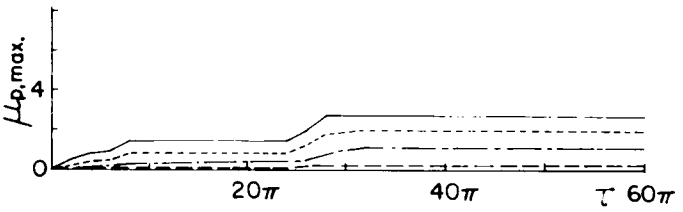

(b) The Absolute Maximum Plastic Deformation

Fig.2.22 Effects of Intensity Parameter r_s to Modified Jennings Hysteretic Structures (h_o=0.05, α=0.1, η=1.0)

structures with smaller value of η which could be called "relatively short period" or "relatively rigid" structures. The effect of duration of the excitation is also significant for smaller value of η. Almost similar effects are found for $\mu_{p,max}$ shown in Fig.2.23 (b).

These results indicate that the response of the relatively short period structures ($\eta \leq 1.0$) shows the larger values and also grows more rapidly after yielding on the time history than that of the relatively long period structures ($\eta > 1.0$). Therefore from engineering view point, yielding of short period structures with strong nonlinearity should especially be avoided not to let the response grow rapidly up to failure due to many number of loading cycles in the state of resonance.

Response of the modified Jennings hysteresis (α=0.1, r=9, h_o=0.05, r_s =1.0) is also plotted in Fig.2.24 (a) and (b) for a set of parameter η. Plotted μ_{max} and especially $\mu_{p,max}$ in these figures are found to be smaller than those of the elasto-plastic hysteresis. However, it is the same tendency for modified Jennings hysteresis loops that the smaller values of η gives the bigger response of μ_{max} and $\mu_{p,max}$. The effect of duration of the excitation is also similar to that of the elasto-plastic hysteresis.

These results suggest that the effects of η to the response of hysteretic structures are almost identical even for different type of hysteresis loops. That is, the relatively short period hysteretic structures recieve the duration effect more strongly and show bigger response than the relatively long period hysteretic structures.

The reason of this effect of η could reasonably be explained by taking acount of the resonance between hysteretic structures with the amplitude-depending natural frequency and the random excitation with the single predominant frequency.

Every hysteretic model adopted in this chapter has soft-spring type restoring force characterisitcs to let the natural period of structures grow large after yielding. Hence, when the response of relatively short period hysteretic structures goes over the yielding limit, the peak of

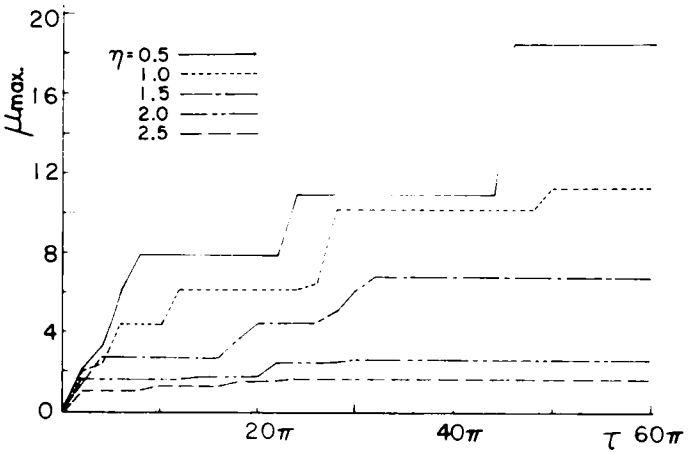

(a) The Absolute Maximum Ductility Factor Response

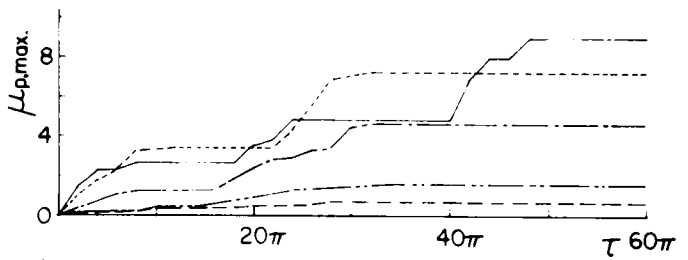

(b) The Absolute Maximum Plastic Deformation

Fig.2.23 Effects of Frequency Parameter η to Elasto-Plastic Hysteretic Structures (h_o=0.05, n=1.0, r_s=1.0)

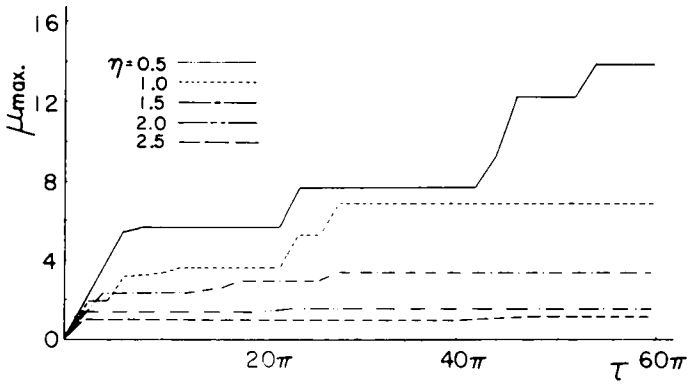

(a) The Absolute Maximum Ductility Factor Response

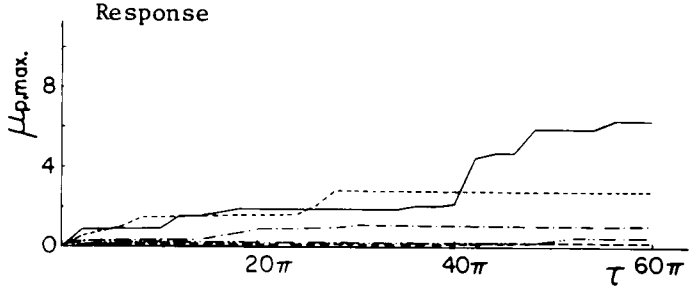

(b) The Absolute Maximum Plastic Deformation

Fig.2.24 Effects of Frequency Parameter η to Modified Jennings Hysteretic Structures (h_o=0.05, α=0.1, r=9, r_s=1.0)

the receptance of the structures moves closer to the predominant frequency of the excitation. On the contrary, the peak of the receptance of the relatively long period structures goes far from the predominant frequency of the excitation due to yielding to suppress the response. As the result of this receptance shifting, the response neither grows large nor recieves the duration effects.

The results in this section seem to allow to conclude that the frequency-depending response characteristics of hysteretic structures which had been said to be very small due to additional damping are almost as significant as those of linear structures. Further theoretical studies are strongly needed for general discussions of earthquake response characteristics of hysteretic structures.

As one of the important suggestions for earthquake engineers obtained in this section, it is strongly noted that the response of the relatively short period hysteretic structures after yielding is expected to grow very rapidly up to failure due to the high number of loading cycles in the state of resonance.

2-5 Conclusions

In this chapter, the plastic deformation of elasto-plastic structures in strong earthquakes has been discussed by means of numerical simulation on a digital computer. Main results derived from the study in this chapter are as follows.

(1) The dimensionless representation of the equation of motion of a single-degree-of-freedom (simple) structures with arbitrary types of restoring force has been proposed to reduce the number of parameters of excitation and hysteretic structures. Consequently, the effects of different types of restoring force of structures to their random response have been discussed and examined more generally than for the conventional investigations with dimensions.

(2) Displacement response of hysteretic structures has been separated

into elastic and plastic components. The amount of plastic deformation has been estimated by means of the moving average technique by which local vibration of elastic component has been eliminated. The suitable time interval of the averaging section has been found as 4 times as long as the natural period of structures to take out the plastic deformation from total displacement response.

(3) Effects of shapes of hysteresis loops to the plastic deformation have been checked for bilinear and modified Jennings types of representation. For bilinear hysteresis loops, the plastic deformation grows very rapidly when the stiffness after yielding becomes close to zero. When the stiffness in the plastic region is greater than one quarter of that in the elastic region, the plastic deformation was found to grow little. For modified Jennings hysteresis loops, the plastic deformation was observed even for r=3 which shows the weakest nonlinearity of the hysteresis loop. The Plastic deformation increased gradually for stronger nonlinearity of the hysteresis loops, however, it did not reach to so large as that of the elasto-plastic hysteresis loop.

(4) Effects of intensity of the excitation have been examined for two specified hysteresis loops. For the elasto-plastic hysteresis loops, the plastic deformation was found to grow significantly out of the principle of linear superposition when the r.m.s. intensity of the excitation is greater than half of the yielding level. Relatively proportional relation was found between the plastic deformation and the intensity of the excitation for the modified Jennings hysteresis loops (r=9).

(5) Effects of natural period of structures were found almost the same between the elasto-plastic hysteresis and the modified Jennings hysteresis loops (r=9). Response of "relatively short period structures" of which natural period is shorter than the predominant period of the excitation has shown the larger values and also grown more rapidly after yielding than that of "relatively long

period structures". This frequency effect seems due to the soft-spring type restoring force which lets the natural period of structures grow longer and shift more close to the predominant period of the excitation.

(6) Effects of the duration of the excitaion have been found not so small as had been suggested before, especially for "relatively short period structures" with strong nonlinearity of hysteresis loops. Accumulation of plastic deformation of these structures should strongly be avoided not to cause structural collapse due to severe ground motion.

The study in this chapter has also derived next three topics to be investigated for more realistic, statistical and theoretical discussions about earthquake response characteristics of hysteretic structures.

(a) Only two idealized models were used in this chapter as the presentation of nonlinear hysteretic restoring force characteristics of structures to examine their random response. However, restoring force characteristics of real structures have not yet been well investigated, particularly in the large amplitude range from the yielding level up to failure. From this point of view, experimental studies both in laboratories and in fields are strongly needed to measure more realistic behavior of restoring forces.

(b) Main features of hysteretic response of structures with weak nonlinearity were found not so different from those of linear ones. This result suggested that nonlinear response could be predicted theoretically by choosing equivallent linear structures and applying linear theories to them. From this point of view, investigation of linearization techniques and their application to earthquake response of hysteretic structures are of strong necessity.

(c) Plastic deformation was found to grow significantly only for structures with strong nonlinearity. Theoretical investigation of

plastic deformation is also needed to predict the probabilistic amount of it, particularly for discussions of structural reliability during strong earthquakes.

These three topics will be discussed intensively in the following three chapters of this dissertation.

References for Chapter 2

1) P.C. Jennings: Response of Simple Yielding Structures to Earthquake Excitation, The Thesis for the Degree of Doctor of Philosophy (Ph. D.), California Institute of Technology (Cal Tech), 1963.
2) J. Penzien and S.-C. Liu: Nondeterministic Analysis of Nonlinear Structures Subjected to Earthquake Excitataions, Proc. of the fourth WCEE, Vol. I, January, 1969, pp. A1-114∿129.
3) S.-C. Liu: Earthquake Response Statistics of Nonlinear Systems, Proc. of ASCE, EM2, April, 1969, pp. 397-419.
4) N.C. Nigam and G.W. Housner: Elastic and Inelastic Response of Framed Structures During Earthquakes, Proc. of the fourth WCEE, Vol. II, January, 1969, pp. A4-89∿104.
5) D. Karnopp and T.D. Scharton: Plastic Deformation in Random Response, The Journal of ASA, Vol. 39, Number 6, 1966, pp.1154-1161.
6) M. Hakuno and M. Shidawara: Dynamic "Force-Displacement" Relations of Cantilever Test Piece Applied by Earthquake Type External Force, Proc. of JSCE, No. 162, February, 1969, pp. 11-20, (in Japanese).
7) M. Hamuno, M. Shidawara and T. Hara: Dynamic Destructive Test of a Cantilever Beam, Controlled by An Analog-Computer, Proc of JSCE, No. 171, Novermber, 1969, pp. 1-9, (in Japanese).
8) P.C. Jennings: Periodic Response of a General Yielding Structure, Proc. of ASCE, EM2, April 1964, pp. 131-166.
9) H. Goto, K. Toki, Y. Ando and A. Ohta: On Restoring-Force Characteristics of Soil-Foundation Systems, The Annual Report on Research Activities, The Kansai District of JSCE, May, 1968, No. I-15, (in Japanese).
10) M. Shinozuka and Y. Sato: Simulation of Nonstationary Random Process, Proc. of ASCE, EM1, February, 1967, pp. 11-40.
11) J.D. Robson: An Introduction to Random Vibration, Edinburgh University Press, 1964, p. 40.
12) H. Goto, K. Toki and T. Akiyoshi: Generation of Artificial Earth-

quakes on Digital Computer for Aseismic Design of Structures, Proc. of the second Japan Earthquake Engineering Symposium (JEES), 1966, pp. 25-30, (in Japanese).

13) K. Toki: Simulation of Earthquake Motion and Its Application, Annual Report of DPRI, Kyoto Univ., No. 11A, 1968, pp. 1-13., (in Japanese).

14) T. Kimura: On Functions of RANDOM and KUNIRN to generate Uniform Random Variables, Report of Data Processing Center, Kyoto Univ., Vol. 7. No. 1, 1974, pp. 7-10., (in Japanese).

15) T.K. Caughey and H.J. Stumpf: Transient Response of A Dynamic System under Random Excitation, Journal of Applied Mechanics (AM), No. 4, 1961, pp. 563-566.

16) T.K. Caughey: Sinusoidal Excitation of A System with Bilinear Hysteresis, Journal of AM, Vol. 27, December, 1960, pp. 640-643.

17) P.C. Jennings: Earthquake Response of A Yielding Structure, Proc. of ASCE, EM4, August, 1965, pp. 41-68.

18) S. Yoshihara: Studies on Dynamic Characteristics of Caisson Foundation and its Earthquake Response, The Dissertation for Ph. D. at Kyoto Univ., September, 1973, pp. 130-176.

19) R. Tanabashi: Nonlinear Transient Vibration of Structures, Proc. of the Second WCEE, Vol. II, July, 1960, pp. 1223-1238.

20) D.E. Hudson: Equivalent Viscous Friction for Hysteretic Systems with Earthquake-like Excitations, Proc. of the third WCEE Vol. II, January, 1965, pp. II-185∿206.

APPENDIX 2-A

Frequency Response Curve of Hysteretic Structures with Viscous Damping

Frequency response curves of hysteretic structures without viscous damping were theoretically investigated by T.K.Caughey[16] and P.C.Jennings[8] using the slowly varying parameter method. In this appendix, similar investigation is made for hysteretic structures with viscous damping.

The equation of motion of simple hysteretic structures with damping subjected to sinusoidal excitation is written as

$$\ddot{\mu}(\tau)+2h_o\dot{\mu}(\tau)+q(\alpha,\beta,\mu,\tau) = -r_s\cos\eta\tau \tag{2-A-1}$$

Let's assume slowly varying amplitude $\mu_o(\tau)$ and phase angle $\phi(\tau)$ of the response of the above equation, i.e.;

$$\mu(\tau) = \mu_o(\tau)\cos\{\eta\tau+\phi(\tau)\} \tag{2-A-2}$$

where

$$d\mu_o(\tau)/d\tau \simeq 0, \quad d\phi(\tau)/d\tau \simeq 0 \tag{2-A-3}$$

Substituting Eq.(2-A-2) into Eq.(2-A-1) and taking the first term of sine and cosine Fourier expansion series of Eq.(2-A-1) with conditions of Eq.(2-A-3) will give the relation among response amplitude μ_o, frequency parameter η and phase angle ϕ_o as

$$\left.\begin{aligned} -2h_o\eta\mu_o + S(\mu_o) &= -r_s\sin\phi_o \\ -\eta^2\mu_o + C(\mu_o) &= -r_s\cos\phi_o \end{aligned}\right\} \tag{2-A-4}$$

where

$$\left.\begin{aligned} S(\mu_o) &= \frac{1}{\pi}\int_0^{2\pi} q(\alpha,\beta,\mu_o\cos\theta,\tau)\sin\theta d\theta \\ C(\mu_o) &= \frac{1}{\pi}\int_0^{2\pi} q(\alpha,\beta,\mu_o\cos\theta,\tau)\cos\theta d\theta \end{aligned}\right\} \tag{2-A-5}$$

The frequency response curve will be obtained by elimination of phase

angle ϕ_o from Eq.(2-A-4), that is

$$\{S(\mu_o)-2h_o\eta\mu_o\}^2 + \{C(\mu_o)-\eta^2\mu_o\}^2 = r_s^2 \tag{2-A-6}$$

The phase angle is also shown from Eq.(2-A-4) as

$$\phi_o = \tan^{-1}\{\frac{-2h_o\eta\mu_o+S(\mu_o)}{C(\mu_o)-\eta^2\mu_o}\} \tag{2-A-7}$$

$S(\mu_o)$ and $C(\mu_o)$ defined by Eq.(2-A-5) are calculated for bilinear hysteresis loops as[16]

$$\left.\begin{aligned} S(\mu_o) &= \begin{cases} \frac{n\mu_o}{\pi}\sin^2\theta^* & ;\ \mu > 1.0 \\ 0 & ;\ \mu \le 1.0 \end{cases} \\ C(\mu_o) &= \begin{cases} \frac{\mu_o}{\pi}[n\theta^*+(1-n)\pi-n/2\sin 2\theta^*] & ;\ \mu > 1.0 \\ \mu_o & ;\ \mu \le 1.0 \end{cases} \\ \text{where}\quad \theta^* &= \cos^{-1}(1-2/\mu_o) \end{aligned}\right\} \tag{2-A-8}$$

Those for modified Jennings hysteresis loops are obtained as follows[8].

$$\left.\begin{aligned} S(\mu_o) &= -\frac{4\alpha(r-1)\ q_o^r}{\pi(r+1)(1+\alpha q_o^{r-1})} \\ C(\mu_o) &= -\frac{2}{\mu_o\pi}\int_{-\mu_o}^{\mu_o}\frac{zq(\alpha,r,z,\tau)}{\sqrt{\mu_o^2-z^2}}dz \end{aligned}\right\} \tag{2-A-9}$$

3. ANALYTICAL PREDICTION OF PLASTIC DEFORMATION IN RANDOM RESPONSE

3-1 General Remarks

In the occasion of extremely strong earthquakes which might occur once or less in the life time of structures, it would be inevitable for structures to recieve damages, even though they are designed to resist earthquakes following the current aseismic codes. In some cases, structural damages may be permissible unless occupants are injured or killed due to serious collapse of structures. However, it is quite difficult to estimate the extent of structural damages caused by random ground motion of strong earthquakes. Main reasons of the difficulty are 1) there are no effective parameters by which the degree of structural damages can be measured simply, 2) probabilistic approach can not be easily applied to nonlinear response of structures.

Plastic deformation discussed in the previous chapter could be considered as one of the important parameters which represent the degree of structural damages due to random ground motion. When plastic deformation caused by earthquakes is small, structures can be repaired for further use. However when it is large, structures are collapsed or they can not be used anymore. In these cases, structures should be demolished. Hence probabilistic estimation of plastic deformation is expected to give crucial informations on the reliability of structures especially in the plastic range.

As discussed in Chapter 2, most studies on plastic deformation have dealt only with numerically simulated values[1]. In these studies, probabilistic approach needs large amount of calculated results and theoretical prediction of plastic deformation is almost impossible. D.Karnopp and T.D.Scharton[2] proposed the linearization technique to predict the plastic deformation of elasto-plastic structures. This technique is adopted by E.H.Vanmarke[3] and D.Veneziano[4] for estimation of probabilistic seismic response of simple inelastic systems with the effect of gravity. Although the linearization technique is

promissing for probabilistic discussions of plastic deformation, accuracy of basic assumptions has not been investigated.

In this chapter, an improved linearization technique is proposed to predict the accumulated plastic deformation in random response of the elasto-plastic structures. The structures are modeled by single-degree-of-freedom (simple) oscillators in which plastic drifting occurs only in one direction. The accumulated plastic deformation of this model can easily be found proportional to the total energy dissipated by conventional elasto-plastic hysteresis loops. Hence it is expected that prediction of the accumulated plastic deformation would give significant information to measure the degree of structural damages due to strong earthquakes.

In the section of 3-2, analytical methods are developed for probabilistic estimation of plastic deformation. Firstly, plastic deformation for each yielding is predicted from the velocity at the yielding point neglecting the effects of external force during plastic drifting. Then the lienarization technique is adopted for probabilistic prediction of the accumulated plastic deformation which is computed from the expected values of number of upward crossing of the yielding level and of relative velocity at the level. The proposed analytical method which estimates the equivalent damping factor due to plastic drifting is expected to improve the equivalent linear response for accurate prediction. In the section of 3-3, numerical simulations are performed on a digital computer to check the accuracy of theoretical methods of prediction. Random response of the proposed model subjected to recorded seismogram and also to artificially generated white noise accelerogram is numerically calculated by the Runge-Kutta methods. Basic assumptions involved in the theoretical analyses are examined from the comparison of simulated and predicted results.

3-2 Analytical Method to Predict Plastic Deformation

3-2-1 One-Way Yielding Elasto-Plastic Force-Deflection Relation

Force-deflection relations of structures during strong earthquakes would have different hysteresis loops when they respond over the yielding limit. These relations have been represented by various types or shapes of hysteretic models such as bilinear, trilinear[5], curved loops[6] and so on as stated on the previous chapters. Each of them is an ideal model for the dynamic property of structural element derived from empirical studies. Among them, bilinear hysteretic model has been used most commonly for earthquake response analyses. The way of representation of this model is very simple, although different shapes of hysteretic restoring force; linear elastic, bilinear and perfect elasto-plastic loops can be represented.

In this chapter, the perfect elasto-plastic hysteresis loop in which yielding occurs toward only one direction is adopted to investigate the accumulation of plastic deformation which is proportional to the dissipated energy due to conventional elasto-plastic hysteresis loops in random response. The model shown in Fig.3.1 indicates that the plastic deformation after the yielding (A-B and B-C in the figure) is irreversible and the linear fluctuation within the elastic region (A-A', B-B', C-C' in the figure) is reversible. x, $f(x)$, x_y and F_y denote relative displacement, restoring force, yielding displacement and yielding force, respectively. This type of monotonous accumulation of plastic deformation is noticed when the yielding structures with strong nonlinearity receive the effect of the gravity and collapse occurs towards the only one direction[7].

Let structures be expressed by simple nonlinear oscillators with mass of M and viscous damping coefficient C. Then the equation of motion of the oscillator subjected to ground acceleration of $\ddot{Z}(t)$ becomes as

$$M\ddot{x}(t)+C\dot{x}(t)+f(x(t)) = -M\ddot{Z}(t) \qquad (3\text{-}1)$$

The above equation will be reduced to the following form with ductility

factor μ, damping ratio h_o, natural frequency ω_o in the elastic region, and intensity parameter of excitation r_s, as

$$\ddot{\mu}(t)+2h_o\omega_o\dot{\mu}(t)+\omega_o^2 q(\mu(t)) = -r_s\ddot{Z}(t) \tag{3-2}$$

where

$$\left.\begin{aligned} \mu(t) &= x(t)/x_y, \qquad \omega_o = \sqrt{F_y/M} \\ h_o &= C/(2\sqrt{F_y M}), \qquad r_s = 1/x_y \end{aligned}\right\} \tag{3-3}$$

$q(\mu)$ is the dimensionless force and ductility factor relation shown in Fig.3.2.

3-2-2 Prediction of Plastic Deformation from the Velocity at the Yielding Point

Suppose that response of a structure with a unit mass has reached to the yielding point A shown in Fig.3.2 with the relative velocity $\dot{\mu}_y$, then the total energy at this point will be evaluated from the sum of the potential energy $P_a(E)$ and the kinetic enrgy $K_a(E)$ which is calculated from the velocity at the point A as

$$K_a(E) = \dot{\mu}_y^2/2 \tag{3-4}$$

During the plastic drifting from A to B in Fig.3.2, the kinetic energy $K_a(E)$ will be dissipated and relative velocity $\dot{\mu}$ will become zero at the point B. If it is possible to ignore the effect of external force to the energy balance between points A and B, next relation will be reduced.

$$P_a(E) + K_a(E) = P_b(E) + D_b(E) \tag{3-5}$$

D_b in the above equation is the dissipated energy due to plastic drifting and it is obtained from the hatched area shown in Fig.3.2. $P_b(E)$ is the potential energy at the point B which is equal to $P_a(E)$ in this study. Hence following simple relations are brought out.

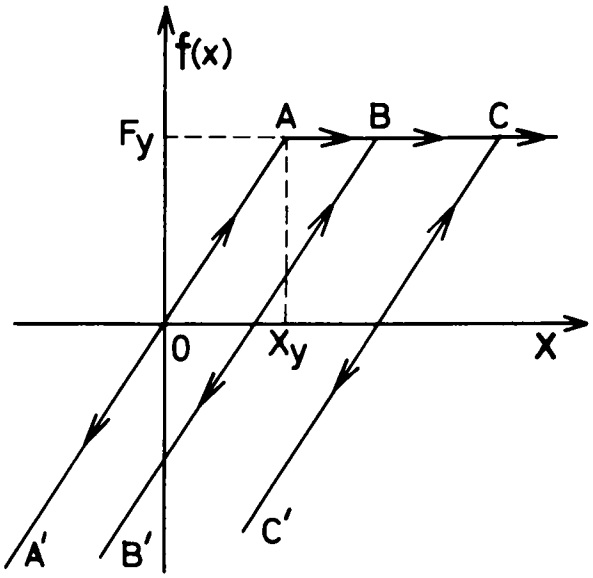

Fig.3.1 One Way Yielding Elasto-Plastic Force-Deflection Relation

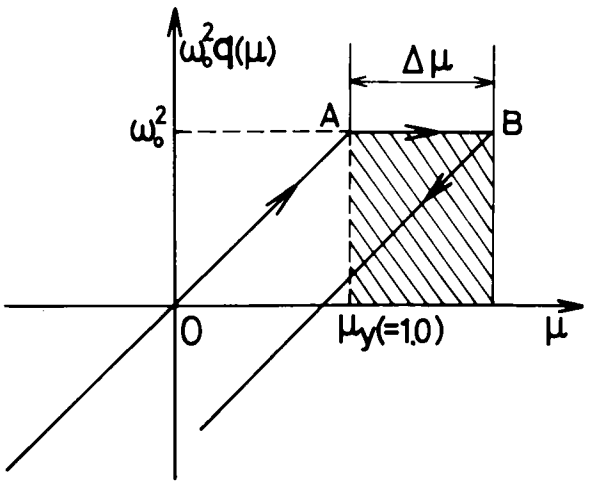

Fig.3.2 Plastic Deformation in Ductility Factor and the Dissipated Energy

$$K_a(E) = D_b(E) \ , \quad D_b(E) = \omega_o^2 \Delta\mu \tag{3-6}$$

Using Eqs.(3-4) and (3-6), the plastic deformation $\Delta\mu$ is estimated from the velocity at the yielding point as

$$\Delta\mu = \dot{\mu}_y^2/(2\omega_o^2) \tag{3-7}$$

The time interval Δt during the plastic drifting from the point A→B, is evaluated by solving the next equation of motion

$$\ddot{\mu}(t) + \omega_o^2 = 0 \tag{3-8}$$

under the initial conditions of

$$\mu(t) = \mu_y = 1.0 \quad \text{and} \quad \dot{\mu}(t) = \dot{\mu}_y \quad \text{at} \quad t=0 \tag{3-9}$$

At the point B, relative velocity $\dot{\mu}$ is zero, then

$$\Delta t = \dot{\mu}_y/\omega_o^2 \tag{3-10}$$

The result of Eq.(3-7) can also be obtained from the solution of Eq.(3-8). The relation between Δt and $\Delta\mu$ ($\Delta\mu=\omega_o^2\Delta t^2/2$) is plotted in Fig.3-3. It is seen that the plastic deformation is proportional to the square of the time interval of plastic drifting and also to the square of the natural frequency of the model in the linear oscillation.

Above discussions are brought out without considering the effects of external force. When input acceleration $r_s\ddot{Z}(t)$ is considered, Eq.(3-8) becomes as

$$\ddot{\mu}(t) + \omega_o^2 = -r_s\ddot{Z}(t) \tag{3-11}$$

The solution of the above equation is obtained by the sum of the free vibration $\mu_f(t)$ due to the initial conditions and the forced vibration due to the external force as

$$\mu(t) = \mu_f(t) + r_s\int_0^t h(t-t')\ddot{Z}(t')dt' \tag{3-12}$$

where $h(t)$ is the unit impulse response function of Eq.(3-11). For discussions of Eq.(3-12) in the sense of an average of random response, let's take the ensemble average of the equation; i.e.,

$$\begin{aligned} E[\mu(t)] &= E[\mu_f(t)] + E[r_s \int_0^t h(t-t')\ddot{Z}(t')dt'] \\ &= E[\mu_f(t)] + r_s \int_0^t h(t-t')E[\ddot{Z}(t')]dt' \end{aligned} \tag{3-13}$$

Since ensemble average of random external force like earthquake ground motion is usually zero, the effect of the external force in Eq.(3-13) can be neglected. Therefore, the plastic deformation can be evaluated from Eq.(3-7) in the sense of an average of random samples. The accuracy of the method discussed in this section to measure the plastic deformation will be examined through simulation in the next section.

3-2-3 Prediction of Accumulated Plastic Deformation through the Linearization Technique

From the technique shown in the previous term, the expected amount of plastic deformation can be predicted from the expected value of the mean-square of the relative velocity at the yielding point. However, it is still quite difficult to estimate the expected mean-square of relative velocity response of structures with one-way yielding perfect elasto-plastic restoring force. An approximate linearization technique is introduced in this term to make the linear random vibration theory applicable for statistical estimation of nonlinear response.

The time history of ductility factor response of a structure with the one-way yielding restoring force shown in Fig.3.1 exhibits one-way drifting as schematically illustrated in Fig.3.4 (a). Subtraction of the plastic deformation from the time history gives the portion of response only in the linear range as seen in Fig.3.4 (b). In this figure, ductility factor response has no specified value during the time interval of plastic drifting. Connection of the portaions of linear response eliminating the small portion of plastic drifting brings the semi-linear response shown in Fig.3.4 (c). If it is possible to apply linear vibra-

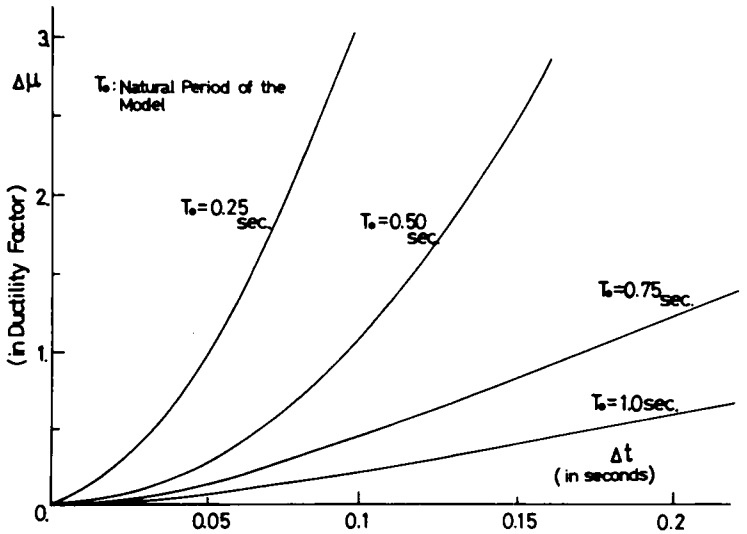

Fig.3.3 Theoretical Relation between Plastic Deformation $\Delta\mu$ and Time Interval Δt

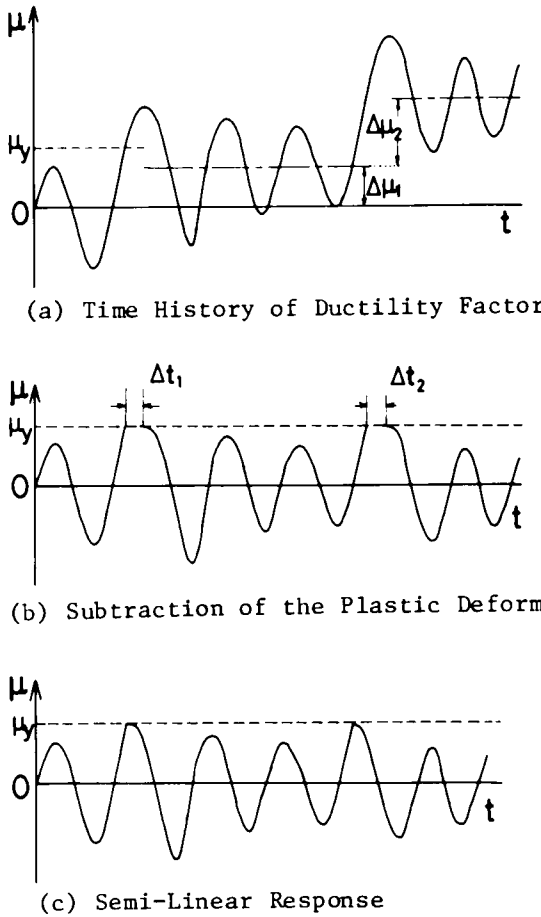

(a) Time History of Ductility Factor

(b) Subtraction of the Plastic Deformation

(c) Semi-Linear Response

Fig.3.4 Construction of Semi-Linear Response

tion theory to the semi-linear response, expected value of the accumulated plastic deformation which is proportional to the total energy dissipated by conventional elasto-plastic hysteresis loops can be evaluated from product of the expected number of upward crossing of the yielding level and the expected plastic deformation per yielding.

Firstly, it is assumed that the semi-linear response is at the stationary state subjected to stationary white noise excitation of which power spectrum intensity is D. The intensity parameter of excitation r_s is proportional to root of D. From the stationality of the response, Gaussian probability density function $p(\mu,\dot{\mu})$ has no correlation between displacement μ and velocity $\dot{\mu}$; i.e.,

$$p(\mu,\dot{\mu}) = 1/(2\pi\sigma_\mu\sigma_{\dot{\mu}})\exp\{-\mu^2/(2\sigma_\mu^2)-\dot{\mu}^2/(2\sigma_{\dot{\mu}}^2)\} \tag{3-14}$$

where σ_μ and $\sigma_{\dot{\mu}}$ are the r.m.s. response of ductility factor μ and velocity $\dot{\mu}$. These values are obtained from integration of power spectrum density of the response over all frequency range as

$$\left.\begin{aligned}\sigma_\mu^2 &= \int_{-\infty}^{\infty} D/\{(\omega^2-\omega^2)^2+4h_o^2\omega_o^2\omega^2\}d\omega = \pi D/(2h_o\omega_o^3)\\ \sigma_{\dot{\mu}}^2 &= \int_{-\infty}^{\infty} D\omega^2/\{(\omega^2-\omega_o^2)^2+4h_o^2\omega_o^2\omega^2\}d\omega = \pi D/(2h_o\omega_o)\end{aligned}\right\} \tag{3-15}$$

in which h_o is the damping factor of the semi-linear system.

Using the probability density function $p(\mu,\dot{\mu})$ of the semi-linear response, the expected number ν of upward crossing of the yielding level $\mu=\mu_y=1.0$ in a unit time is calculated as[8)]

$$\nu = \int_0^{\infty}\dot{\mu}p(\mu_y,\dot{\mu})d\dot{\mu} = \sigma_{\dot{\mu}}/(2\pi\sigma_\mu)\exp\{-\mu_y/(2\sigma_\mu^2)\} \tag{3-16}$$

Hence, the expected total number $E[N]$ of the upward crossing during time interval of T is written as

$$E[N] = \nu T \tag{3-17}$$

Taking the ensemble average of Eq.(3-7), the expected value of plastic

deformation per yeilding is estimated from the following relation

$$E[\Delta\mu] = E[\dot{\mu}_y^2]/(2\omega_o^2) \tag{3-18}$$

The expected mean-square value $E[\dot{\mu}_y^2]$ of relative velocity at the yeilding point is derived as follows,

$$\begin{aligned} E[\dot{\mu}_y^2] &= \int_0^\infty v^2 p(\dot{\mu}=v \,|\, \mu=\mu_y)\,dv \\ &= \int_0^\infty v^2 p(\mu=\mu_y, \dot{\mu}=v)/p(\mu=\mu_y)\,dv = \sigma_{\dot{\mu}}^2/2 \end{aligned} \tag{3-19}$$

in which $p(A|B)$ represents the conditional probability density of event A on the hypothesis of event B. It is noted that $E[\dot{\mu}_y^2]$ does not depend on yielding level but only on mean-square of velocity response.

Combining the above discussed results, the accumulated plastic deformation $E[D_\mu]$ is obtained as follows.

$$E[D_\mu] = E[N]E[\Delta\mu] = T\omega_o\sigma_\mu^2/(4\pi)\exp\{-\mu_y/(2\sigma_\mu^2)\} \tag{3-20}$$

In the estimation of Eq.(3-20) so far discussed, effects of energy dissipation of plastic drifting to the semi-linear response have not been considered. So, Eq.(3-20) is expected to estimate larger accumulated plastic deformation than actual response. From this point, it is preferable to add substitute damping factor to the equivalently linearized structure.

The equivalent damping factor h_{eq} of plastic deformation can be evaluated by equating the dissipated energy due to plastic drift to that of viscous damping. The total amount of dissipated energy E_{dp} due to plastic drifting is obtained by the product of the accumulated plastic deformation and the yielding force as

$$E_{dp} = \omega_o^2 E[D_\mu] \tag{3-21}$$

It is noted that E_{dp} is exactly the same as the total energy dissipated

by conventional elasto-plastic hysteresis loops in random response. The amount of dissipated energy due to substitute damping factor h_{eq} in one cycle with response amplitude μ_o is obtained as [9]

$$\oint 2h_{eq}\omega_o\dot{\mu}d\mu = 2\pi h_{eq}\omega_o^2\mu_o^2 \tag{3-22}$$

in which $\oint d\mu$ denotes the integration over one cycle of oscillation. The probability density function of peaks μ_o of random response derived by S.O.Rice[8] is given in the form of

$$p(\mu_o) = \mu_o/\sigma_\mu^2 \exp\{-\mu^2/(2\sigma_\mu^2)\} \tag{3-23}$$

From the above two equations, the expected amount of dissipated energy due to h_{eq} in one cycle with random amplitude is computed as,

$$\int_0^\infty 2\pi h_{eq}\omega_o^2\mu_o^2 p(\mu_o)d\mu_o = 4\pi h_{eq}\omega_o^2\sigma_\mu^2 \tag{3-24}$$

Equating the total dissipated enrgy of plastic deformation during the time interval T to that of equivalent damping factor, we have

$$\omega_o^2 E[D_\mu] = 4\pi h_{eq}\omega_o^2\sigma_\mu^2 T/T_o \qquad (T_o=2\pi/\omega_o) \tag{3-25}$$

Hence, the equivalent damping factor h_{eq} is computed in the form of

$$h_{eq} = E[D_\mu]/(2\omega_o\sigma_\mu^2 T) \tag{3-26}$$

For accurate estimation of the accumulated plastic deformation, it is preferable to use the damping factor of (h_o+h_{eq}) instead of h_o in Eq. (3-15). The accuracy of the methods will be examined in the next section from comparison of predicted and simulated results.

3-3 Numerical Simulations

3-3-1 Simulation of Plastic Deformation

To check the accuracy of prediction of plastic deformation from the velocity at the yielding point neglecting the effects of external

force during plastic drifting, numerical simulation is carried out on a digital computer. Random response of the proposed model with one-way yielding elasto-plastic restoring force is numerically calculated by the Runge-Kutta method. As the input acceleration, two different types of excitation are used. One is the S69°E component of the recorded accelerogram at Taft during the Kern County California earthquake in July 21, 1952[10]. The other is the stationary white noise acceleration which is generated using the technique discussed in Chapter 2. Its duration is 54 seconds.

Predicted and simulated results of the models subjected to the recorded acceleration and the white noise acceleration are shown in Figs.3.5 and 3.6, respectively. The abscissa represents dimensionless yielding level r_y which is the ratio between yielding acceleration $\omega_o^2\mu_y(=\omega_o^2)$ and the maximum acceleration of excitation $\ddot{Z}_{max}$, i.e., $r_y = \omega_o^2/\ddot{Z}_{max}$. It is noted r_y is proportional to $1/\sqrt{D}$. The total number of plastic drifting N shown in (a) of the figures is found decreasing with the increasing yielding level. This tendency is quite clear when excitation is white noise presumably due to stationality of input acceleration. Averaged plastic deformation shown in (b) of the figures represents the mean value of plastic deformation per yielding during the course of random response. $E[\Delta\mu_s]$ is the simulated plastic deformation which is obtained from the direct integration of Eq.(3-2) with the effects of the external force. $E[\Delta\mu_p]$ is the predicted plastic deformation which is calculated from the relative velocity at the yielding point by Eq.(3-7) neglecting the effects of the external force during plastic drifting. $E[\Delta t_s]$ and $E[\Delta t_p]$ shown in (c) of the figures are the simulated and predicted mean value of time interval of plastic drifting per yielding, respectively. From these figures, no significant discrepancy is found between predicted and simulated values of plastic deformation and time interval.

In Fig.3.7, relation between the simulated plastic deformation and the time interval for each yielding is plotted. Theoretical relation

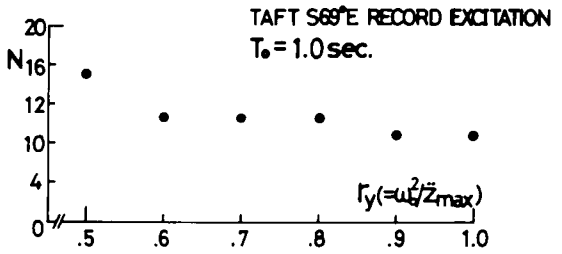

(a) Total Number of Yielding

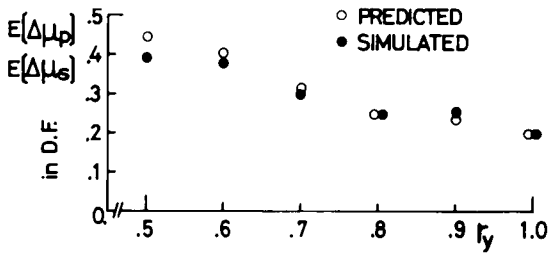

(b) Expected Plastic Deformation

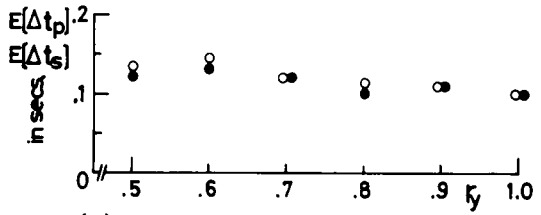

(c) Expected Time Interval

Fig.3.5 Predicted and Simulated Plastic Deformation and Time Interval per Yielding

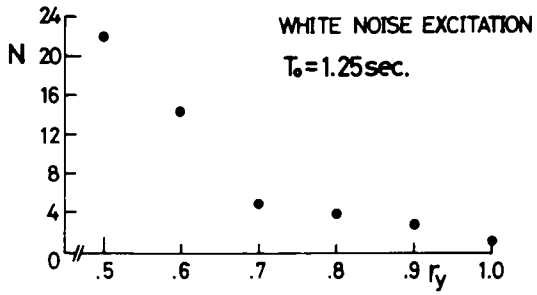

(a) Total Number of Yielding

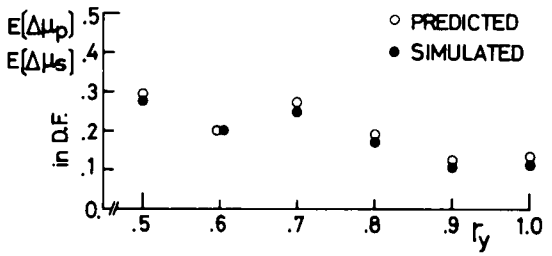

(b) Expected Plastic Deformation

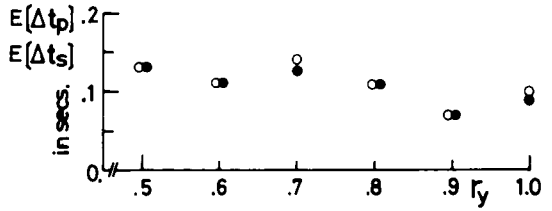

(c) Expected Time Interval

Fig.3.6 Predicted and Simulated Plastic Deformation and Time Interval per Yielding

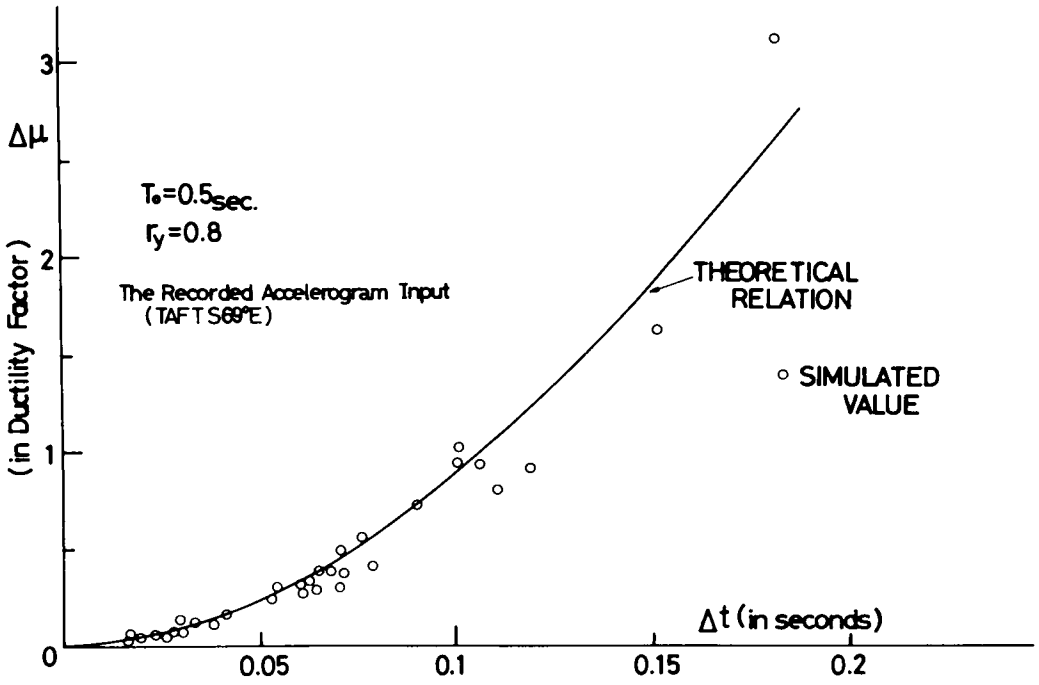

Fig. 3.7 Predicted and Simulated Relation between Plastic Deformation $\Delta\mu$ and Time Interval Δt

between $\Delta\mu$ of Eq.(3-7) and Δt of Eq.(3-10) is also plotted in this figure. Although simulated values show fluctuation along the theoretical curve recieving the effects of local external acceleration, both results agree quite well in the sense of average. From discussion in Figs.3.5~3.7, it is concluded that the effects of external force during plastic drifting can be neglected for estimation of plastic deformation in the sense of average. Hence it is concluded that the expected value of plastic deformation can be predicted fairly well from the expected value of relative velocity at the yielding point by Eq.(3-18).

3-3-2 Accuracy Evaluation of the Linearization Technique

The accuracy of the linearization technique to predict accumulated plastic deformation discussed in the previous section is also examined through numerical simulation. Firstly, construction of the semi-linear response from the time history of ductility factor response is tried.

In Fig.3.8, shown are the numerically calculated results of the model subjected to the recorded acceleration at Taft for a set of parameters, $T_o(=2\pi/\omega_o)$=1.0sec., and r_y=0.6. Response of the one-way yielding elasto-plastic restoring force plotted in figure (a) verifies that numerical simulation is well performed. It is recognized that yielding occurred 11 times during random earthquake response. The figure (b) shows the time history of plastic drifting of ductility factor response. The accumulated plastic deformation at the end of vibration is found about 3.9 in ductility factor. The semi-linear response is constructed following the process discussed in the previous section and plotted in the figure (c). It is noticed in this figure that no upward crossing of yielding level (μ_y=1.0) occurs in one direction and the duration of response is shorter than real response by about 2 seconds due to subtraction of plastic deformation. However general feature of the response seems similar to linear response, which suggests the possibility of application of equivalent linearization technique. Input acceleration during the plastic drifting is plotted in the figure (d). Although perfect symmetry is not found, no significant effects of

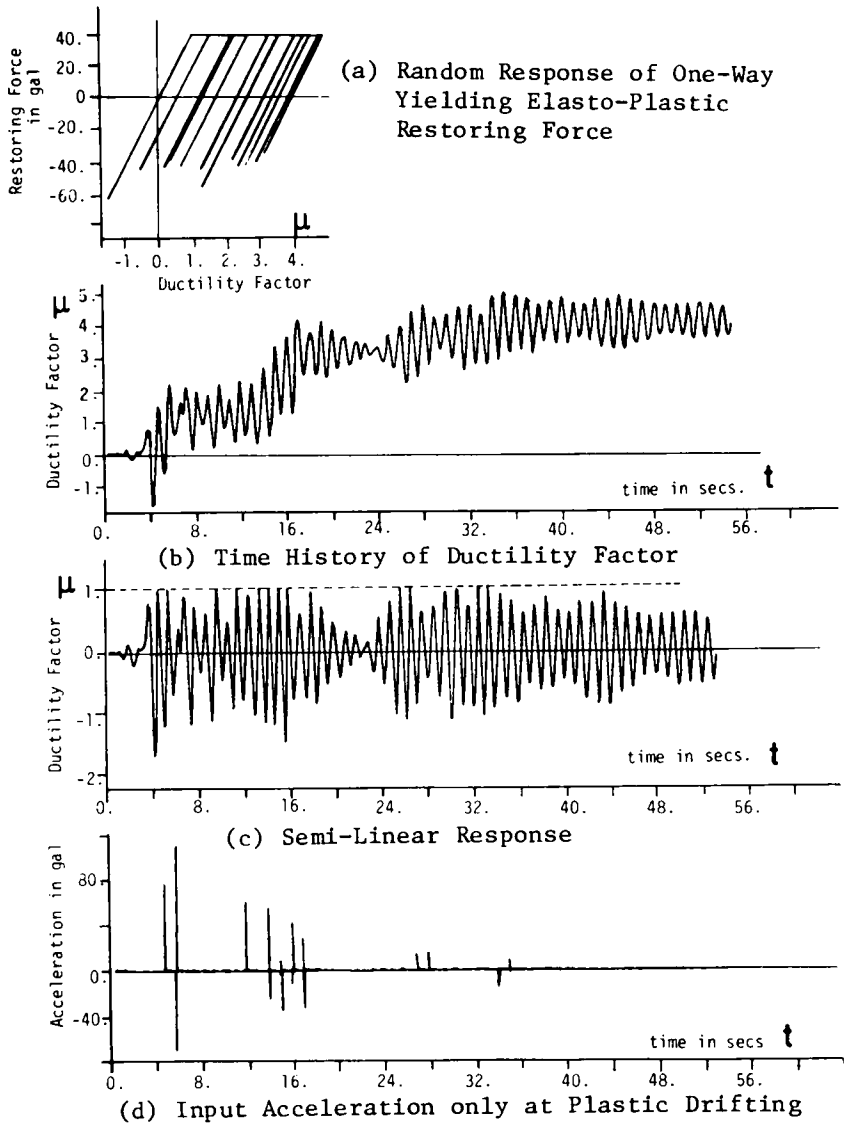

Fig.3.8 Calculated Results of the Model to the Recorded Acceleration (T_o=1.0sec., r_y=0.6)

input acceleration during plastic drifting to the accumulated plastic deformation is expected.

In Fig.3.9, similar calculated results of the model subjected to the white noise excitation are plotted for a set of parameters T_o=0.8sec., r_y=0.8. This figure also suggests the applicability of equivalent linearization technique. Especially the artificially generated white noise excitation gives more symmetric input acceleration during the plastic drifting than the recorded seismograms.

Using the linearization technique discussed in the term of 3-2-3, the accumulated plastic deformation of the model in stationary response subjected to white noise excitation is predicted for a set of parameters h_o=0.06 and T=40 seconds. Eqs.(3-17)∿(3-19) which give the expected total number E[N] of upward crossing of the yielding level and the expected mean-square of the relative velocity E[$\dot{\mu}_y^2$] are used for prediction. Both predicted and simulated results of E[N], E[$\dot{\mu}_y^2$] and the expected accumulated plastic deformation E[D_μ] are shown in Table 3-1 for different sets of natural period T_o and yielding level r_y of the model. Good agreement is found for sets of parameters T_o=1.25 and r_y=0.4, 0.5. In other cases, predicted values show larger values than simulated results. The cause of the over estimation is due to neglection of effects of energy dissipation of plastic drifting to the semi-linear response. Predicted results of E[$\dot{\mu}_y^2$] are found not depending on r_y. This is the result of Eq.(3-19) in which no correlation between μ and $\dot{\mu}$ is considered.

As discussed in the term of 3-2-3, it is preferable to adopt the damping factor of (h_o+h_{eq}) instead of h_o in Eq.(3-15) for accurate prediction. To estimate the order of h_{eq} which is due to plastic deformation, theoretically predicted and simulated results of the expected number ν of upward crossing of the yielding level in a second are plotted in Fig.3.10 for a parameter T_o=1.25sec.. Theoretical values are predicted from Eq.(3-16) in which no equivalent damping factor is considered. Hence the predicted results show a little larger value than

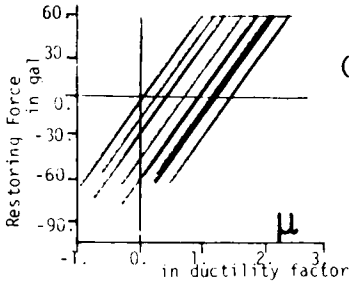

(a) Random Response of One-Way Yielding Elasto-Plastic Restoring Force

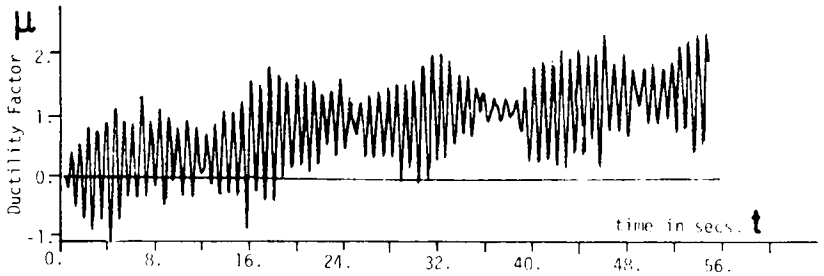

(b) Time History of Ductility Factor

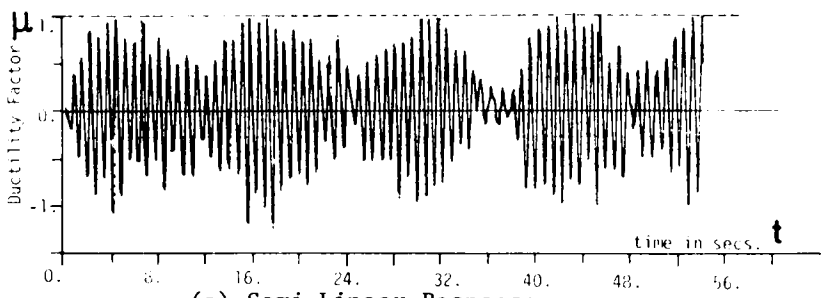

(c) Semi-Linear Response

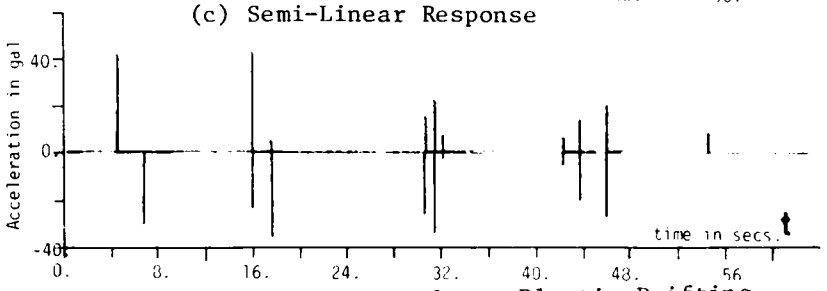

(d) Input Acceleration only at Plastic Drifting

Fig.3.9 Calculated Results of the Model to the White Noise Acceleration (T_o=0.8sec., r_y=0.8)

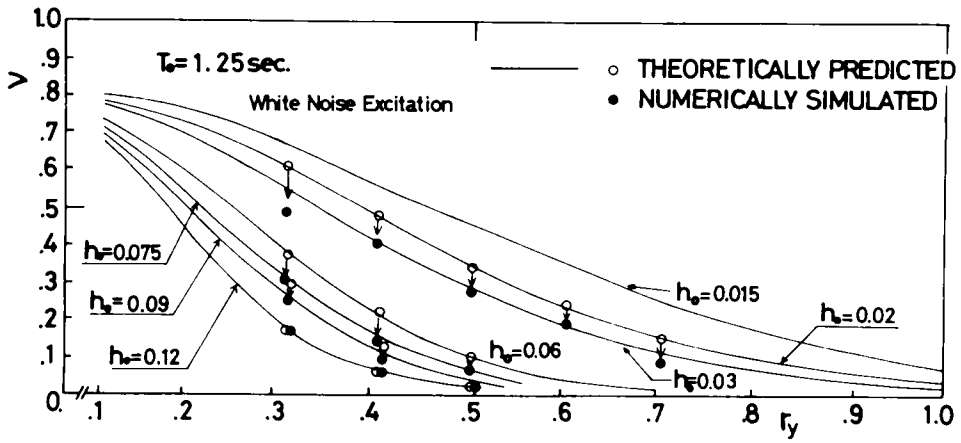

Fig. 3.10 Predicted and Simulated Expected Number of Upward Crossing of the Yielding Level per Second

Table 3.1 Predicted and Simulated Results (h_o=0.06, T=40sec.)

$T_o=\frac{2\pi}{\omega_o}$ (sec)	r_y	E[N]		E[$\dot{\mu}_y^2$]		E[D_μ]	
		Predicted	Simulated	Predicted	Simulated	Predicted	Simulated
0.50	0.4	46	25	6.62	4.08	21.34	9.96
	0.5	23	14	6.62	4.34	10.03	3.52
	0.6	14	7	6.62	3.62	4.81	0.88
1.25	0.4	8	6	16.65	18.70	1.15	1.17
	0.5	2	2	16.65	17.05	0.42	0.38
	0.6	2	1	16.65	7.68	0.12	0.03
1.50	0.3	10	4	19.87	13.98	2.77	0.84
	0.4	5	1	19.87	9.14	0.79	0.07

simulated ones when ν is greater than 0.2. In this range, additional a few percent of critical damping is expected to let the predicted results close to simulated values. When ν is less than 0.2, little discrepancy is found between predicted and simulated values. In this range, no additional damping is needed because of infrequent yielding. The order of additional damping factor found in Fig.3.10 agrees well with the equivalent damping factor given by Eq.(3-26). Therefore, it's concluded that the equivalent damping factor due to plastic drifting should be taken into account in establishing the equivalent linear response for probabilistic estimation of the accumulated plastic deformation of the proposed model in random response.

3-4 Conclusions

In this chapter, an improved linearization technique which is based on the study done by D.Karnopp and T.D.Sharton is proposed to predict the accumulated plastic deformation in random response of the one-way yielding elasto-plastic structures. It is expected that the predicted plastic deformation which is found proportional to the total energy dissipated by the conventional elasto-plastic hysteresis loops would give significant information on measuring the degree of structural damages due to severe ground motions. Basic assumptions involved in the analyses are examined from the comparison between predicted results and numerically simulated values on a digital computer. Main conclusions obtained in this chapter are as follows.

(1) Plastic deformation and time interval of drifting for each yielding are predicted from the relative velocity at the yielding point neglecting the effects of external force during plastic drifting. Simulated values both to the recorded seismogram and the artificially generated white noise accelerogram are found close to predicted values to suggest applicability of the technique for estimation of accumulated plastic deformation in random response.

(2) The semi-linear response is constructed by subtracting the simulated plastic deformation from the one-way drifting ductility factor response subjected to the recorded and artificially generated accelerograms. General feature of the response is found similar to linear response, which verifies applicability of linear vibration theory to the constructed semi-linear system to calculate expected value of relative velocity at the yielding level. Although simulated input acceleration only at the time interval of plastic drifting does not show perfect summetry, no significant effects of it are noticed for estimation of expected value of plastic deformation.

(3) Accumulated plastic deformation of the model in stationary response subjected to white noise excitation is predicted from product of the expected total number $E[N]$ of upward crossing of the yielding level and the expected mean-square $E[\dot{\mu}_y^2]$ of relative velocity at the level. Predicted values of $E[N]$ and $E[\dot{\mu}_y^2]$ are found mostly larger than simulated results. The cause of the over estimation is attributable to neglection of effects of energy dissipation during plastic drifting to the constructed equivalent linear system.

(4) A theoretical method to estimate the equivalent damping factor for energy dissipation during plastic drifting is proposed to improve construction of the equivalent linear system. From comparison between predicted and simulated values of expected number of upward crossing of the yielding level in a unit time, it is concluded that adoption of the proposed equivalent damping factor improves the accuracy of prediction fairly well.

References for Chapter 3

1) For an example, S.-C. Liu: Earthquake Response Statistics of Nonlinear Systems, Proc. of ASCE, EM 2, April, 1969, pp. 397∿419.
2) D. Karnopp and T.D. Sharton: Plastic Deformation in Random Response, The Journal of ASA, Vol. 39, No. 6, 1966, pp. 1154∿1161.
3) E.H. Vanmarke and D. Veneziano: Probabilistic Seismic Response of Simple Inelastic Systems, Proc. of the fifth WCEE, Vol. 2, June, 1973, pp. 2851∿2863.
4) D. Veneziano: Analysis and Design of Hysteretic Structures for Probabilistic Seismic Resistance, Proc. of the fifth WCEE, Vol. 2, June, 1973, pp. 2839∿2850.
5) H. Umemura et al: Analysis of the Behavior of Reinforced Concrete Structures during Strong Earthquakes Based on Empirical Estimation of Inelastic Restoring Force Characteristics of Members, Proc. of the fifth WCEE, Vol. 2, 1973, pp. 2201∿2210.
6) P.C. Jennings: Periodic Response of a General Yielding Structures, Proc. of ASCE, EM 2, April, 1964, pp. 131∿166.
7) H. Goto, H. Iemura and T. Nakata: Aseismic Displacement Requirements of Highway Bridge Girder Supports, U.S.-Japan Seminar on Earthquake Engineering Research with Emphasis on Lifeline Systems, Nov., 1976, (in Press).
8) S.O. Rice: Selected Papers on Noise and Stochastic Processes, edited by N. Wax, Dover Pub., 1954, pp. 133∿294.
9) H. Goto and H. Iemura: Linearization Techniques for Earthquake Response of Simple Hysteretic Structures, Proc. of JSCE, No. 212, April, 1973, pp. 109∿119.
10) Strong-Motion Earthquake Accelerograms, Corrected Accelerograms and Integrated Ground Velocity and Displacement Curves, Vol. II , Part A EERL 71-50, Cal Tech, Sept., 1971.

4. LINEARIZATION TECHNIQUES FOR EARTHQUAKE RESPONSE OF SIMPLE HYSTERETIC STRUCTURES

4-1 General Remarks

In recent years, statistical aspects of structural vibration induced by earthquake excitation have received considerable attension of many research workers because of the randomness found in the strong motion seismograms. A majority of these statistical works has dealt only with structures with linear restoring force[1]. Response statistics of these linear structures could be estimated relatively easily through the linear random vibration theory if the statistics of random excitation are clearly defined.

To evaluate more realistic reliability of structures during strong earthquakes, however, it is considered essential to investigate statistical properties of the response of structures with hysteretic restoring force, since most of structures subjected to severe ground motion show weak or strong yielding behaviour. In spite of these inevitable necessities, it is generally quite difficult to make theoretical analyses on earthquake response statistics of hysteretic structures from the reason that the principle of linear superposition (Duhamel's Integral) cannot be applied to them.

As an exact analytical method for nonlinear response problems, we have the Fokker-Plank equation[2]. But at the present stage, it is applicable only to the stationary response of hysteretic structures subjected to white noise excitation. However it is of great importance in investigations of earthquake response to consider the frequency characteristics of excitations and the nonstationarity of structural response, because most of strong earthquake motions have the predominant frequency and structures start or vibrate from the static state. These importatnt characteristics of the excitation and of the response cannot be discussed from the solution of the Fokker-Plank equation which is now available.

On the other hand, the numerical methods such as step-by-step integration of nonlinear equations of motion on digital or analog

computers have great applicability for almost any kind of hysteresis loops and for any kind of excitations. However these methods consume a lot of time for the calculation of many samples which are needed for statistical discussions of random response of hysteretic structures. Moreover additional ruling parameters due to hysteretic characteristics of the structures should be taken into account, which makes the investigations more complex than for linear structures. Hence, accumulation of a great amount of numerical samples whch are sufficient enough to cover wide range of each parameter seems quite difficult to make general and theoretical statements about earthquake response characteristics of nonlinear hysteretic structures.

To overcome these difficulties, equivalent linearization techniques seem to be very powerful in the range of admissible error, since the results of linear random vibration theory can be available to predict the response statistics analytically.

The linearization technique for random response of simple hysteretic systems was proposed in the field of applied mechanics firstly by T.K.Caughy[3] using the method of slowly varying parameters based on the work of Kryloff and Bogoliuboff. In this technique, equivalent natural frequency and damping factor of linearized second order systems are determined so as to make the mean-square error due to linearization minimum. T.Kobori and R.Minai[4] showed the fundamental technique to estimate the nonstationary hysteretic response combining the linearization technique by T.K.Caughey[5] and the step-by-step parameter method proposed by Y.Sawaragi et al[6].

W.D.Iwan[7] and L.D.Lutes[8),9] estimated time-average statistics of the response of simple bilinear hysteretic systems to an excitation with white power spectrum density. The applicability of the Krylov and Bogoliubov method of equivalent linearization to the problem was investigated by comparing predicted and experimentally measured mean-square level of the response. H.Takemiya[10] additionally discussed the equivalent linearization by 3rd order system and tried to extend

the results on the stationary response to the case of transient response.

In the field of earthquake engineering, six conceivable equivalent linearization techniques for the steady state harmonic motion were proposed by P.C.Jennings[11] based on the works by L.S.Jacobsen[12] and T.K.Caughey[3]. In these techniques, main interest was put in the estimation of equivalent linear damping factors which show different values depending on each difinition of linearization. An energy balance method to determine the equivalent linear system in the steady state random motion was proposed by D.Karnopp and R.N.Brown[13].

Another linearization technique which lets the response spectrum of a hysteretic structure equal to that of a linearized structures was proposed by D.E.Hudson[14] to conclude that the equivalent damping factor under initial stiffness for earthquake-type excitation is about several percent of the critical.

These works of equivalent linearization contributed considerably toward general understandings of the stationary response of hysteretic structures subjected to stationary harmonic or stationary random excitations. From earthquake engineering point of view, however, more detailed investigations which represent closer conditions of real structures and excitations are strongly needed.

Among these problems, next five issues are strong concern of this chapter for intensive discussions.

1) The phisical relation between two different types of equivalent linearization techniques; one is the least mean-square error method and the other is the energy balance method.
2) Effects of non-white frequency components of random excitation and yielding level of hysteretic structures to r.m.s. response with relative to the transition of the structural receptance due to yielding.
3) Application of step-by-step linearization technique to predict nonstationary mean-square response of hysteretic structures subjected to the nonstationary excitation represented by the product of the

nonstationary envelope function and the stationary random process.

4) Probability distribution of maximum response of hysteretic structures both in stationary and nonstationary state predicted by pure-birth and envelope methods for reliability analysis of structures during strong earthquakes.

5) Monte Carlo simulations on a digital computer to calculate time and ensemble average of generated response for discussions of accuracy of theoretically predicted r.m.s. response and probability distribution of maximum response.

4-2 Equivalent Linearization Techniques

To make theoretical and general discussions about the earthquake response characteristics of nonlinear hysteretic structures, a dimensionless representation of the equation of motion is tried in Chapter 2, which leads to the following equation of motion of a single-degree-of-freedom structure with viscous damping and with arbitrary types of nonlinear hysteretic characteristics:

$$\ddot{\mu}(t) + \beta_o\dot{\mu}(t) + q(\alpha,\beta,\mu,\dot{\mu},t) = -r_s\psi(t)f(\eta,h_f,t) \qquad (4\text{-}1)$$

where $\mu(t)$: ductility factor, α and β: parameters which show characteristics of dimensionless hysteresis $q(\alpha,\beta,\mu,\dot{\mu},t)$, β_o: damping coefficient in small oscillation of yielding structures, $\cdot$: derivative by dimentionless time t, r_s: a constant showing the intensity of the excitation, $\psi(t)$: a deterministic shape function which exclusively assumes positive values, $f(\eta,h_f,t)$: a stationary non-white random process with zero mean value and the variance of unity, $\eta=\omega_f/\omega_o$ and h_f: parameters showing the characteristics of the power spectrum of $f(t)$, ω_f: predominant frequency of $f(t)$, $\omega_o(=1.0)$:natural frequency of small oscillation of yielding structure, respectively.

By using the equivalent damping coefficient β_{eq} and the equivalent natural frequency ω_{eq}, the equation of motion of the equivalent linear

structure can be written as follows:

$$\ddot{\mu}(t) + \beta_{eq}\dot{\mu}(t) + \omega_{eq}^2\mu(t) = -r_s\psi(t)f(\eta, h_f, t) \tag{4-2}$$

Concerning the techniques to determine β_{eq} and ω_{eq} both in sinusoidal and in random vibration, discussions have been made by many investigators using mainly two different types of linearization criteria; one is the least mean-square error method and the other is what we may call the energy balance method as briefly explained in the previous section. These two methods have been discussed separately and their relation with each other has never been discussed as far as the author concerned. However we shall see in the following sections that they are closely correlated to each other.

4-2-1 The Least Mean-Square Error Method

This method is based on the work of N.Wiener[15] to find the optimum linear controlling system which filters out the random noise involved in the output of the system as much as possible. The criterion which deals with mean-square values of error terms between output of the system and true signal is called the Wiener's criterion.

T.K.Caughey[3] adopted this Wiener's criterion firstly in random vibration of hysteretic systems to find equivalently linearized systems. In this method, the two equivalent linearization parameters β_{eq} and ω_{eq} of the second order linear system are determined so as to minimize the least mean-square error between Eqs.(4-1) and (4-2). The mean-square error in one cycle $(\tau, \tau+\tau_T)$ can be written as follows:

$$I(\beta_{eq}, \omega_{eq}) = \frac{1}{\tau_T}\oint_{\tau}^{\tau+\tau_T}\{\beta_o\dot{\mu}+q-\beta_{eq}\dot{\mu}-\omega_{eq}^2\mu\}^2 dt \tag{4-3}$$

Now let's minimize $I(\beta_{eq}, \omega_{eq})$ with respect to β_{eq} and ω^2_{eq}.

$$\left.\begin{aligned}\frac{\partial I}{\partial \beta_{eq}} &= \beta_o\oint\dot{\mu}^2 dt+\oint q\dot{\mu}dt-\beta_{eq}\oint\dot{\mu}^2 dt-\omega_{eq}^2\oint\mu\dot{\mu}dt = 0\\ \frac{\partial I}{\partial \omega^2_{eq}} &= \beta_o\oint\mu\dot{\mu}dt+\oint q\mu dt-\beta_{eq}\oint\mu\dot{\mu}dt-\omega_{eq}^2\oint\mu^2 dt = 0\end{aligned}\right\} \tag{4-4}$$

in which $\oint dt$ denotes the integration over one cycle of oscillation.

If the nonlinearity of the hysteresis loops is weak and the damping is slight, we can assume that the response $\mu(t)$ is a sinusoidal time function with a slowly varying random amplitude $\mu_o(t)$ and a random phase angle $\phi(t)$; i.e.,

$$\mu(t) = \mu_o(t)\cos\{\omega_{eq}t+\phi(t)\} \tag{4-5}$$

By substituting Eq.(4-5) to Eq.(4-4), we obtain equivalent linear parameters as functions of response amplitude.

$$\left.\begin{aligned} \beta_{eq}(\mu_o) &= \beta_o+\oint q\dot{\mu}dt/\oint\dot{\mu}^2dt \\ \omega_{eq}^2(\mu_o) &= \oint q\mu dt/\oint\mu^2dt \end{aligned}\right\} \tag{4-6}$$

4-2-2 Energy balance method

Energy balance method was firstly proposed in the earthquake engineering field by D.E.Hudson[14] and P.C.Jennings[11] after the preliminary work done by L.S.Jacobsen[16]. Although the definition of the equivalent damping factor by Jacobsen originated from the ratio between dissipated energy and the maximum potential energy of hysteretic structures, the energy balance between hysteretic and linearized structures is guaranteed when the potential energy is taken appropriately.

In this method, the equivalent damping coefficient is determined so as to equate the energy dissipation by the hysteresis loops to that of the linear viscous damping; i.e.,

$$\oint\{\beta_o\dot{\mu}+q\}d\mu = \oint\beta_{eq}\dot{\mu}d\mu \tag{4-7}$$

From the above equation, β_{eq} can be determined without any reference to ω_{eq}.

It is interestingly noted that various values of equivalent damping factor h_{eq} will be obtained according to conceivable definitions of ω_{eq} since

$$h_{eq} = \beta_{eq}/(2\omega_{eq}) \tag{4-8}$$

In the study of this section, it is considered reasonable to estimate ω_{eq} as the resonant frequency of hysteretic structures. In the previous study (Appendix 2-A), the resonance curve was obtained as

$$\{S(\mu_o)-\beta_o\mu_o\omega\}^2 + \{C(\mu_o)-\mu_o\omega^2\}^2 = r_s^2 \tag{4-9}$$

where

$$\left.\begin{aligned} S(\mu_o) &= \frac{1}{\pi}\int_0^{2\pi} q(\alpha,\beta,\mu_o\cos\theta)\sin\theta d\theta \\ C(\mu_o) &= \frac{1}{\pi}\int_0^{2\pi} q(\alpha,\beta,\mu_o\cos\theta)\cos\theta d\theta \end{aligned}\right\} \tag{4-10}$$

The resonant frequency is determined by letting

$$\partial\mu_o(\omega)/\partial\omega = 0 \tag{4-11}$$

From Eqs.(4-8)∿(4-11), the equivalent linearization parameters can be obtained as functions of response amplitude.

$$\left.\begin{aligned} \beta_{eq}(\mu_o) &= \beta_o + \oint q\,d\mu/\oint \dot{\mu}\,d\mu \\ \omega_{eq}^2(\mu_o) &= C(\mu_o)/\mu_o \end{aligned}\right\} \tag{4-12}$$

Under the assumption of Eq.(4-5) and considering the relation of

$$d\mu = (d\mu/dt)dt = \dot{\mu}dt \tag{4-13}$$

the results of Eqs.(4-6) and (4-12) completely coincide with each other for any types of hysteresis loops[17]. It is very interesting from the physical point of view that the quite different methods based on the different criteria of linearization conclude the same expressions of

the equivalent linear damping coefficient and natural frequency. That is to say, the equivalent linear structure determined from the least mean-square error method has the same resonant frequency and moreover dissipates the same amount of energy as that of hysteretic structures. Therefore, it may be concluded that the least mean-square error method is physically well-grounded in the sense of frequency matching and energy balance in linearizing the hysteretic structures.

As a typical example of dimensionless hysteretic characteristics[18], bilinear hysteresis loop shown in Fig.4.1 is considered in this chapter. The yielding point is defined as the point at which $\mu=q=1$. The initial stiffness before yielding is unity and the second stiffness after yielding is $(1-n)$, where n is the parameter which shows the nonlinearity of the hysteresis. So, this hysteresis shows the linear structure when $n=0$, and the perfect elasto-plastic structure when $n=1$. Then after some algebraic treatments, expressions in Eqs.(4-6) and (4-12) for the bilinear hysteresis yield

$$\left.\begin{aligned}
&\omega_{eq}^2(\mu_o) = 1 \\
&\beta_{eq}(\mu_o) = \beta_o
\end{aligned}\right\} \quad \mu_o \leq 1$$

$$\left.\begin{aligned}
&\omega_{eq}^2(\mu_o) = \frac{2n(2-\mu_o)}{\pi\mu_o^2}\sqrt{\mu_o-1} + \frac{n}{\pi}\cos^{-1}(1-2/\mu_o) + (1-n) \\
&\beta_{eq}(\mu_o) = \beta_o + \frac{4n(\mu_o-1)}{\pi\omega_{eq}(\mu_o)\mu_o^2}
\end{aligned}\right\} \quad \mu_o \geq 1 \qquad (4\text{-}14)$$

Numerical values for Eq.(4-14) are shown in Fig.4.2 for the parameters $n=0.25$, 0.50, 0.75, 1.00. The values of the equivalent damping coefficient $\beta_{eq}(\mu_o)$ and the equivalent natural frequency $\omega_{eq}(\mu_o)$ within the linear elastic region ($\mu_o \leq 1.0$) are β_{eq} and unity respectively.

When the response goes into the plastic region ($\mu_o > 1.0$), β_{eq} grows large showing its maximum value around $\mu_o = 2 \sim 4$, then decreases gradually to zero for infinite amplitude. The maximum values of β_{eq} suggest

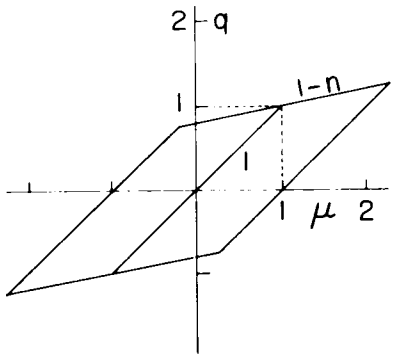

Fig.4.1 Nondimensional Representation of Bilinear Hysteresis Loop

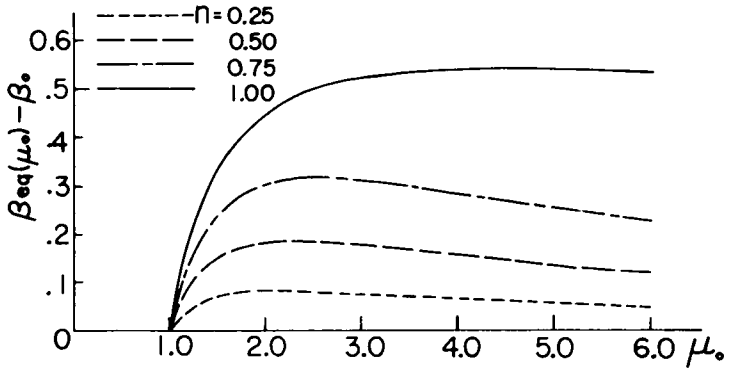

(a) Equivalent Damping Coefficient

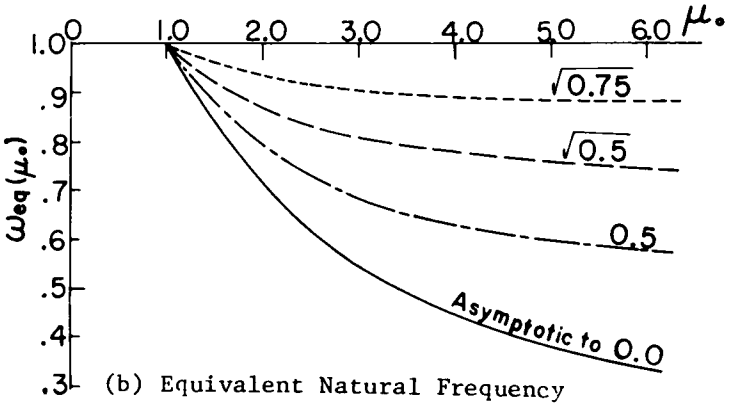

(b) Equivalent Natural Frequency

Fig.4.2 Equivalent Linear Parameters of Bilinear Hysteresis Loops

that there exists the optimum ductility factor which would suppress the response most efficiently due to the largest hysteretic energy dissipation. The larger value of the nonlinear parameter n resulted in the larger value of β_{eq}, because the area of the bilinear hysteresis loops is proportional to n as known from the next equation.

$$\oint q d\mu = 4n(\mu_o - 1) \tag{4-15}$$

The equivalent natural frequency shows smaller value with the increase of n which shows the stronger nonlinearity. The values of ω_{eq} decreases monotonously and in the limit of infinite amplitude, it is asymptotic of $\sqrt{1-n}$, since the stiffness of the bilinear hysteresis loops would become almost the same as the second spring constant $(1-n)$.

4-2-3 Equivalanet Linearization Parameters in Random Response

From the analyses in the previous section, the equivalent damping coefficient and the equivalent natural frequency are obtained as a function of slowly varying amplitude μ_o of almost sinusoidal oscillation with slowly varying phase angle. Direct application of these results to random response is impossible because of the difficulty to define the amplitude during random time history. However, if the probability density $p(\mu_o)$ of the peak amplitude μ_o in random response can be estimated, the equivalent linearization parameters in random response would be defined as their expectations using $p(\mu_o)$, following the suggestion by S.-C. Liu[19] and theoretical result by T.Kobori and R.Minai[4].

Thus in the case of stationary random response, the equivalent linearization parameters will be defined as a function of standard deviation σ_μ of ductility response μ in the following form;

$$\left.\begin{aligned} \omega_{eq}^2(\sigma_\mu) &= \int_0^\infty \omega_{eq}^2(\mu_o) p(\mu_o, \sigma_\mu) d\mu_o \\ \beta_{eq}(\sigma_\mu) &= \int_0^\infty \beta_{eq}(\mu_o) p(\mu_o\ \sigma_\mu) d\mu_o \end{aligned}\right\} \tag{4-16}$$

in which the probability density of μ_o has been obtained by S.O.Rice[21] for

narrow band response as

$$p(\mu_o,\sigma_\mu) = (\mu_o/\sigma_\mu^2)\exp\{-\mu^2/(2\sigma_\mu^2)\} \tag{4-17}$$

The values of $\beta_{eq}(\sigma_\mu)$ and $\omega_{eq}(\sigma_\mu)$ have been calculated from Eqs. (4-14), (4-16), (4-17) and plotted in Fig.4.3 with the experimental results by L.D.Lutes[9]. The experimental values of equivalent linear parameters were determined by applying linear theory to the experimentally simulated response of bilinear systems subjected to white noise excitation on an analog computer.

For the moderately nonlinear hysteresis loop (n=1/2), $\beta_{eq}(\sigma_\mu)$ and $\omega_{eq}(\sigma_\mu)$ predicted theoretically in this section show close to these of experimental results. This agreement suggests that random response of the bilinear hysteretic structures with moderate nonlinearity (n=1/2) could reasonably be predicted without large errors, using equivalent linear parameters above mentioned.

The discrepancy between theoretically predicted and experimentally determined equivalent linear parameters of strong nonlinear hysteresis loop (n=20/21) suggests that applicability of the techniques used herein is limitted only for structures with moderate nonlinearity.

In the case of nonstationary random response, the probability density of peak amplitude $p(\mu_o,\sigma_\mu,\rho_{\mu\dot{\mu}},\sigma_{\dot{\mu}})$ which was obtained by T.Kobori and R.Minai[4] as a function of standard deviation of μ and $\dot{\mu}$ and the correlation coefficient between them $\rho_{\mu\dot{\mu}}$ shall be used. Then we obtain

$$\left.\begin{aligned}\beta_{eq}(\sigma_\mu,\rho_{\mu\dot{\mu}},\sigma_{\dot{\mu}}) &= \int_0^\infty \beta_{eq}(\mu_o)p(\mu_o,\sigma_\mu,\rho_{\mu\dot{\mu}},\sigma_{\dot{\mu}})d\mu_o \\ \omega_{eq}^2(\sigma_\mu,\rho_{\mu\dot{\mu}},\sigma_{\dot{\mu}}) &= \int_0^\infty \omega_{eq}^2(\mu_o)p(\mu_o,\sigma_\mu,\rho_{\mu\dot{\mu}},\sigma_{\dot{\mu}})d\mu_o\end{aligned}\right\} \tag{4-18}$$

where

$$\left.\begin{aligned}p(\mu_o,\sigma_\mu,\rho_{\mu\dot{\mu}},\sigma_{\dot{\mu}}) = \exp(-\frac{\mu_o}{2\sigma_\mu^2})[&\frac{\mu_o}{\sigma_\mu^2}\exp\{-\frac{\rho\mu_o^2}{2(1-\rho^2)\sigma_\mu^2}\} \\ &+ \frac{\rho}{\sqrt{1-\rho^2}}\sqrt{\frac{\pi}{2\sigma_\mu^2}}(\frac{\mu_o^2}{\sigma_\mu^2}-1)\mathrm{erf}\{\frac{\rho\mu_o^2}{\sqrt{2(1-\rho^2)}\sigma_\mu^2}\}]\end{aligned}\right\} \tag{4-19}$$

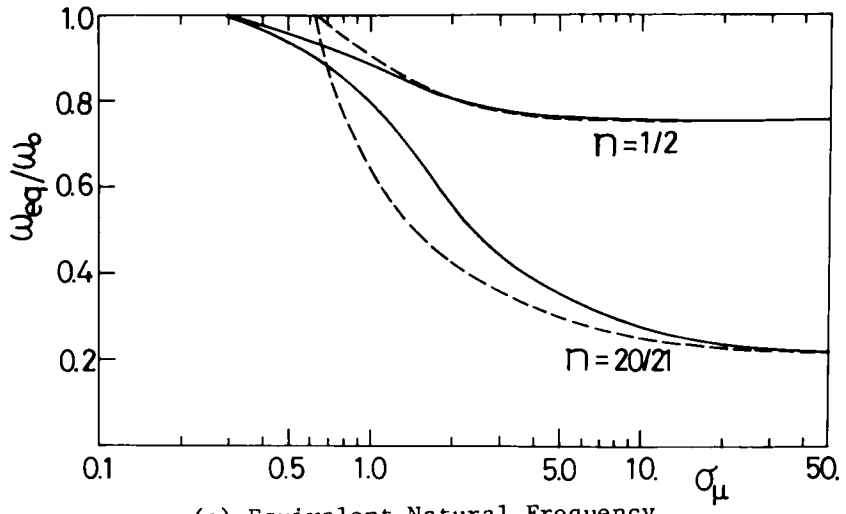

(a) Equivalent Natural Frequency

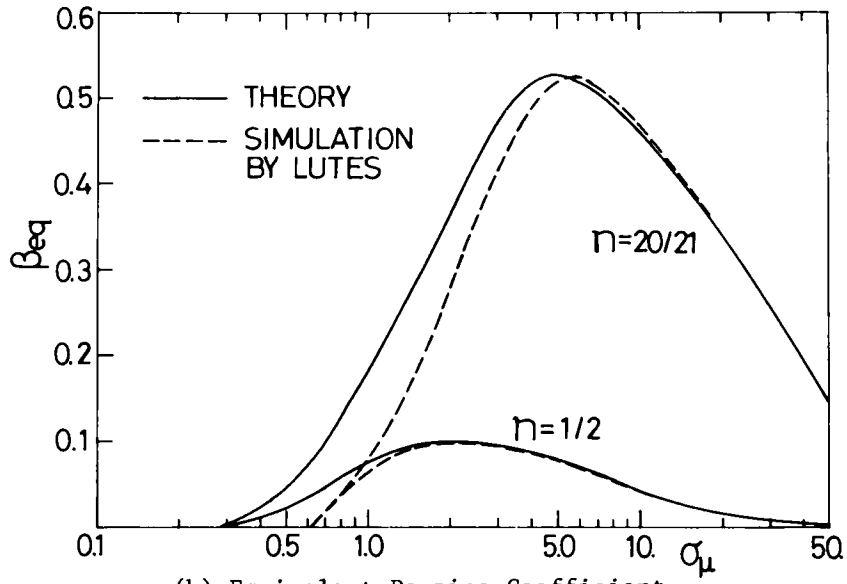

(b) Equivalent Damping Coefficient

Fig.4.3 Equivalent Linear Parameters of Bilinear Structures in Random Response

$$\rho = \rho_{\mu\dot{\mu}} = \sigma_{\mu\dot{\mu}}/(\sigma_{\mu}\sigma_{\dot{\mu}}) \qquad \Big|$$

4-3 Stationary Response

4-3-1 Iterative Method for Stationary Response

In this section, stationary response of structures with bilinear hysteresis loops subjected to stationary random excitation $r_s f(t)$ which has the predominant frequency ω_f will be investigated by both analytical and experimental methods[21].

In the previous section, equivalent linearization parameters have been determined analytically as a function of the r.m.s. value of random response. But stationary r.m.s. response to be predicted is still unknown. From the experimental methods such as numerical simulations on digital or analog computers, we would be able to obtain it for specified cases like the simulation performed by W.D.Iwan and L.D.Lutes[7]. Analytical methods to predict the response of hysteretic structures are considered to be much more important not only to make discussions about the random response of these structures theoretical and therefore general but also for practical purposes to estimate accurate structural reliability during strong earthquakes.

When the power spectrum density of excitation is constant (white noise excitation) as,

$$S_f(\omega) = K \qquad (4\text{-}20)$$

the mean-square value of ductility response of equivalent linear structures with parameters of ω_{eq} and β_{eq} will be obtained after residue integral as

$$\sigma_\mu^2 = \frac{1}{\pi}\int_0^\infty K|H(\omega_{eq},\omega_{eq})|^2 d\omega = \frac{K}{\pi}\int_0^\infty \frac{d\omega}{(\omega_{eq}^2-\omega^2)^2+(\beta_{eq}\omega)^2} = \frac{K}{\beta_{eq}\omega_{eq}^2} \qquad (4\text{-}21)$$

From Eqs.(4-16) and (4-17), β_{eq} and ω_{eq} have been determined as functions of σ_μ. Hence we now have three equations which are sufficient enough to solve three unknowns β_{eq}, ω_{eq} and σ_μ.

Menwhile it is desirable in earthquake response analyses to consider the frequency characteristics of the excitation because of following two reasons: 1) Most of recorded seismograms have their predominant frequency reflecting local ground conditions. 2) Effects of natural frequency of hysteretic structures with relative to the predominant frequency of excitation were found significant in the Chapter 2.

In the study of this chapter, therefore, we take the stationary excitation of $f(t)$ of which power spectrum density shall be represented in the following form analogous to the receptance of the relative velocity of a simple linear structure against acceleration excitation.

$$S_f(\omega) = \frac{4h_f}{\pi\omega_f}\frac{(\omega/\omega_f)^2}{\{1-(\omega/\omega_f)^2\}^2 + 4h_f^2(\omega/\omega_f)^2} \qquad (4\text{-}22)$$

in which h_f is the damping factor and ω_f is the natural frequency of a simple system. It is readily verified that Eq.(4-22) satisfies the condition that $f(t)$ should have the variance of unity.

The stationary mean-square response of the equivalent linear structure with parameters of β_{eq} and ω_{eq} subjected to the excitation of $r_s f(t)$ can easily be estimated by using the random vibration theory for linear structures as

$$\sigma_\mu^2 = \frac{1}{\pi}\int_0^\infty S_f(\omega)|H(\omega)|^2 d\omega = \frac{1}{\pi}\int_0^\infty \frac{r_s^2 S_f(\omega)(\omega_f/\eta)^4}{(\omega_{eq}^2-\omega^2)^2+(\beta_{eq}\omega)^2} d\omega \qquad (4\text{-}23)$$

Hence, the following three relations are obtained so far for the estimation of stationary random response of hysteretic structures including Eq.(4-16).

$$\left.\begin{aligned} \beta_{eq} &= \text{func}(\sigma_\mu, n, \beta_o) \\ \omega_{eq} &= \text{func}(\sigma_\mu, n, \beta_o) \\ \sigma_\mu &= \text{func}(\beta_{eq}, \omega_{eq}, \eta, r_s, h_f) \end{aligned}\right\} \qquad (4\text{-}24)$$

Using these three relations, equivalent linear parameters β_{eq} and ω_{eq} would be determined as those of the optimum equivalent linear structure corresponding to the hysteretic structure and the r.m.s. response σ_μ of it would also be predicted. However it is quite hard to solve the relations in Eq.(4-24) explicitly. Therefore, an iterative method on a digital computer was used to find the numerical result of Eq.(4-24). In this method we first estimate the r.m.s. response of the linear structure with ω_o and β_o which correspond to the initial dynamic parameters of the hysteretic structure, then we obtain the equivalent linear parameters ω_{eq} and β_{eq} for the first approximation from Eq.(4-16) based on the r.m.s. response just obtained. By substituting these parameters into Eq.(4-23), we have the r.m.s. response σ_μ. Repeating this iterative method, the response approaches to a constant value to fix the optimum equivalent linear structure and its response.

4-3-2 Calculated Results

(i) Frequency Characteristics of Hysteretic Response

The numerical results for the stationary r.m.s. response of structures with bilinear hysteresis loops and corresponding equivalent linear parameters are shown in Fig.4.4 for the set of parameters r_s=0.5, β_o=0.1, n=0.00, 0.25, 0.50, 0.75.

In Fig.4.4 (a), it is apparent that the peaks of r.m.s. response curves of hysteretic structures are suppressed and shifted to the lower frequency range with relative to that of linear structures. This tendency becomes more prominent for larger value of n presumably because of stronger nonlinearity and larger area of hysteresis loop. It will be found from close-up observation that the r.m.s. response of the bilinear

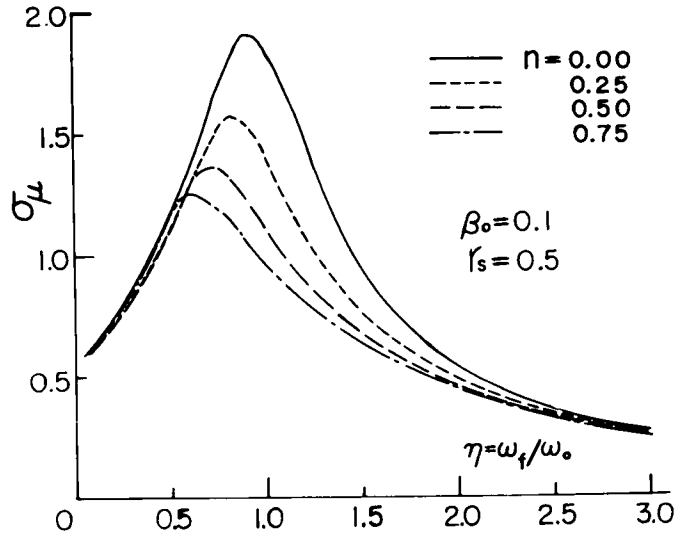

(a) R.M.S. of Ductility Factor Response

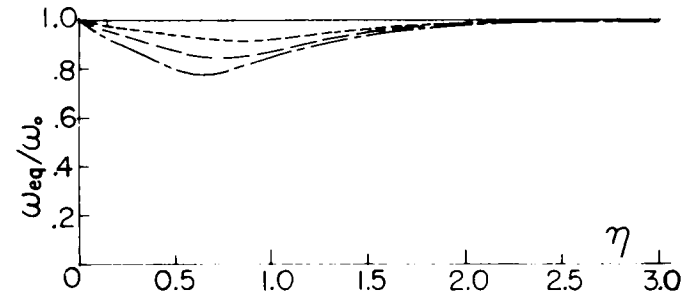

(b) Ratio of the Equivalent Natural Frequency

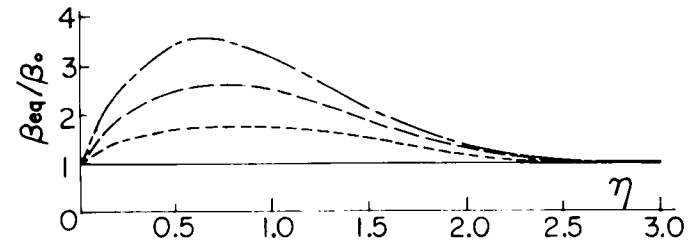

(c) Ratio of the Equivalent Damping Coefficient

Fig.4.4 Stationary Response of Structures with Bilinear Hysteresis Loops

structure with a stronger nonlinearity of hysteresis loop in the frequency range from $\eta=\omega_f/\omega_o=0.75$ to 3.0 is comparatively less than that of linear structure ($n=0.00$) of which structural parameters are $\omega_{eq}=\omega_o$ and $\beta_{eq}=\beta_o$. On the contrary, in the frequency range of $\eta\leq 0.75$, the r.m.s. response is not necessarily smaller than that of the linear structure.

To discuss these response characteristics of hysteretic structures in terms of equivalent linear parameters, the variation of ω_{eq} and β_{eq} which are shown in Fig.4.4 (b) and (c) should be investigated. The equivalent natural frequency ω_{eq} is always less than ω_o because of the softening type spring constant characteristics, and for the bigger n, ω_{eq} shows the less value. The equivalent damping coefficient β_{eq} is necessarily greater than β_o in consequence of hysteretic energy dissipation. It increases with increasing n.

The effects of such properties of ω_{eq} and β_{eq} to the stationary r.m.s. response σ_μ would reasonably be explained from the concept of the transition of the receptance of the structure due to its hysteretic properties schematically illustrated in Fig.4.5 in terms of the spectrum coordinate. That is to say, as the structure softens due to yielding behaviour and consequently ω_{eq} decreases, the receptance of a "relatively rigid" structure ($\eta=0.5$; $\omega_o>\omega_f$) moves closer to the peak of the spectrum of the excitation and tends to increase the response. On the contrary, such shift of the receptance tends to suppress the response of a "relatively soft" structure ($\eta=2.0$; $\omega_o<\omega_f$). Meanwhile, the increase of β_{eq} due to hysteretic energy dissipation reduces the peak of the structural receptance in Fig.4.5 to limit the response over the whole frequency range. The compound effects of ω_{eq} and β_{eq} above explained result in the r.m.s. response shown in Fig.4.4 (a).

(ii) Yielding Level Characteristics of Hysteretic Response

Another significant characteristic of hysteretic response is that the gain of structures (the normalized response amplitude by the measure of the input amplitude) changes when the excitation level grows higher. The existence of the optimum yielding level which lets the gain of

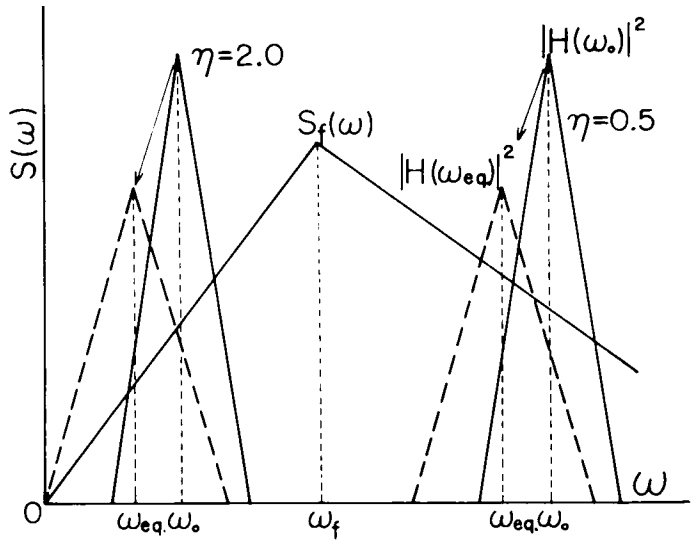

Fig.4.5 Transition of the Receptance due to Nonlinearity and Hysteresis

hysteretic structures minimum was found by J.Penzien and T.Odaka el al for sinusoidal or earthquake-type excitations as discussed in Chapter 1.

The same characteristic was also pointed out by W.D.Iwan and L.D.Lutes[7] for the case of random white noise excitation. However, as stated in the former part of this section, frequency shift of the receptance of a hysteretic structure has the remarkable effects on its random response, especially when the excitation has the predominant frequency. So in the latter part of this section, the yielding level characteristics of hysteretic structures subjected to the non-white random excitation are investigated through the iterative linearization technique.

In Figs.4.6∿4.8, shown are the r.m.s. response of bilinear hysteretic structures normalized by the r.m.s. response of linear structures in ductility factor and corresponding equivalent linear parameters against the r.m.s. response of linear structures for the sets of parameters; n=0.25, 0.75, η=0.5, 1.0, 2.0, h_f=0.9, β_o=0.2.

Predicted response of "relatively rigid" (η=0.5) hysteretic structures is shown in Fig.4.6. The normalized r.m.s. response of n=0.75 shows its minimum value when the linear r.m.s. response σ_l is about 1.0 in ductility factor. When the excitation level becomes higher (,which has the same effects as when the yielding level becomes lower), the hysteretic r.m.s. response is found much bigger than the linear r.m.s. response.

This yielding (excitation) level characteristics of "relatively rigid" hysteretic structures could also be explained reasonably through the concept of the transition of the structural receptance. For relatively high yielding level (σ_l<2.0), the shift of the equivalent natural frequency is small although the equivalent damping coefficient approaches to its maximum value as can be seen in Fig.4.6 (c). In this range, therefore, the energy absorption due to hysteresis loops lets the hysteretic response less than the corresponding linear response. On the contrary, for lower yielding level (σ_l>2.0), the shift of the natural frequency becomes large and the equivalent damping coefficient decreases gradually to its original

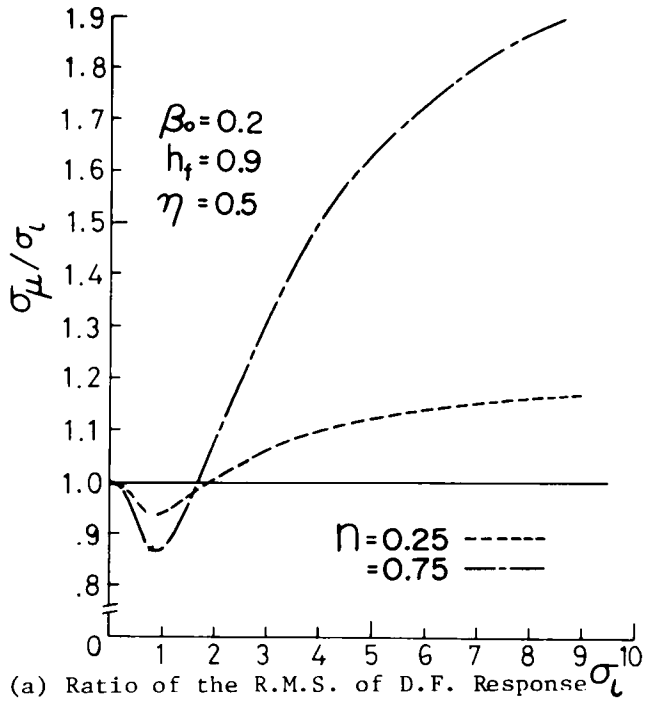

(a) Ratio of the R.M.S. of D.F. Response

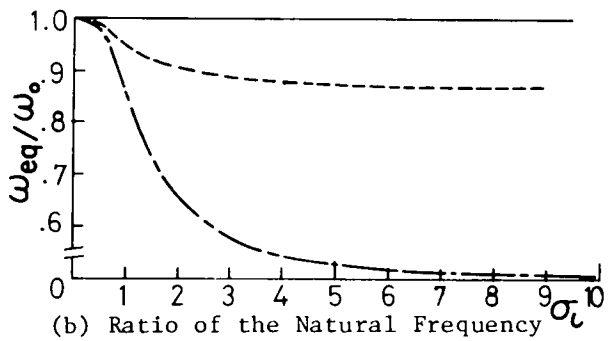

(b) Ratio of the Natural Frequency

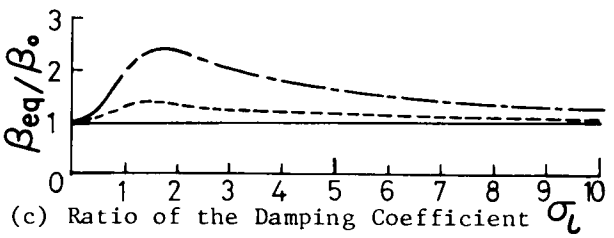

(c) Ratio of the Damping Coefficient

Fig.4.6 Effects of Yielding Level to Stationary R.M.S. Response of "Relativley Rigid" Bilinear Structures

value. Especially for n=0.75 in Fig.4.6 (b), ω_{eq} approaches to the half of ω_o to let the peak of the receptance close to the peak of the spectrum of the excitation. Then the hysteretic r.m.s. response in this range grows much bigger than that of linear response.

Similar response characteristics of the yielding level are found for the parameter of n=0.25 in Fig.4.6.

In Fig.4.7, shown are the similar results for hysteretic structures of which natural frequency in small vibration is the same as the predominant frequency of the excitation (η=1.0). The hysteretic r.m.s. response is found less than the linear r.m.s. response in wider range of σ_l than "relatively rigid" structures in Fig.4.6. This is attributable to the decrease of ω_{eq} which lets the peak of the structural receptance far from the peak of the spectrum of the excitation. The minimum value of hysteretic response is found when σ_l is around 1.5. When the yielding level becomes lower (σ_l>4.0∿6.0), the hysteretic response shows a little larger values than the linear response presumably due to the decrease of β_{eq} to its original value and the excitation which has broad band spectrum (h_f=0.9). These yielding level characteristics of the hysteretic response agree well with the simulated results on an analog computer carried out by W.D.Iwan and L.D.Lutes[7].

When hysteretic structures are "relatively soft" (η=2.0), the hysteretic response is found less than the linear response for full range of the yielding level σ_l shown in Fig.4.8. This result is also attributable to the decrease of the stiffness of the restoring force which lets ω_{eq} very far from ω_f to filter out the random excitations of which frequencies are around ω_f. For n=0.75, the minimum value of the hysteretic response which is about 65% of the corresponding linear response is found when σ_l is around 2.5.

In the latter part of this section, the yielding level characteristics have also been explained by means of variation of equivalent linear parameters ω_{eq} and β_{eq} relative to the spectrum of the excitation. Thus the concept of the transition of the structural receptance could be

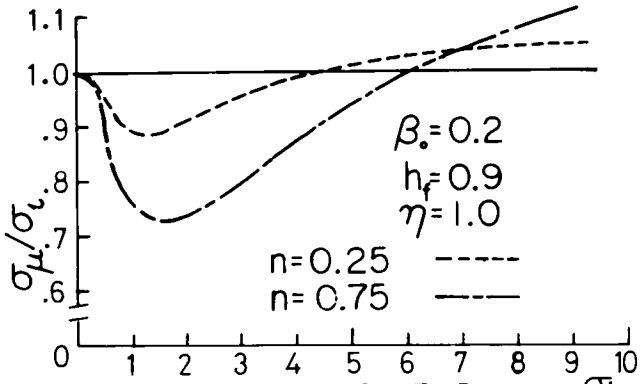

(a) Ratio of the R.M.S. of D.F. Response

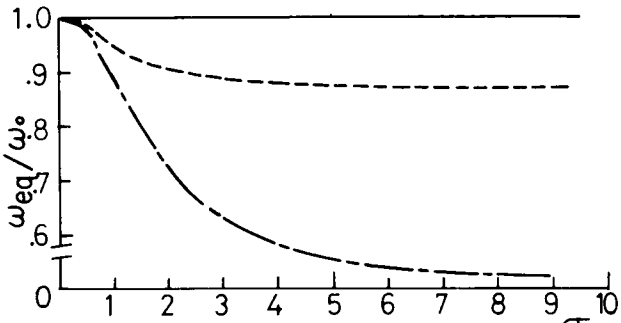

(b) Ratio of the Natural Frequency

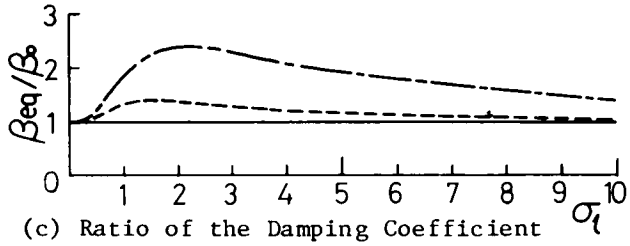

(c) Ratio of the Damping Coefficient

Fig.4.7 Effects of Yielding Level to Stationary R.M.S. Response of"Relatively Intermediate" Bilinear Structures

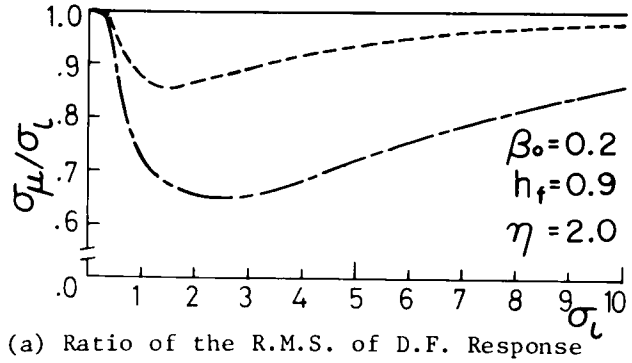

(a) Ratio of the R.M.S. of D.F. Response

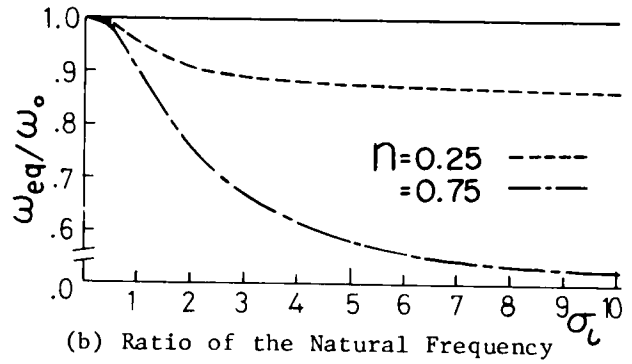

(b) Ratio of the Natural Frequency

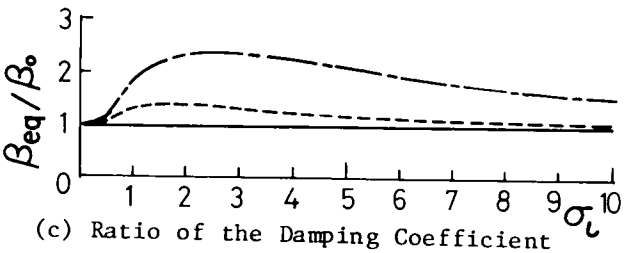

(c) Ratio of the Damping Coefficient

Fig.4.8 Effects of Yielding Level to Stationary R.M.S. Response of "Relatively Soft" Bilinear Structures

considered reasonable to make theoretical discussions about the random response characteristics of structures with any kind of hysteresis loops in terms of equivalently determined linear parameters.

It is noted that the effects of natural period of hysteretic structures in small oscillation to the plastic deformation discussed in the Chapter 2 can also be explained from this concept of the transition of structural receptance.

4-3-3 Numerical Simulations

To check the accuracy of the prediction of the r.m.s. response of hysteretic structures through the iterative linearization technique discussed in the previous section, numerical simulations have been carried out on a digital computer.

Firstly the stationary artificial earthquakes have been generated by following the procedure precisely explained in Chapter 2. A white noise random process is made from the summation of 500 sinusoidal time functions of which circular frequencies and phase angles are random variables with uniform probability densities. Then the velocity response of a simple oscillator with natural frequency ω_f and damping factor h_f subjected to the white noise is calculated by the linear acceleration method. The stationary part of the relative velocity response is taken as the excitation $f(t)$ for numerical simulations in this section.

Using the excitation $f(t)$ above mentioned, response of structures with bilinear hysteresis loops is calculated through step-by-step integration of the governing equation of motion. The r.m.s. response σ_μ of the ductility factor μ is calculated as the time average over the stationary part of which duration is 20 times as long as the natural period of infinitesimal vibration.

Both predicted and simulated results for frequency response of hysteretic structures are shown in Fig.4.9 for the same sets of parameters in Fig.4.4. It is observed that the predicted and simulated results agree well for the parameters of n=0.25, 0.50 and 0.75 from Figs.4.9 (a), (b) and (c). So within the limits of these parameters of n, r_s and β_o, it could be said that the iterative linearization technique

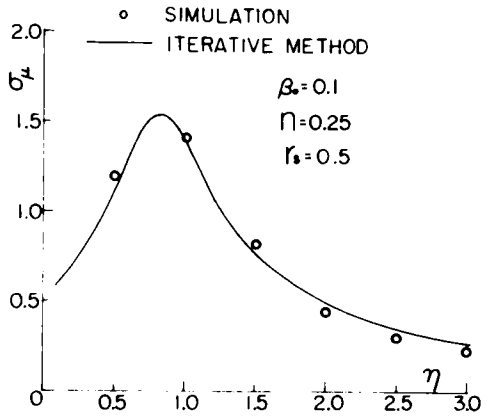

(a) Bilinear Hysteresis (n=0.25)

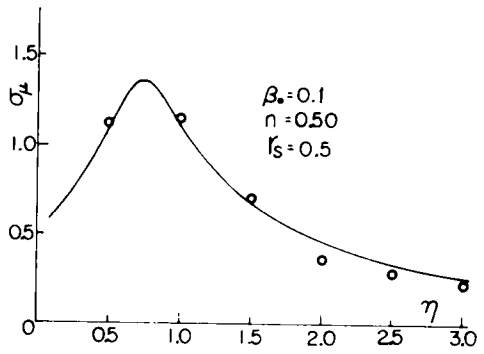

(b) Bilinear Hysteresis (n=0.50)

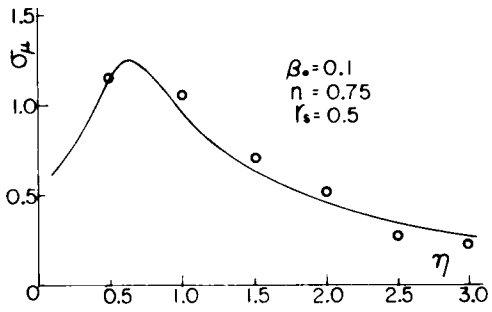

(c) Bilinear Hysteresis (n=0.75)

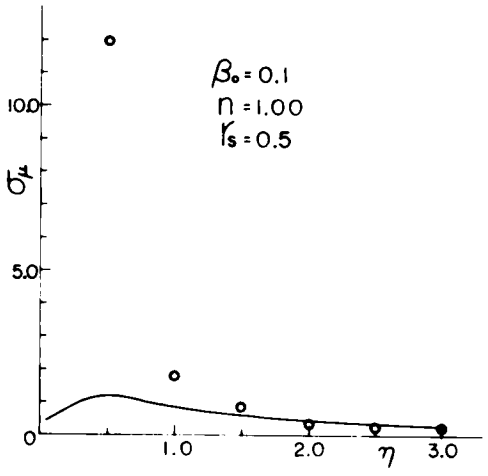

(d) Elasto-Plastic Hysteresis (n=1.00)

Fig.4.9 Simulated and Predicted Results of Stationary R.M.S. Response of Bilinear and Elasto-Plastic Hysteretic Structures

investigated in the previous section has satisfactory accuracy to predict the r.m.s. response of the bilinear structures.

On the other hand, in Fig.4.9 (d), the simulated result shows much greater values than the predicted result for the structure with perfect elasto-plastic hysteresis loop (n=1.00). This discrepancy is remarkable especially for a "relatively rigid" structure (η=0.5). For a "relatively soft" structure, the discrepancy is not found since the response remains almost in the elastic region (μ<1.0). The cause of the discrepancy between simulated and predicted response is mainly attributable to the growth of the plastic deformation due to an excessive yielding behavior. In Chapter 2, it is pointed out by the moving average method that conspicuous plastic deformation occurs only for structures with perfect elasto-plastic hysteresis. Therefore satisfactory estimation of the response of the perfectly elasto-plastic structures would need the combination of two techniques. One is a linearization technique to evaluate the elastic component of the response as discussed in this chapter and the other is a technique to evaluate the plastic deformation as discussed in Chapter 3.

The yielding level characteristics of predicted bilinear hysteretic response are also compared with the simulated results in Fig.4.10 for the same sets of parameters as in Fig.4.6∿4.8. When the nonlinearity is small (n=0.25), the predicted results show quite good agreement with the simulated ones, suggesting that the iterative equivalent linearization technique is applicable and powerful for hysteretic response analyses in wide range of the yielding level. The discrepancy between predicted and simulated results is noticed when the nonlinearity becomes strong (n=0.75). The simulated response shows a little bigger value than predicted one presumably because of the higher estimation of hysteretic energy dissipation in theoretical analysis than in the real hysteretic history which does not always enclose the loops.

In spite of the discrepancy found in Fig.4.10, the general trends of yielding level characteristics of hysteretic response predicted by the iterative linearization technique agree well with the simulated

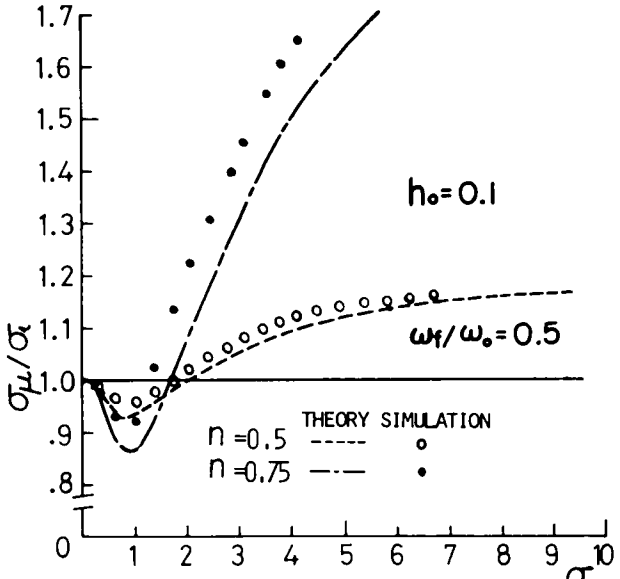

(a) "Relatively Rigid" Bilinear Structures

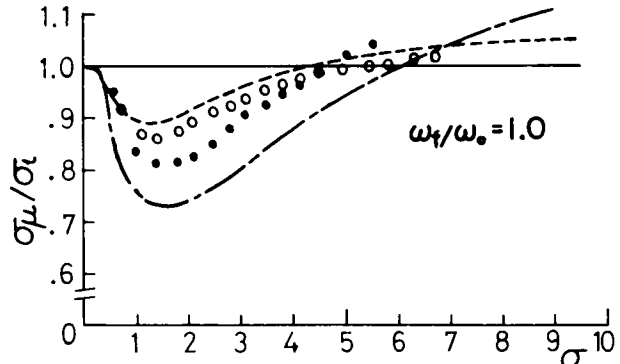

(b) "Relatively Intermediate" Bilinear Structures

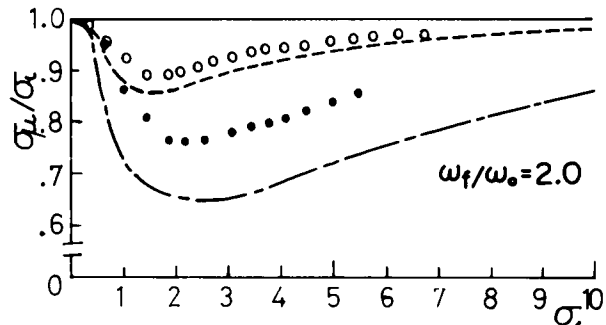

(c) "Relatively Soft" Bilinear Structures

Fig.4.10 Simulated and Predicted Ratio of Stationary R.M.S. Response of Bilinear Structures to that of Linear Structures

results. From these analyses, it could be concluded that the "relatively soft" hysteretic structures show smaller response than that of linear structures. Response of "relatively intermediate" (η=1.0) hysteretic structures show smaller value when the yielding level is high (σ_y<4∿6) and becomes larger than corresponding linear response for the lower yielding level (σ_y>4∿6). Response of "relatively rigid" (η=0.5) hysteretic structures is found larger than that of linear structures in broad range of yielding level except at σ_y<1.5.

4-4 Statistical Properties of Hysteretic Response

4-4-1 Probability Distribution of Hysteretic Response

(i) Simulated Probability Distribution

In the previous section, the equivalent linearization technique was found applicable and powerful to predict r.m.s. response of moderately nonlinear structures. From engineering point of view, it is of great needs to know not only r.m.s. values but also probability distributions of response amplitude of hysteretic structures for further discussions of structural reliability during strong earthquakes.

In this section, probability distributions of simulated response of hysteretic structures are compared with those of equivalent linear structures of which parameters are determined from the technique proposed in the previous section. These distributions give the probability that the response is less than a given level and are plotted in Figs.4.11∿4.13. In these figures, the probability distribution of the response of the linear structures of which natural periods and damping factors are the same as those of hysteretic structures in the elastic region are also plotted in order to investigate the difference between the linear and the hysteretic response. For the estimation of probability distributions, the stationary portion of the simulated response of which interval is 50 times as long as the natural period of the structures in small oscillation is taken.

In Figs.4.11 (a), (b) and (c), shown are the simulated results of linear and hysteretic structures for the set of parameters n=0.25, r_s=1.2, h_f=0.9, β_o=0.2. The distributions of hysteretic response are found very close to those of the linear responses for a "relatively rigid" (η=0.5) and a "relatively soft" (η=2.0) structures, because of the weak nonlinearity (n=0.25). Hence the discrepancy between the hysteretic and the equivalent linear response is not found either for these structures. For a "relatively intermediate" (η=1.0) structure, the probability distribution of the hysteretic response shows greater probability than that of the linear response in the positive range. On the contrary, the smaller probability is found in the negative range. This result corresponds to the fact that the r.m.s. response of the hysteretic structures is less than that of the linear structure as shown in Fig.4.10 (b). Although the shift of the receptance is small due to the weak nonlinearity and the small area of hysteresis loop, the effect of shifting to the hysteretic response becomes significant around the predominant frequency of the excitation. The discrepancy between the hysteretic and the equivalent linear response is very small to suggest that the probability distribution of hysteretic response can also be predicted satisfactorily through the equivalent linearization technique when the nonlinearity of the hysteresis is weak.

In Fig.4.12 (a), (b) and (c), shown are the results of the hysteretic structures with medium nonlinearity (n=0.5). Other parameters are the same as those in Fig.4.11. For a "relatively rigid" (η=0.5) structure, the probability distribution of the hysteretic response shows smaller probability than that of linear response in the positive range of response amplitude. The greater probability is found in the negative range. This result corresponds to the fact that the r.m.s. response of a "relatively rigid" (η=0.5) structure grows greater than that of linear structure as discussed in Fig.4.10 (a). For "relatively intermediate (η=1.0) and soft (η=2.0)" structures, the characteristics of the probability distributions of the hysteretic response relative to those of linear response

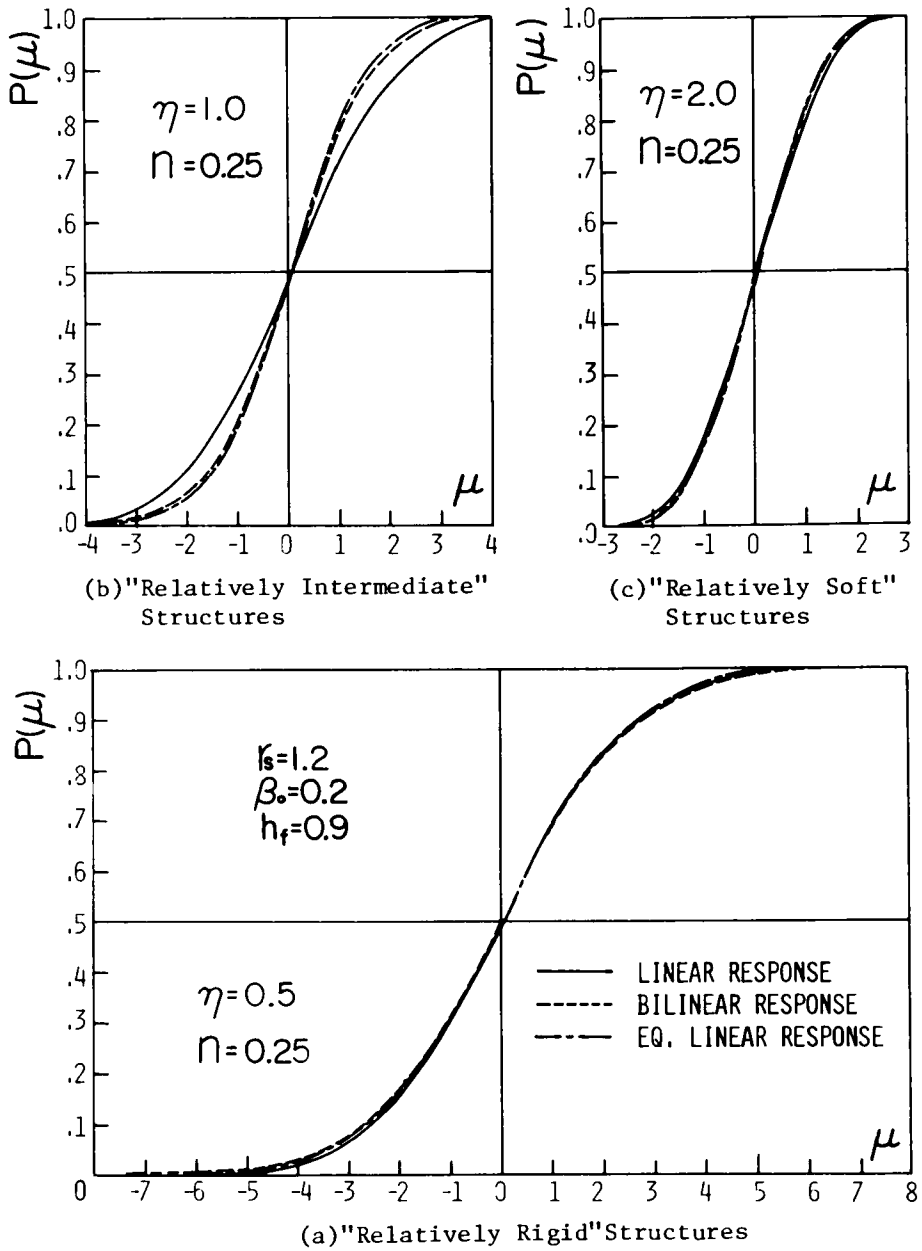

Fig.4.11 Simulated Probability Distribution of Ductility Factor (D.F.) Response of Linear, Bilinear(n=0.25), and Equivalent Linear Structures

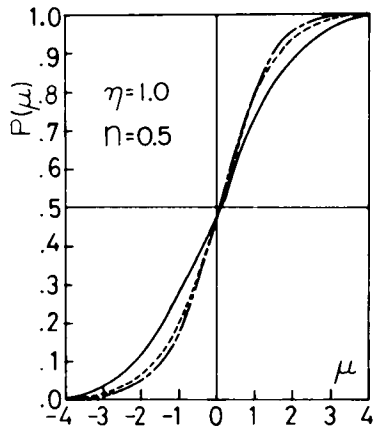

(b)"Relatively Intermediate" Structures

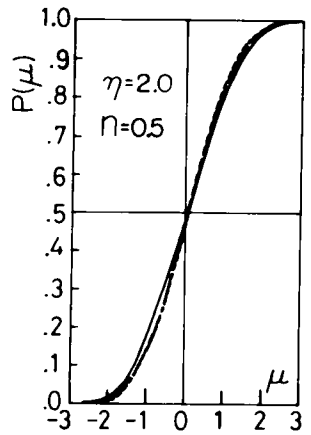

(c)"Relatively Soft" Structures

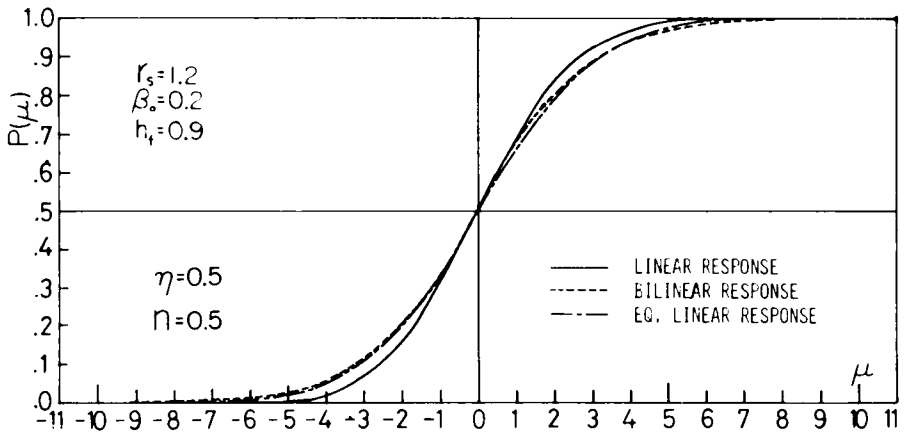

(a)"Relatively Rigid"Structures

Fig.4.12 Simulated Probability Distribution of Ductility Factor (D.F.) Response of Linear, Bilinear(n=0.50) and Equivalent Linear Structures

becomes contrary, which corresponds to the smaller r.m.s. response of these hysteretic structures as discussed in Fig.4.10 (b) and (c). The probability distributions of the equivalent linear structures are found close to those of the hysteretic structures to suggest that the equivalent linearization technique is still powerful for the medium nonlinearity (n=0.5).

The simulated results for hysteretic structures with strong nonlinearity (n=0.75) are shown in Fig.4.13 (a), (b) and (c). The characteristics of the probability distributions are almost the same as those in Fig.4.12 (a), (b) and (c). However the discrepancy is found between the probability distributions of hysteretic structures and those of equivalent linear structures. The cause of the difference may be attributable to the growth of the plastic deformation which lets the simulated hysteretic r.m.s. response bigger than the equivalent linear r.m.s. response and also the simulated hysteretic distribution unsymmetric. Although no plastic deformation is taken into account for the prediction of r.m.s. response by the equivalent linearization technique, this amount of discrepancy could be permissible to grasp general trends of hysteretic response.

(ii) Deviation from the Gaussian Distribution

In order to check the deviation from the Gaussian distributions which have exactly the same r.m.s. values as the hysteretic response, the distributions of hysteretic structures with strong nonlinearity (n=0.75) are again plotted in Fig.4.14 (a), (b) and (c). For a "relatively rigid" (η=0.5) structure, the hysteretic response shows larger probability than the Gaussian distribution in the positive low range of response amplitude (μ=0$\sim$4), and smaller probability in the positive high range (μ>4). This result shows that the probability of being at the intermediate level (around $\mu\simeq$4) is shifted both to lower and higher level. The relatively large amplitude (μ>4) is enlarged due to strong softening-type nonlinearity which makes the structure easy to slip toward larger amplitude. On the contrary, the relatively small amplitude (μ<4) is

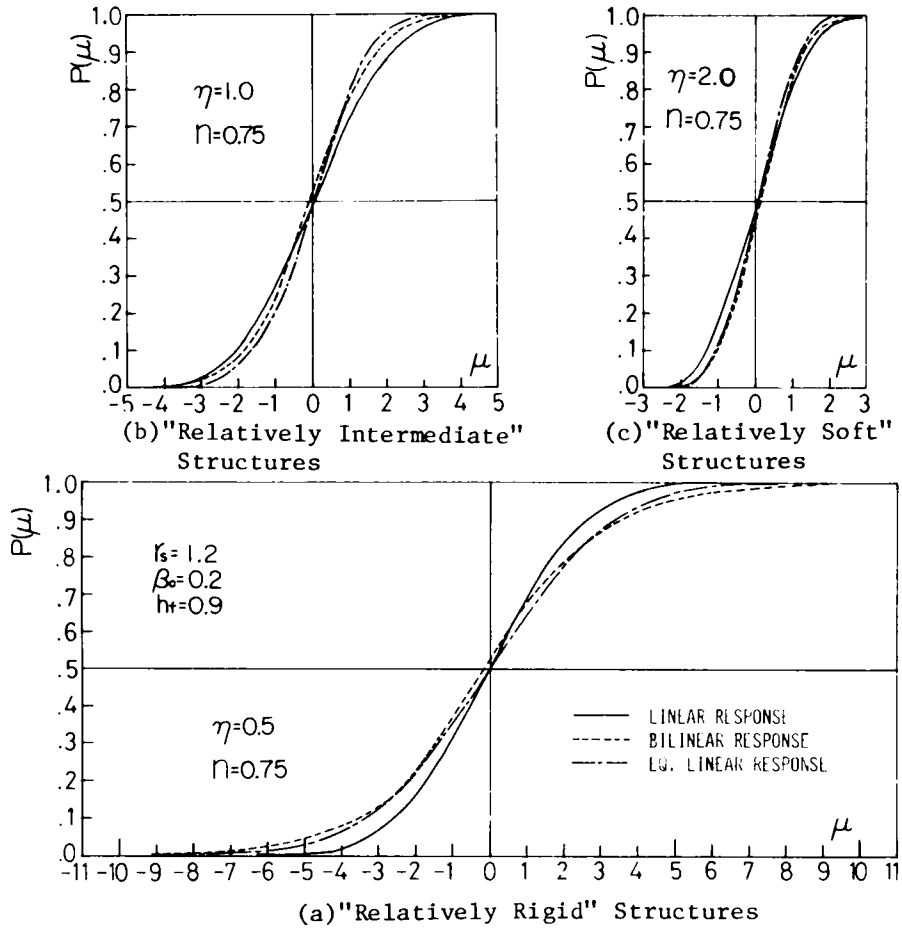

Fig.4.13 Simulated Probability Distribution of Ductility Factor (D.F.) Response of Linear, Bilinear(n=0.50) and Equivalent Linear Structures

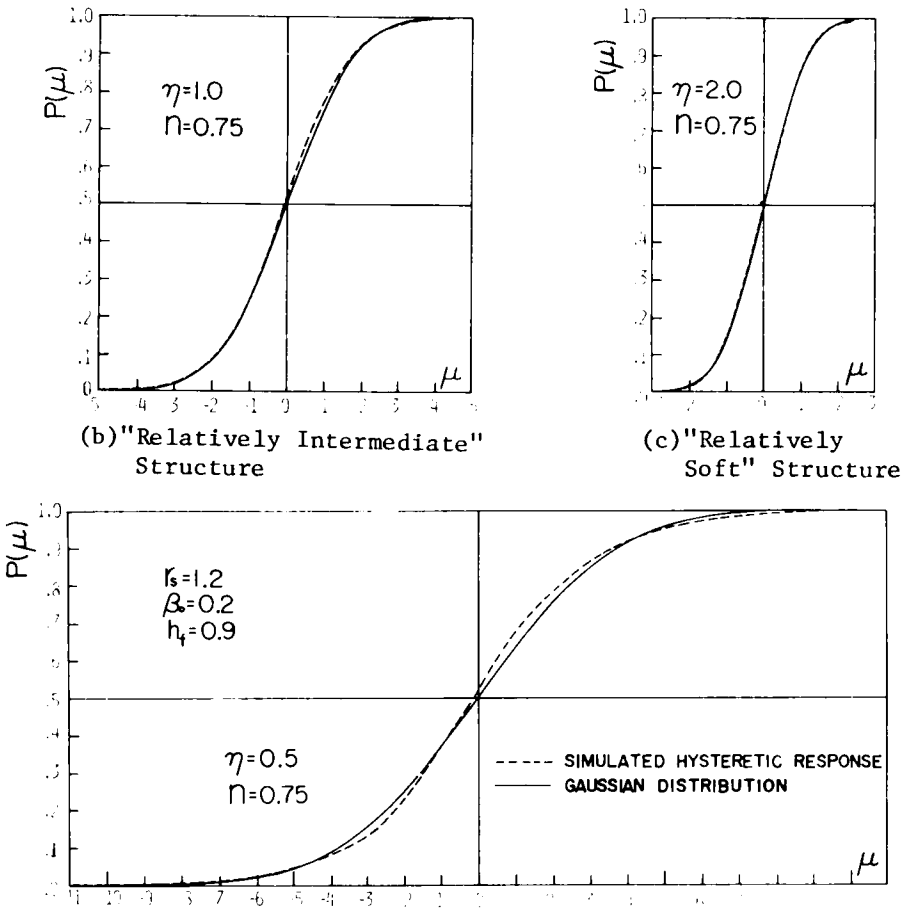

Fig.4.14 Simulated Probability Distribution of Bilinear (n=0.75) and the Gaussian Distribution

suppressed due to hysteretic behavior which absorbs kinetic energy. Hence, even if the r.m.s. values of hysteretic response are predicted accurately through the linearization technique, the probability distribution of it shows the deviation from the Gaussian distribution. When the assumption of Gaussian distribution is adopted for statistical response analysis of hysteretic structures, it would conclude the higher estimation of structural reliability than the real value in the above discussed "amplitude-enlarging" range.

For "relatively intermediate (μ=1.0) and soft (μ=2.0)" structures shown in Fig.4.14 (b) and (c), the hysteretic response shows very close values to the Gaussian distribution. The nonlinear hysteretic properties of the restoring force seems to have little effects on the shapes of the probability distributions. Hence the assumption of the Gaussian distribution would be reasonable for the hysteretic structures with the limited sets of parameters.

Similar investigations for the structure with moderate (n=0.5) and weak (n=0.25) nonlinearity have shown little deviation from the Gaussian distribution.

(iii) Approximate Gaussian Distribution

From the above discussed simulations, probability distributions of moderately nonlinear hysteretic structures are found not exactly the same but close to those of equivalent linear structures and they could be regarded as Gaussian depending on the accuracy of the problem. Hence for the further discussions of statistical properties of hysteretic structures, such as probability distribution of maximum response which will be discussed in the next section, the following Gaussian probability density of ductility factor μ and velocity $\dot{\mu}$ in the stationary state will be used.

$$p(\mu,\dot{\mu}) = \frac{1}{2\pi\sigma_{\mu}\sigma_{\dot{\mu}}}\exp\{-\frac{1}{2}(\frac{\mu^2}{\sigma_{\mu}^2} + \frac{\dot{\mu}^2}{\sigma_{\dot{\mu}}^2})\} \qquad (4\text{-}25)$$

Where σ_{μ} is the r.m.s. value of velocity response which will be estimated

from the next equation.

$$\sigma_{\dot{\mu}}^2 = \frac{1}{\pi}\int_0^\infty \frac{r_s S_f(\omega)(\omega_f/\eta)^4\omega^2}{(\omega_{eq}^2-\omega^2)^2+(\beta_{eq}\omega)^2}d\omega \tag{4-26}$$

Where ω_{eq} and β_{eq} are determined by the iterative method proposed in the previous section.

4-4-2 Probability Distribution of Maximum Response

(i) Basic Formulation

Prediction of probability distribution of maximum response (PDMR) of structures subjected to random excitation is quite essential especially for reliability analysis, because PDMR is considered as distribution of dynamic load to structural elements. When distribution of strength of structural elements is known, reliability of structures in random response will easily be estimated. From this point of view, the PDMR of linear structures subjected to earthquake type random excitation has been intensively investigated by H.Kameda[1]. In this section, effects of hysteretic restoring force upon PDMR of structures are analytically examined through the pure-birth-process method[20] applied to equivalently linearized structures.

Let the absolute maximum value of hysteretic response $\mu(\tau)$ at the time interval (o, τ_o) be μ_{max}. Then the probability distribution $\Phi(\mu_{max}, \tau_o)$ of μ_{max} will be obtained from the pure-birth-process equation similary as that of the first passage time: i.e.,

$$\begin{aligned}\Phi(\mu_{max}, \tau_o) &= P[\max|\mu(\tau)| \le \mu_{max}; 0 \le \tau \le \tau_o] \\ &= a_o(\mu_{max})\exp\{-\int_0^{\tau_o} e_o(\mu_{max}, \tau)d\tau\}\end{aligned} \tag{4-27}$$

where

$$\left.\begin{aligned} e_o(\mu_{max}, \tau)d\tau &= P[\{|\mu(\tau+d\tau)| > \mu_{max} \,|\, \max|\mu(\tau'')| \le \mu_{max}\}; 0 \le \tau'' \le \tau] \\ a_o(\mu_{max}) &= P[|\mu(0)| \le \mu_{max}] \end{aligned}\right\} \tag{4-28}$$

It should be noted that P[A] represents the probability of event A and P[A|B] indicated the conditional probability of event A on the hypothesis of event B. Hence $C_o(\mu_{max},\tau)d\tau$ is the probability of first crossing of the level of amplitude μ_{max} at the time interval $(\tau, \tau+d\tau)$. It is almost impossible to obtain the exact solution of Eq.(4-28) for an explicit form. Assuming the Poisson Process arrival of the maximum response to the level μ_{max}, the first step appromixation of Eq.(4-28) will be induced as

$$\bar{C}_o(\mu_{max},\tau)d\tau \simeq \frac{P[|\mu(\tau+d\tau)| \geq \mu_{max} \cap |\mu(\tau)| \leq \mu_{max}]}{P[|\mu(\tau)| \leq \mu_{max}]} \tag{4-29}$$

The probability of crossing the level μ_{max} at the time interval $(\tau, \tau+d\tau)$, which is the numerator of right hand term of Eq.(4-29), is estimated from the results by S.O.Rice[21] for stationary Gaussian process. From discussion in the previous section, Gaussian process approximation of hysteretic response seems to be reasonable unless nonlinearity is strong. Then substituting Eq.(4-29) for Eq.(4-28), Eq.(4-27) will be approximated as

$$\Phi(\mu_{max},\tau_o) \simeq \mathrm{erf}\left(\frac{\mu_{max}}{\sqrt{2}\sigma_\mu}\right)\exp\left[-\frac{\dot{\sigma}_\mu}{\pi\sigma_\mu}\exp\left\{-\frac{1}{2}\left(\frac{\mu_{max}}{\sigma_\mu}\right)^2\right\}\tau_o \Big/ \mathrm{erf}\left(\frac{\mu_{max}}{\sqrt{2}\sigma_\mu}\right)\right] \tag{4-30}$$

where erf(x) is an error function of x.

(ii) Predicted and Simulated Results

Calculated results of above equation are shown in Figs.4.15 (a), (b) and (c) for the sets of parameters; n=0.0, 0.50, 0.75, η=0.5, 1.0, 2.0, r_s=1.2, h_f=0.9, β_o=0.2. Duration τ_o of stationary response is set 20 times the natural period of linear structures.

The PDMR of "relatively rigid" (η=0.5) hysteretic structures are found larger than that of a linear structure (n=0.0). The larger mean

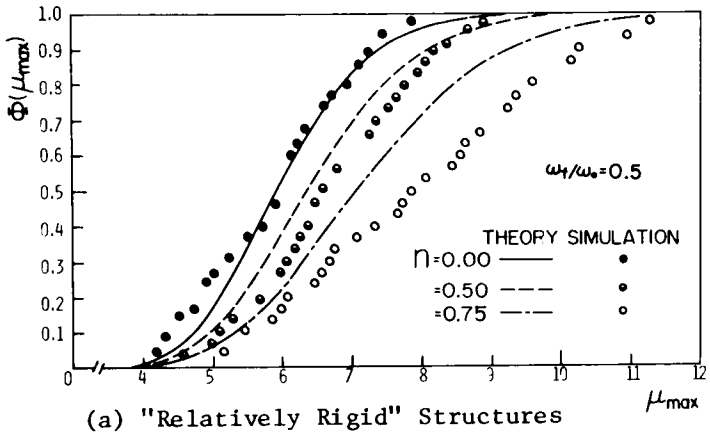

(a) "Relatively Rigid" Structures

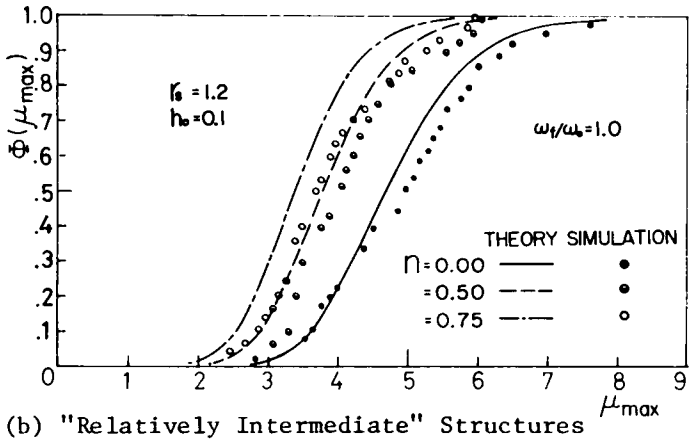

(b) "Relatively Intermediate" Structures

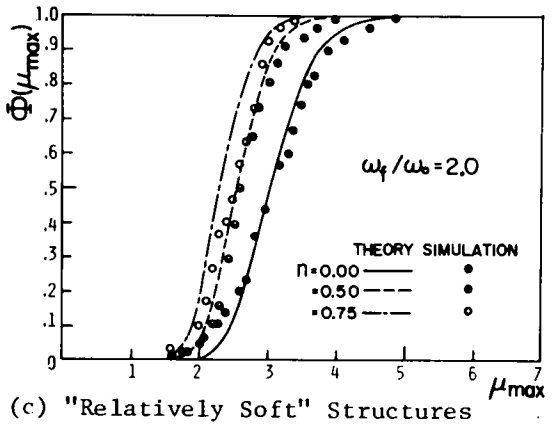

(c) "Relatively Soft" Structures

Fig.4.15 Probability Distribution of Maximum Ductility Factor of Bilinear Structures in Stationary Response

response and variation of distribution is noticed for the stronger nonlinearity of hysteresis loops. On the contrary, hysteretic effects suppress the PDMR of "relatively intermediate (η=1.0) and soft (η=2.0)" structures as seen in Fig.4.15 (b) and (c). These frequency-dependent characteristics of the PDMR of hysteretic structures can also be explained from transition of the receptance of equivalently linearized structures as discussed in previous sections.

Simulated results are also plotted in Fig.4.15 (a), (b) and (c). Predicted and simulated results show satisfactory agreement for linear structures. This is due to relatively large damping factor (h_o=0.1) which lets the Poisson Process assumption in Eq.(4-29) reasonable. Difference between theoretical and experimental results increases with the nonlinearity parameter. The large discrepancy found in "relatively rigid" (η=0.5) bilinear structures with strong nonlinearity (n=0.75) suggests that the component of plastic deformation can not be neglected in this case. Frequency and nonlinearity dependent properties of the PDMR of hysteretic structures are almost consistent with those of r.m.s. response discussed in the previous section.

4-5 Nonstationary Response

4-5-1 Step-by-Step Method for Linear Structures

(i) Variances and Correlation Coefficient of Linear Response

In the previous section, the equivalnet linear structures and their response in the stationary state are investigated. It is, however, one of very important factors in the reliability analysis of strctures in strong earthquakes to investigate the nonstationarity of response of linear and hysteretic structures from following reasons. 1) The strength of earthquake motions varies with time. This time variation seems to depend on the location of the observation site relative to the hypocenter and also on the path characteristics and so on. 2) Even it might be assumed simply that the earthquake excitation is stationary, structures in the occasion of

earthquakes start to vibrate from the static state.

In this section, the step-by-step method shall be discussed to estimate the time depending variances of displacement and velocity response of linear structures, and the correlation coefficient between them at each step of time shown in Fig.4.16.

First, consider the response of a simple linear structure under the initial conditions that

$$\mu(t)\big|_{t=t_i} = \mu_i, \quad \dot{\mu}(t)\big|_{t=t_i} = \dot{\mu}_i, \quad \psi(t)\big|_{t=(t_i+t_{i+1})/2} = \psi_i \qquad (4\text{-}31)$$

Then the solution of Eq.(4-2) at any time of t between t_i and t_{i+1} is obtained by the summation of the free vibration due to the initial conditions and the forced vibration due to the excitation $r_s\psi_i f(t)$ as follows.

$$\left.\begin{aligned} \mu(t) &= -(r_s\psi_i)/p \int_{t_i}^{t} h(t-t')f(t')dt' + I(t-t_i) \\ \dot{\mu}(t) &= -(r_s\psi_i)/p \int_{t_i}^{t} \dot{h}(t-t')f(t')dt' + \dot{I}(t-t_i) \end{aligned}\right\} \qquad (4\text{-}32)$$

where

$$\left.\begin{aligned} &p=\sqrt{\omega_{eq}^2-\beta_{eq}^2/4},\ I(t)=g_1(t)\mu_i+g_2(t)\dot{\mu}_i,\ \dot{I}(t)=g_3(t)\mu_i+g_4(t)\dot{\mu}_i \\ &h(t)=\exp(-\beta_{eq}t)\sin pt,\ \dot{h}(t)=p\exp(-\beta_{eq}t/2)\{\cos pt-(\beta_{eq}/2p)\sin pt\} \\ &g_1(t)=\exp(-\beta_{eq}t/2)\{\cos pt+(\beta_{eq}/2p)\sin pt\} \\ &g_2(t)=(1/p)\exp(-\beta_{eq}t/2)\sin pt \\ &g_3(t)=-(\omega_{eq}^2/p)\exp(-\beta_{eq}t/2)\sin pt \\ &g_4(t)=-(\beta_{eq}/2p)\exp(-\beta_{eq}t/2)\sin pt+\exp(-\beta_{eq}t/2)\cos pt \end{aligned}\right\} \qquad (4\text{-}33)$$

From Eqs.(4-32) and (4-33), the variances of displacement and velocity response and the correlation coefficient between them at any time t between t_i and t_{i+1} is readily expressed as

$$\sigma_{\mu}^2(t)=E[\mu^2(t)]=(r_s^2\psi_i^2/p^2)\int_{t_i}^{t}\int_{t_i}^{t}h(t-t')h(t-t'')E[f(t')f(t'')]dt'dt''$$

$$-(2r_s\psi_i/p)E[I(t-t_i)\int_{t_i}^{t}h(t-t')f(t')dt']+E[I^2(t-t_i)] \qquad (4-34)$$

$$\sigma_{\dot{\mu}}^2(t)=E[\dot{\mu}^2(t)]=(r_s^2\psi_i^2/p^2)\int_{t_i}^{t}\int_{t_i}^{t}\dot{h}(t-t')\dot{h}(t-t'')E[f(t')f(t'')]dt'dt''$$

$$-(2r_s\psi_i/p)E[\dot{I}(t-t_i)\int_{t_i}^{t}\dot{h}(t-t')f(t')dt']+E[\dot{I}^2(t-t_i)] \qquad (4-35)$$

$$\rho_{\mu\dot{\mu}}(t)\sigma_{\mu}(t)\sigma_{\dot{\mu}}(t)=E[\mu(t)\dot{\mu}(t)]$$

$$=(r_s\psi_i^2/p^2)\int_{t_i}^{t}\int_{t_i}^{t}h(t-t')\dot{h}(t-t'')E[f(t')f(t'')]dt'dt''$$

$$-(r_s\psi_i/p)E[I(t-t_i)\int_{t_i}^{t}\dot{h}(t-t'')f(t'')dt'']$$

$$-(r_s\psi_i/p)E[\dot{I}(t-t_i)\int_{t_i}^{t}h(t-t')f(t')dt']$$

$$+E[\dot{I}(t-t_i)I(t-t_i)] \qquad (4-36)$$

where

$$\left.\begin{aligned}
E[I^2(t-t_i)]&=g_1^2(t-t_i)E[\mu_i^2]+2g_1(t-t_i)g_2(t-t_i)E[\mu_i\dot{\mu}_i]\\
&\quad+g_2^2(t-t_i)E[\dot{\mu}_i^2]\\
E[\dot{I}^2(t-t_i)]&=g_3^2(t-t_i)E[\mu_i^2]+2g_3(t-t_i)g_4(t-t_i)E[\mu_i\dot{\mu}_i]\\
&\quad+g_4(t-t_i)E[\dot{\mu}_i^2]\\
E[I(t-t_i)\dot{I}(t-t_i)]&=g_1(t-t_i)g_3(t-t_i)E[\mu_i^2]\\
&\quad+\{g_1(t-t_i)g_4(t-t_i)+g_2(t-t_i)g_3(t-t_i)\}E[\mu_i\dot{\mu}_i]\\
&\quad+g_2(t-t_i)g_3(t-t_i)E[\dot{\mu}_i^2]
\end{aligned}\right\} \qquad (4-37)$$

Expected values of initial conditions at $t=t_i$ in above equation will be determined from the response statistics at the end of the previous time segment as

$$\left.\begin{aligned} E[\mu_i^2] &= \sigma_\mu^2(t_i) \\ E[\dot{\mu}_i^2] &= \sigma_{\dot{\mu}}^2(t_i) \\ E[\mu_i\dot{\mu}_i] &= \rho_{\mu\dot{\mu}}(t_i)\sigma_\mu(t_i)\sigma_{\dot{\mu}}(t_i) \end{aligned}\right\} \qquad (4\text{-}38)$$

These response statistics will be obtained from Eqs.(4-34)~(4-36), if expected values of initial conditions at $t=t_{i-1}$ are available.

Repeating this procedure backward on the time axis, one reaches at the beginning of structural vibration. Hence, when the initial conditions at t=0 are defined ($\mu(0)=\dot{\mu}(0)=0$ for most structures in earthquake engineering problems), nonstationary response of linear structures of which natural frequency and damping factor in Eqs.(4-18) and (4-19) are changeable at the beginning of any time segment, can be estimated by applying Eqs.(4-34)~(4-37) and Eq.(4-18) to every one of them.

Following algebraic reductions are used to estimate Eqs.(4-34)~(4-37). Covariances of excitation in Eqs.(4-34)~(4-36) will be expressed by power spectrum density using fourier transform as

$$E[f(t')f(t'')]=R_f(t'-t'')=\int_{-\infty}^{\infty}S_f(\omega)\exp\{i\omega(t'-t'')\}d\omega \qquad (4\text{-}39)$$

From the above relation, the first term of right-hand side of Eq.(4-34) is reduced to following form after tedious algebra.

$$\begin{aligned} \sigma_\mu^2(t)_1 &= (r_s^2\psi_i^2/p^2)\int_{t_i}^{t}\int_{t_i}^{t}h(t-t')h(t-t'')E[f(t')f(t'')]dt'dt'' \\ &= (r_s^2\psi_i^2/p^2)\int_{-\infty}^{\infty}S_f(\omega)\,|H(\omega)|^2 \\ &\times[1-2\exp(-\beta_{eq}\xi/2)\{((\beta_{eq}/2p)\sin p\xi+\cos p\xi)\cos\omega\xi+\omega/p\sin\omega\xi\sin p\xi\} \\ &+\exp(-\beta_{eq}\xi)\}\{(\beta_{eq}/2p)\sin 2p\xi+((\beta_{eq}/2)^2+\omega^2)/p^2\sin^2 p\xi+\cos^2 p\xi\}]d\omega \end{aligned} \qquad (4\text{-}40)$$

where

$$\xi = t - t_i$$
$$|H(\omega)|^2 = 1/\{(\omega_{eq}^2 - \omega^2)^2 + (\beta_{eq}\omega)^2\} \tag{4-41}$$

(ii) White-Noise Excitation

When power spectrum density of excitation is constant (white-noise excitation) as,

$$S_f(\omega) = S_o \tag{4-42}$$

the Eq.(4-40) will be estimated approximately by the integration over the narrow range in the vicinity of the equivalent natural frequency ω_{eq} as T.K.Caughey and H.J.Stumpf[22] have proposed.

$$\sigma_\mu^2(t)_1 \simeq \frac{\pi r_s^2 \psi_i^2 S_o}{2\beta_{eq}\omega_{eq}^2}\{1-\exp(-\beta_{eq}\xi)(1+\frac{\beta_{eq}}{2p}\sin 2p\xi+\frac{\beta_{eq}^2}{2p^2}\sin^2 p\xi)\} \tag{4-43}$$

Similar calculation was made by H.Goto and H.Kameda[23] for the variance and the correlation coefficient in Eqs.(4-35) and (4-36) as

$$\sigma_{\dot\mu}^2(t)_1 = \frac{r_s^2\psi_i^2}{p}\int_{t_i}^t\int_{t_i}^t \dot h(t-t')\dot h(t-t'')E[f(t')f(t'')]dt'dt''$$
$$\simeq \frac{\pi r_s^2\psi_i^2}{2\beta_{eq}}\{1-\exp(-\beta_{eq}\xi)(1-\frac{\beta_{eq}}{2p}\sin 2p\xi-\frac{\beta_{eq}^2}{2p}\sin^2 p\xi)\} \tag{4-44}$$

$$\rho_{\mu\dot\mu}(t)\sigma_\mu(t)\sigma_{\dot\mu}(t)_1 \simeq \frac{r_s^2\psi_i^2}{p^2}\int_{t_i}^t\int_{t_i}^t h(t-t')\dot h(t-t'')E[f(t')f(t'')]dt'dt''$$
$$\simeq \frac{\pi r_s^2\psi_i^2 S_o}{2\omega_{eq}^2}\exp(-\beta_{eq}\xi)\sin^2 p\xi \tag{4-45}$$

The second terms of the right-hand side of the Eqs.(4-34)~(4-36) are the covariance between free vibration due to initial conditions at the beginning of a short time-segment and forced vibration due to excitation

during the segment. When initial conditions at t=0 are all zero as,

$$\mu(t)\big|_{t=0} = 0, \quad \dot{\mu}(t)\big|_{t=0} = 0 \tag{4-46}$$

initial conditions at the beginning of a short segment are determined only from forced vibration at the end of the previous segment. Hence, the covariance is written as

$$\begin{aligned}
&E[I(t-t_i)\int_{t_i}^{t} h(t-t')f(t')dt'] \\
&\quad = E[\{g_1(t-t_i)\mu_i + g_2(t-t_i)\dot{\mu}_i\}\int_{t_i}^{t} h(t-t')f(t')dt'] \\
&\quad = E[\{g_1(t-t_i)\int_{t_{i-1}}^{t_i} h(t_i-t'')f(t'')dt'' + g_2(t-t_i)\int_{t_{i-1}}^{t_i} h(t_i-t''')f(t''')dt'''\} \\
&\qquad \times \int_{t_i}^{t} h(t-t')f(t')dt'] \\
&\quad = g_1(t-t_i)\int_{t_{i-1}}^{t_i}\int_{t_i}^{t} h(t_i-t'')h(t-t')E[f(t')f(t'')]dt'dt'' \\
&\qquad + g_2(t-t_i)\int_{t_{i-1}}^{t_i}\int_{t_i}^{t} \dot{h}(t_i-t''')h(t-t')E[f(t')f(t''')]dt'dt'''
\end{aligned} \tag{4-47}$$

When the power spectrum density of the excitation is constant, its correlation function is given by fourier transform as

$$E[f(t')f(t''')] = S_o\delta(t'-t''') \tag{4-48}$$

where $\delta(t)$ is the Dirac's delta function. Substitution of the above relation into Eq.(4-47) lets the integration zero. Similarly all correlation coefficients between the free vibration and the forced vibration in Eqs.(4-34)∿(4-36) become zero. Therefore, when the excitation is white-noise random process, Eqs.(4-34)∿(4-36) will be estimated relatively easily from the simplified Eqs.(4-43)∿(4-45).

To check the accuracy of the step-by-step method discussed herein, nonstationary response of linear structures subjected to stationary white-noise excitation is firstly compared in Fig.4.17 with the theoreti-

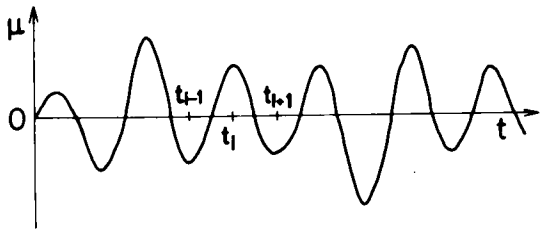

Fig.4.16 Time Steps in Nonstationary Response

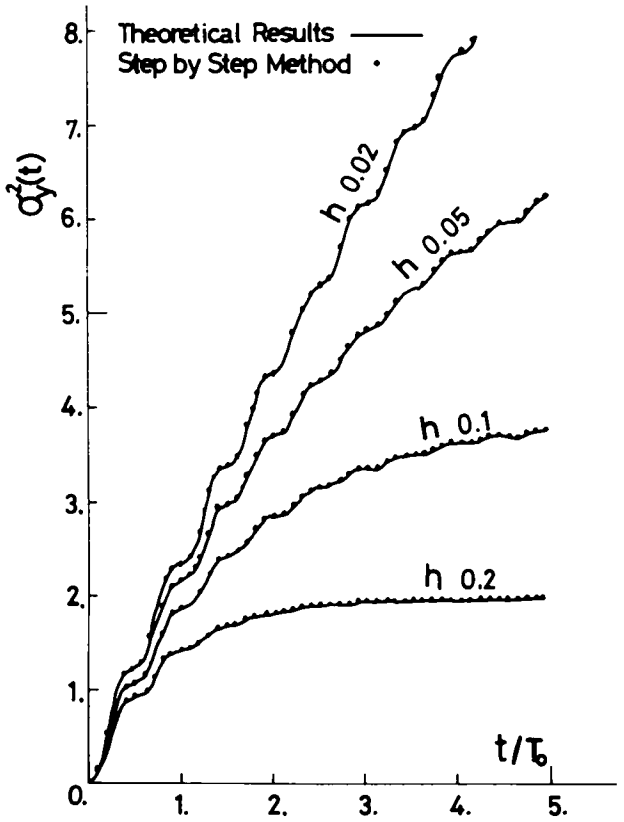

Fig.4.17 Nonstatinary Mean-Square Response of Linear Structures Subjected to Stationary White Noise Excitation

cal results obtained by T.K.Caughey and H.J.Steumph[23]. The nonstationary response of the variance predicted by the step-by-step method of which interval of the time segment is taken as $T_o/10$ (one tenth of natural period of a structure) shows quite good agreement with the theoretical result to verify the technique discussed herein.

(iii) Non-White Random Excitation

When power spectrum density of excitation is not white but has a predominant frequency such as represented by Eq.(4-22), the integration in Eq.(4-40) can not so easily be reduced to a simple form as Eq.(4-43). Besides, the covariance between free and forced vibration expressed in Eq.(4-47) does not vanish to make the calculation of Eqs.(4-34)∿(4-36) very complicated. For an approximate estimation, following techniques are used. First, numerical integration over the limitted range of frequency around ω_f and ω_{eq} is conducted to evaluate $\sigma_\mu{}^2(t)_1$, $\sigma_{\dot\mu}{}^2(t)_1$ $\rho_{\mu\dot\mu}(t)\sigma_\mu(t)\sigma_{\dot\mu}(t)_1$. Then from next two reasons, the second terms of the right-hand side of Eqs.(4-34)∿(4-36) are expected negligibly small. 1) if a peak of power spectrum density function of excitation is not so sharp as receptance of a structure, the covariance between free vibration due to previous excitation and forced vibration due to present excitation would be small, and 2) free vibration dies out with time by virtue of damping coefficient β_{eq}, hence the covariances would also become small.

To check the accuracy of numerical estimation of the linear r.m.s. response through the step-by-step method ignoring the covariance between free and forced vibration, the calculated result is compared with the theoretical result derived by H.Kameda[1] in Fig.4.18 (b). After tedious algebraic treatments, H.Kameda obtained the theoretical r.m.s. response of a simple linear structure subjected to an earthquake-type nonstationary excitation represented by product of nonstationary envelope function $\psi(t)$ shown in Fig.4.18 (a) and stationary random process $f(\eta, h_f, t)$ of which power spectrum density function is given by Eq.(4-22) for the set of parameters η=1.0, τ/T_f=10, h_f=0.9, h_o=0.02, 0.05, 0.20.

In Fig.4.18, τ denotes the equivalent stationary duration for nonstationary excitation defined by him. Both results are found to coincide well with each other except at the first and the second step. The cause of discrepancy between the two results at the first step is considered to be the considerably great time-derivative of the nonstationary envelope function at the beginning of excitation. From this point, it is desirable that length of interval of the time step is short. On the contrary, to ignore the covariance between free and forced vibration, it is desirable to let the interval long. Since both conditions can not be satisfied simultaneously, interval of the section in this study is chosen so as to furnish the same maximum r.m.s. response as that obtained by the theoretical method.

Thus the step-by-step method investigated herein seems very powerful to analyze not only nonstationary linear response but also nonstationary response of hysteretic structures subjected to earthquake motion from the following merits. 1) This method can be applied to any kind of nonstationary envelope function $\psi(t)$ of the excitation. 2) The process of numerical calculation is not complex as long as the intensity of excitation is considered constant during short interval of time segments. 3) Parameters of equivalent linear structures can be changed at the beginning of any time segment.

4-5-2 Predicted and Simulated Mean-Square Response

(i) Analytical Prediction

The mean square response of structures with bilinear hysteretic restoring force subjected to nonstationary excitation is predicted by using both the equivalent linearization technique investigated in the section of 4-2-3 and the step-by-step method discussed in the previous section. Two techniques are used following next procedures. The equivalent linear parameters β_{eq} and ω_{eq} at the first time segment are taken to be equal to β_o and ω_o (parameters of linear structure), respectively and the linear response at the end of the first time segments is calculated from Eqs.(4-34)$\sim$(4-36), since response of structures is considered

to be in the elastic range at the beginning of vibration. Then equivalent linear parameters β_{eq} and ω_{eq} for the second time segment are determined from Eq.(4-18) according to the response level of σ_{μ}^2, $\sigma_{\dot{\mu}}^2$ and $\rho_{\mu\dot{\mu}}$ at the end of the first time segment. At the second time segment, the nonstationary response of the equivalent linear structure with parameters β_{eq} and ω_{eq} is calculated under the initial conditions stipulated by σ_{μ}^2, $\sigma_{\dot{\mu}}^2$ and $\rho_{\mu\dot{\mu}}$. Then the equivalent linear parameters for the third time segment will be determined in the same manner as those for the second time segment. This process of calculation is schematically illustrated in Fig.4.19.

In Fig.4.20 (a), (b), (c) and (d), predicted nonstationary mean-square response of "relatively rigid" hysteretic structures subjected to the nonstationary excitation and corresponding amplitude-dependent equivalent linear parameters ω_{eq} and h_{eq} are plotted for a set of parameters r_s=2.5, η=0.5, h_f=0.9, n=0.00, 0.50, 0.75, h_o=0.1. The larger value of mean-square response is found for the stronger nonlinearity of hysteresis loops. It is also observed that time lag between the peak of response and that of the excitation is enlarged due to nonlinearity. It is obvious that cause of these results is mainly attributable to softening-type of nonlinearity which lets the equivalent natural period longer and consequently shifts the structural receptance closer to the peak of excitation. When nonlinearity parameter n is equal to 0.75, ω_{eq} is found to decrease down to almost half of ω_o. This means that ω_{eq} is becoming very close to predominant frequency ω_f of excitation. Extreme growth of mean-square response is the consequence of above discussed "resonance". As could be expected, h_{eq} grows greater as nonlinearity of hysteresis loop becomes stronger. Increase of equivalent damping factor h_{eq} generally suppresses dynamic response. However,effect of hysteretic energy absorbing is so less than that of frequency shifting that the larger mean-square response is predicted inspite of the larger values of h_{eq}.

The predicted nonstationary mean-square response of "relatively

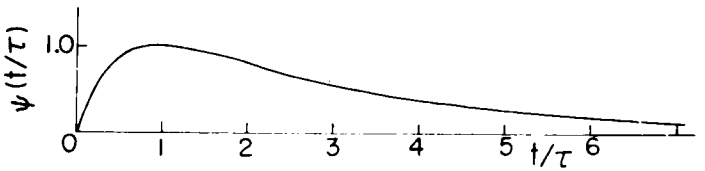

(a) Nonstationary Envelope Function of the Excitation

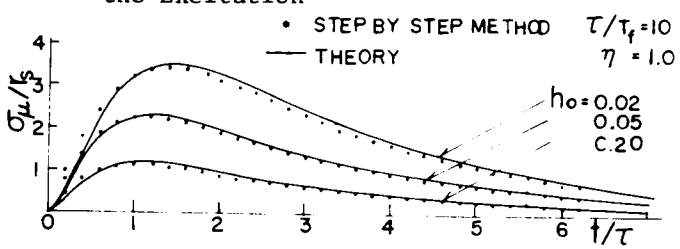

(b) Comparison between Step-by-Step Method and Theoretical Result[1)]

Fig.4.18 Nonstationary R.M.S. Response of Linear Structures

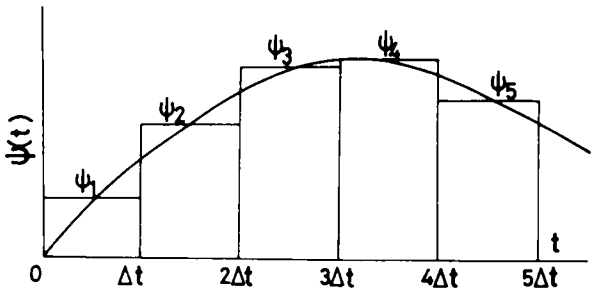

(a) Nonstationary Envelope Function of Excitation

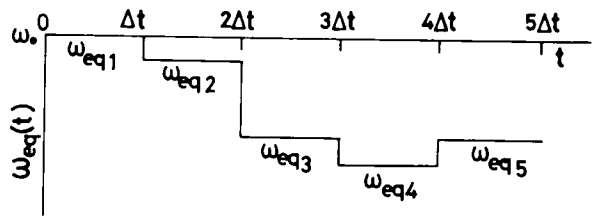

(b) Equivalent Natural Frequencies

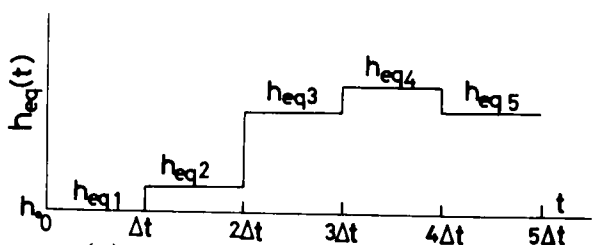

(c) Equivelnt Damping Factors

Fig.4.19 Schematical Illustration of Step-by-Step Equivalent Linearization Technique

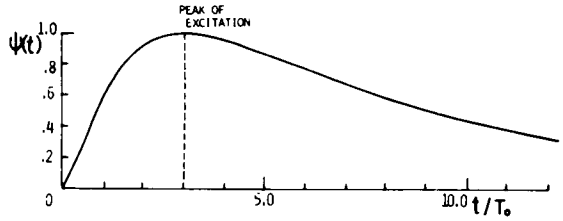

(a) Nonstationary Envelope Function of the Excitation

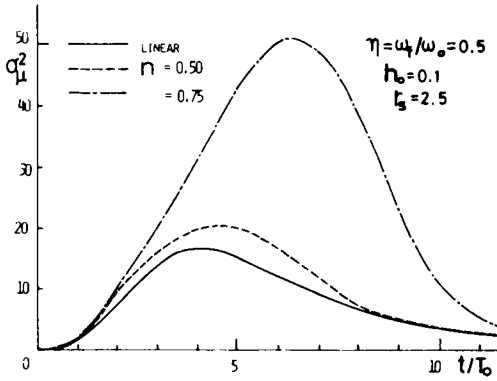

(b) Mean-Square Response of Ductility Factor

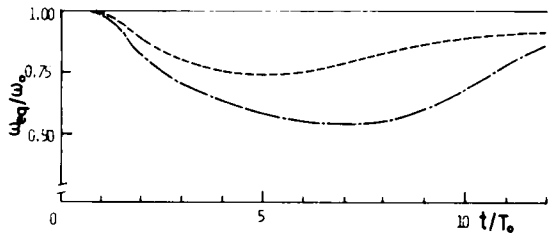

(c) Equivalent Natural Frequency

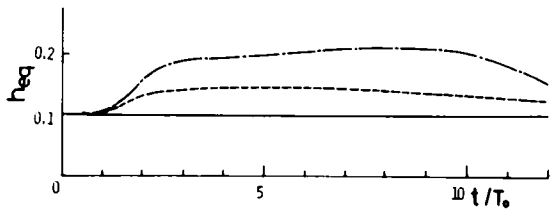

(d) Equivalent Damping Factor

Fig.4.20 Nonstationary Mean-Square Response of Ductility Factor and Transition of ω_{eq} and h_{eq} (Relativley Rigid Bilinear Structures)

intermediate" and "relatively soft" hysteretic structures is plotted in Fig.4.21 (a) and (b). Hysteretic response of "relatively intermediate" structures is found sometimes larger and other times smaller than linear response. This complicated response is a result of combined effects of frequency and yielding level dependent characteristics of hysteretic structures.

In Fig.4.21 (b), it is noticed that hysteretic response of "relatively soft" structures is limited and time lag between the peaks of response and excitation is shortened as nonlinearity becomes strong. Limited mean-square response is attributable both to decrease of ω_{eq} which lets the structural receptance far from the peak of excitation and to increase of h_{eq} due to hysteretic energy absorbing. However, shortened time lag is attributable only to additional damping, because the time lag is generally enlarged when period of structures becomes long[1)].

(ii) Numerical Simulation

To check the accuracy of analytically predicted mean-square response of hysteretic structures, a numerical simulation is carried out on a digital computer. Earthquake type nonstationary random excitations are generated as product of the nonstationary envelope function $\psi(t)$ shown in Fig.4.20 (a) and stationary random process discussed on the section of 4-3-3. 50 samples of the artificial earthquake are made using Monte Carlo method and hysteretic response to each one of them is numerically calculated by linear acceleration method. The nonstationary mean-square response plotted in Fig.4-22 is estimated as the ensemble average of 50 samples of calculated response.

Fig.4.22 (a) shows that the predicted and simulated results agree relatively well when nonlinearity is moderate (n=0.5). Especially at the beginning of vibration, they coincide fairly well, since the history of response is similar to elastic respone. When response grows larger, plots of simulated results fluctuate about theoretically predicted value. This fluctuation is supposed to be an effect of yielding which lets time history of response different from that of elastic response. However, it

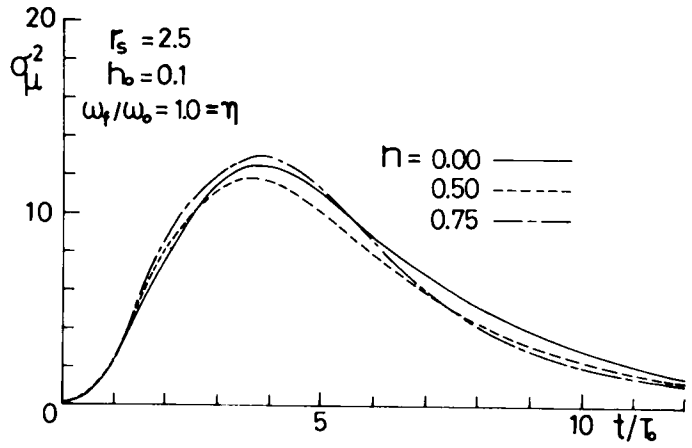

(a) "Relatively Intermediate" Bilinear Hysteretic Structures

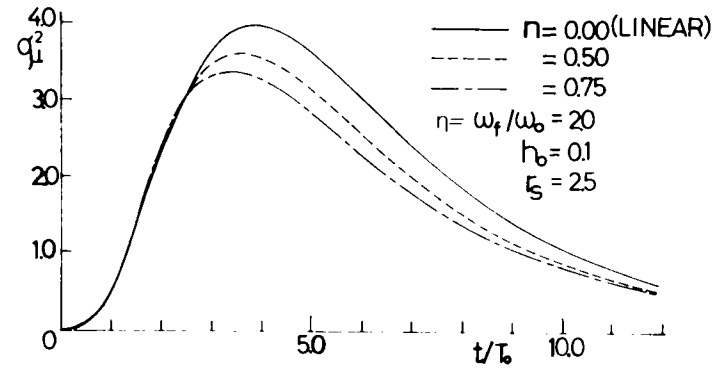

(b) "Relatively Soft" Bilinear Hysteretic Structures

Fig. 4.21 Nonstationary Mean-Square Response of Ductility Factor

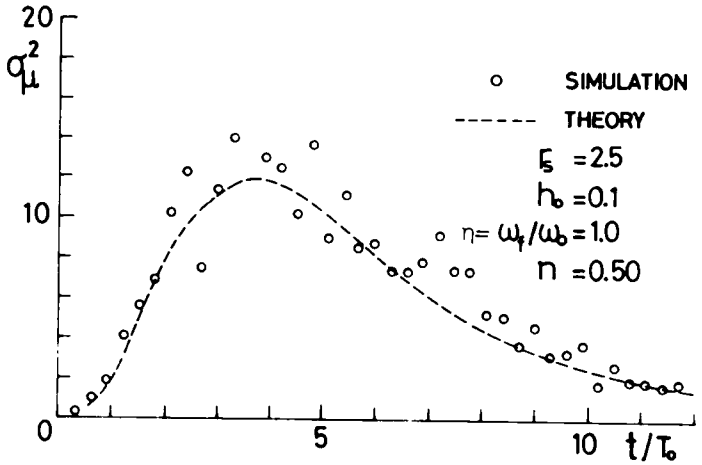

(a) Bilinear Structure with Moderate Nonlinearity (n=0.50)

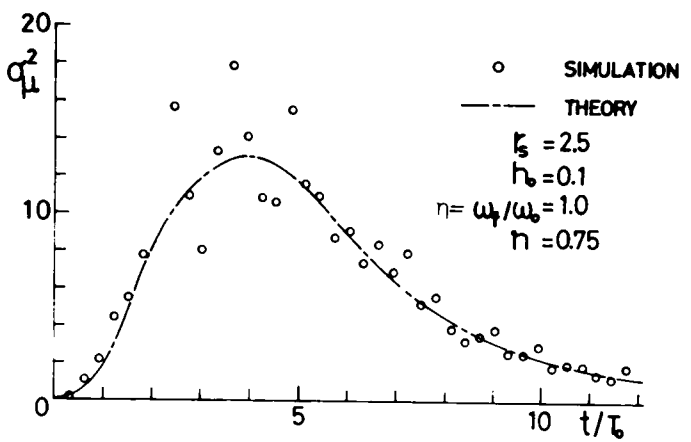

(b) Bilinear Structure with Relatively Strong Nonlinearity (n=0.75)

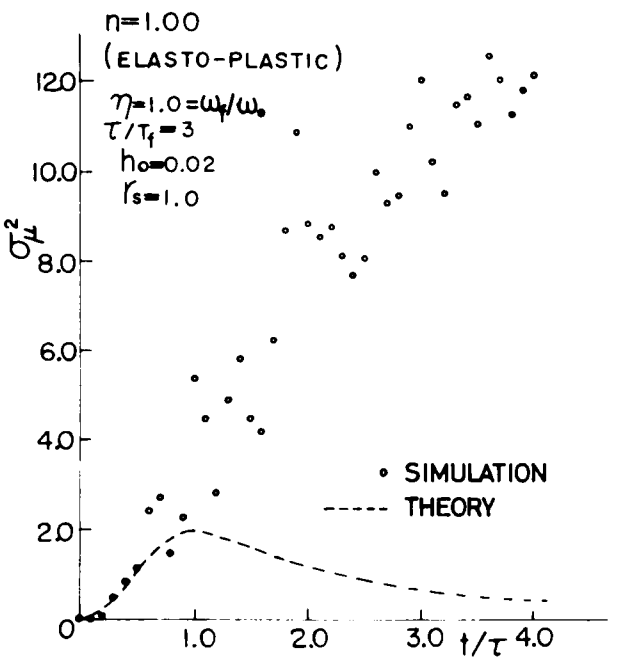

(c) Elasto-Plastic Structure (n=1.0)

Fig.4.22 Predicted and Simulated Nonstationary Mean-Square of Ductility Factor Response

would be gradually eliminated by increasing number of additional samples.

When nonlinearity becomes strong (n=0.75), simulated results plotted in Fig.4.22 (b) shows large fluctuation around peak of response. This fluctuation may also be a result of yielding. However after experiencing the peak of response, predicted and simulated results agree well, which suggests that no significant plastic deformation occurs during course of vibration as pointed out in the Chapter 2.

The discrepancy between the two results becomes quite clear for the structures with perfect elasto-plastic hysteresis loop (n=1.0) shown in Fig.4.22 (c).

4-5-3 Probability Distribution of Maximum Response (PDMR)

As discussed in the section of 4-4-2, estimation of the PDMR of hysteretic structures is quite significant for assessing structural reliability during strong earthquakes, because the PDMR represents the load effects beyond the yielding limit. In this section, the PDMR in nonstationary state is predicted through step-by-step linearization technique and envelope method. Then accuracy of them is checked by numerical simulation.

In the prediction of PDMR in stationary state, $C_o(\mu_{max}, t)dt$ is approximated by the unconditional crossing rate $N_\mu(\mu_{max}, t)$ of ductility factor response $\mu(t)$ at the level of μ_{max}. However it is recently reported that the assumption of Poisson process arrival of response envelope to the level of μ_{max} can be used more successfully than that of $\mu(t)$ itself because structural response is not white but narrow band process. The unconditional crossing rate $N_W(\mu_{max}, t)$ of response envelope $W(t)$ at the level of μ_{max} is obtained by H.Kameda[24] as

$$N_W(\mu_{max}, t) = \int_0^\infty \dot{W}\phi_e(\mu_{max}, \dot{W})d\dot{W}$$

$$= \omega_{eq}\frac{\mu_{max}}{\sigma_\mu}\exp\{-\frac{1}{2}(\frac{\mu_{max}}{\sigma_\mu})^2\}[\sqrt{\frac{B}{2\pi}}\exp\{-\frac{\gamma^2}{2B}(\frac{\mu_{max}}{\sigma_\mu})^2\}$$

$$+\frac{\gamma\mu_{max}}{2\,\sigma_\mu}\{1+\mathrm{erf}(\frac{\gamma\mu_{max}}{\sqrt{2B}\sigma_\mu})\}] \qquad (4\text{-}49)$$

where

$$\left.\begin{aligned}\gamma &= \dot{\sigma}_\mu(t)/\{\omega_{eq}\sigma_\mu(t)\}\\ B &= 1-(1-\delta/\pi)^2/(1-h_{eq}^2)\\ \delta &= \tan^{-1}\{2h_{eq}\sqrt{1-h_{eq}^2}/(1-2h_{eq}^2)\}\end{aligned}\right\} \qquad (4\text{-}50)$$

In this study, the PDMR in nonstationary state is predicted by calculating $N_W(\mu_{max}, t)$ for every time segment to conduct the integration in Eq.(4-27). Predicted results are shown in Fig.4.23 (a), (b) and (c). In these figures, simulated results using maximum response of 50 samples calculated in the previous section are also plotted to check the accuracy of precition. Mean value and coefficient of variation of each PDMR are listed in Table-1.

In Fig.4.23 (a), it is noticed that "relatively rigid" structures exhibit larger maximum response for stronger nonlinearity. It is found in Table-1 that nonlinearity of hysteresis loops makes not only mean values but also coefficient of variation larger. General trends of predicted and simulated results agree well except the magnitude of coefficient of variation. Simulated results show always larger coefficients of variation than predicted results presumably due to assumptions in theoretical analysis and also effect of yielding when nonlinearity is strong. This result suggests that higher estimation of structural reliability would result in when the theoretically predicted PDMR is used as distribution of load over structural members during strong earthquakes. Because structural reliability will be increased when small coefficient of variation of load distribution is used, even though its mean value remains unchanged.

Predicted and simulated PDMR of "relatively intermediate (η=1.0)"

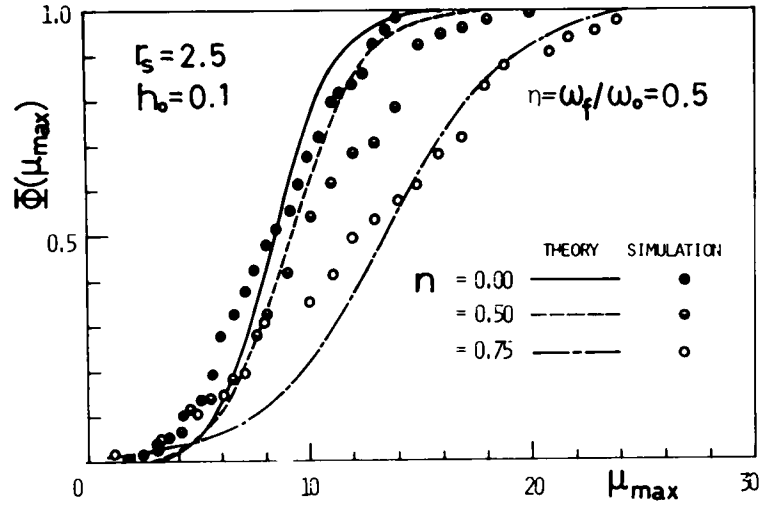

(a) "Relatively Rigid" Biliear Structures

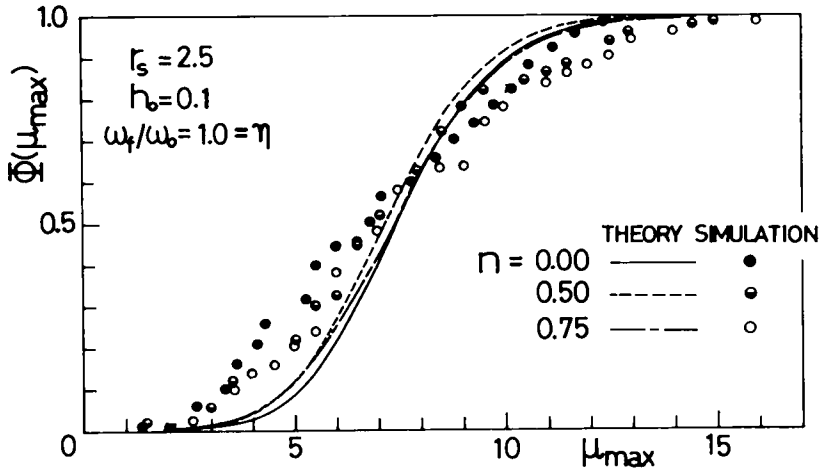

(b) "Relatively Intermediate" Bilinear Structures

Fig.4.23 Probability Distribution of Maximum Ductility Factor in Nonstationary Response

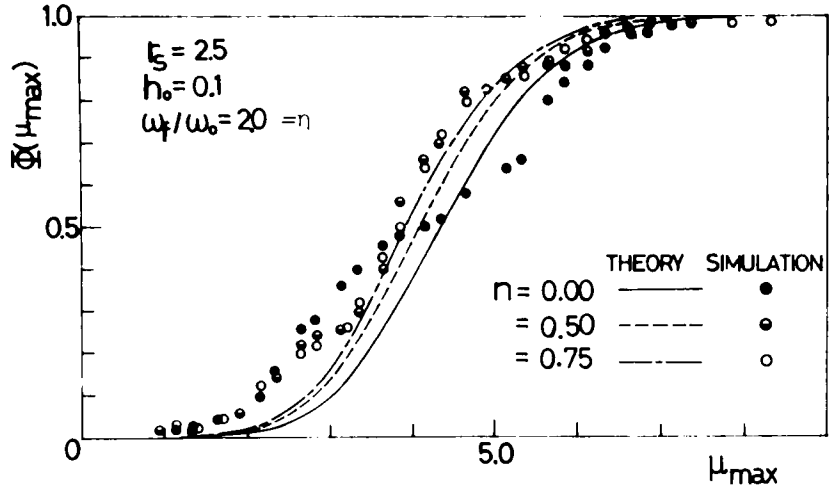

(c) "Relatively Soft" Bilinear Structures

Fig.4.23 Probability Distribution of Maximum Ductility Factor in Nonstationary Response (cont'd)

Table 1 Mean and Coefficient of Variation of Maximum Ductility Factor Response of Linear and Bilinear Structures

Period of Hysteretic Structures	Linearity	Predicted		Simulation	
		Mean Max. Response	Coef. of Variation	Mean Max. Response	Coef. of Variation
η=0.5	Linear	8.31	0.28	7.79	0.39
	n=0.50	9.00	0.30	9.60	0.43
	n=0.75	12.91	0.33	12.09	0.52
η=1.0	Linear	7.35	0.27	6.92	0.49
	n=0.50	7.03	0.28	7.33	0.49
	n=0.75	7.22	0.30	7.61	0.50
η=2.0	Linear	4.21	0.27	4.11	0.47
	n=0.50	3.94	0.27	4.11	0.47
	n=0.75	3.80	0.27	3.95	0.50

hysteretic structures are shown in Fig.4.23 (b), from which no significant hysteretic effects are found. However Table-1 shows that mean values of predicted PDMR are limited due to hysteretic effects, although coefficients of variation are enlarged. Contrary, both mean values and coefficients of variation of simulated PDMR are enlarged with nonlinear parameter n. The difference between predicted and simulated results suggests that theoretically expected hysteretic energy absorption has little effects to suppress simulated response of "relatively intermediate" hysteretic structures. But simulated hysteretic response does not grow so large as "relatively rigid" hysteretic structures, because the peak of structural receptance is shifting away from the peak frequency of the excitation.

Predicted and simulated PDMR of "relatively soft (η=2.0)" hysteretic structures shown in Fig.4.23 (c) and listed in Table-1 indicate that effect of hysteretic energy absorption can be expected in a sense of mean values. However coefficients of variation of simulated PDMR show the larger values for the stronger nonlinearity. Hence it would be concluded that effects of hysteretic energy absorption in nonstationary response can little be expected to make structural reliability increase even if structures are "relatively soft".

4-6 Conclusions

In this chapter, applicability of linearization techniques to predict r.m.s. response and probability distribution of maximum response of bilinear hysteretic structures subjected to stationary and nonstationary excitation is intensively investigated to furnish useful information for aseismic structural design with emphasis on ductility requirements. Main conclusions derived from the study are as follows.

(1) Two equivalent linearization techniques are adopted for theoretical prediction of earthquake response of hysteretic structures; one is the least mean-square error method and the other is the energy

balance method. From the analysis assuming the slowly varying amplitude and phase angle of response, it is found that the final expressions of the equivalent damping coefficient and of the equivalent natural frequency derived from the two methods have the same form.

(2) From examinations of theoretically predicted stationary r.m.s. response by the iterative linearization technique, it is found that hysteretic restoring force has different effects on its response depending both on yielding level and natural frequency ω_o of hysteretic structures relative to intensity and predominant frequency ω_f of random excitation. Existence of the optimum yielding level at which hysteretic energy absorption has the maximum effect to suppress r.m.s. response is confirmed. Response of "relatively rigid ($\eta=\omega_f/\omega_o=0.5$)" bilinear structures is increased with nonlinearity of hysteresis loops although that of "relatively soft ($\eta=2.0$)" structures is decreased.

(3) Frequency and yielding level dependant r.m.s. response characteristics of hysteretic structures are examined in terms of equivalent linear parameters corresponding to predicted response. It is found that response characteristics can reasonably be explained from the concept of the transition of the structural receptance with equivalent linear parameters relative to the power spectrum density of excitation. That is, the receptance of "relatively rigid" structures moves closer to the peak of spectrum of the excitation due to nonlinearity of hysteresis loop. On the contrary, that of "relatively soft" hysteretic structures shifts away from the peak frequency.

(4) The step-by-step linearization technique which defines the equivalent linear parameters varying with the response level of previously determined equivalent linear structures is successfully applied to predict nonstationary mean-square response of hysteretic

structures to earthquake-type random excitation.

(5) Probability distribution of maximum ductility factor response of hysteretic structures in stationary and nonstationary state is theoretically predicted by applying pure-birth and envelope methods. The mean value of maximum response of "relatively rigid" structures is found to increase with nonlinearity of hysteresis loop, where as those of "relatively intermediate" and "relatively soft" hysteretic structures are noticed to decrease. This tendency is attributable to the same reason discussed in prediction of r.m.s. response. However, effects of hysteretic energy absorbing in nonstationary maximum response of "relatively intermediate and soft" structures can not be expected so much as in stationary maximum response.

(6) From error survey made with the aid of numerical simulations on a digital computer, it is concluded that the equivalent linearization techniques dealt with herein are applicable for prediction of stationary and nonstationary r.m.s. response of bilinear hysteretic structures within the nonlinear parameter $0.00 \leq n \leq 0.75$. Simulated probability distribution of maximum ductility factor response shows much larger values of coefficients of variation than predicted values to suggest that theoretical analyses discussed in this study would result in higher estimation of structural reliability than actual probability of safety during strong earthquakes.

References for Chapter 4

1) For an example, H. Kameda: On Estimation of the Maximum Response of Structures Subjected to Random Earthquake Motion, Proc. of JSCE, No. 201, 1972, pp. 1-12, (in Japanese).

2) T.K. Caughey: Deviation and Application of the Fokker-Planck Equation of Discrete Nonlinear Dynamic Systems Subjected to White Random Excitation, Journal of ASA, Vol. 35, 1963, pp. 1683-1692.

3) T.K. Caughey: Random Excitation of A System with Bilinear Hysteresis, Journal of Applied Mechanics, ASME, Vol. 27, 1960, pp. 649-652.

4) T. Kobori and R. Minai: Linearization Technique for Evaluating the Elasto-Plastic Response of A Structural System to Non-Stationary Random Excitations, Annual Report of the DPRI, Kyoto Univ., No. 10A, 1967, pp. 235-260, (in Japanese).

5) T.K. Caughey: Equivalent Linearization Techniques, Journal of ASA, Vol. 35, No. 11, 1968, pp. 1706-1711.

6) Y. Sawaragi, Y. Sunahara and K. Soeda: Non-Stationary Response of Nonlinear Control Systems with Randomly Time-Varying Characteristics Subjected to A Suddenly Applied Stationary Gaussian Random Input, Proc. of JSME, No. 197, 1963, pp. 211-218, (in Japanese).

7) W.D. Iwan and L.D. Lutes: Response of the Bilinear Hysteretic System to Stationary Random Excitation, Journal of ASA, Vol. 43, No. 3, 1968, pp. 545-552.

8) L.D. Lutes: Stationary Random Response of Bilinear Hysteretic Systems, Ph.D. Thesis, Cal Tech, 1967.

9) L.D. Lutes: Equivalent Linearization for Random Vibration, Journal of the E.M. Division, ASCE, Vol. 96, No. EM3, 1970, pp. 229-242.

10) H. Takemiya: Equivalent Linearization for Randomly Excited Bilinear Oscillator, Proc. Of JSCE, No. 219, November, 1973, pp. 1-14, (in Japanese).

11) P.C. Jennings: Equivalent Viscous Damping for Yielding Structures, Journal of the EM Division, Vol. 94, No. EM1, 1968, pp. 103-116.

12) L.S. Jacobsen: Steady Forced Vibration as Influenced by Damping, Journal of Applied Mechanics, ASME, Vol. 52, No. 22, 1930, pp. 169-181.

13) D. Karnopp and R.N. Brown: Random Vibration of Multi-Degree-of-Freedom Hysteresis, Journal of ASA, Vol. 42, No. 1, 1967, pp. 54-59.

14) D.E. Hudson: Equivalent Viscous Friction for Hysteretic Systems with Earthquake-like Excitations, Proc. of the third WCEE, Vol. II, 1965, pp. II-185∿206.

15) N. Wiener: Extrapolation, Interpolation and Smoothing of Stationary Time Serries with Engineering Applications, The MIT Press, 1949.

16) L.S. Jacobsen: Damping in Composite Structures, Proc. of the second WCEE, Vol. II, 1960, pp. 1029-1044.

17) H. Goto and H. Iemura: Linearization Techniques for Earthquake Response of Simple Hysteretic Structures, Proc. of JSCE, No. 212, April, 1973, pp. 109-119.

18) H. Goto and H. Iemura: A Study on the Plastic Deformation of Elasto-Plastic Structures in Strong Earthquakes, Proc. of JSCE, No. 184, December, 1970, pp. 57-67, (in Japanese).

19) S.-C. Liu, discussion of "Equivalent Viscous Damping for Yielding Structures" by P.C. Jennings, Journal of EM Division, ASCE, Vol. 94, No. EM4, August, 1968, pp. 1003-1008.

20) H. Kameda and H. Iemura: Dynamic Response of Single-Degree-of-Freedom Hysteretic Systems, Proc. of the third JEES, 1970, pp. 349-356, (in Japanese).

21) S.O. Rice: Selected Papers on Noise and Stochastic Processes edited by N. Wax, Dover Pub., 1954, pp. 133∿294.

22) T.K. Caughey and H.J. Stumpf: Transient Response of a Dynamic System under Random Excitation, Journal of Applied Mechanics, No. 4, 1961, pp. 563∿566.

23) H. Goto and H. Kameda: On the Probability Distribution of the Maximum Structural Response in Random Vibration, Annuals of the DPRI, Kyoto Univ., No. 124, 1969, pp. 289∿299, (in Japanese).

24) H. Kameda: On Estimation of the Maximum Structural Response to Random Earthquake Motion from Response Envelope, the Memoirs of the Faculty of Engineering, Kyoto Univ., Vol. XXXVI, Part 4, April 1975, pp. 458~471.

5. EARTHQUAKE RESPONSE OF DETERIORATING HYSTERETIC STRUCTURES

5-1 General Remarks

It is the intent of most modern approaches to earthquake-resistant design to produce a structure capable of responding to moderate shaking without damage, and capable to resisting the unlikely event of very strong shaking without seriously endangering the occupants. In the second case, however, structural damage and large deflections are permissible provided collapse is not imminent. To achieve this goal, it is necessary to understand the way buildings and other structures respond to deflections beyond the elastic limit, and much analytical and experimental work has been directed in recent years toward developing the required knowledge. In this effort, the development of analytical models for hysteretic behavior has been guided almost exclusively by static tests of structural elements and assemblages because it is not yet possible to excite full-scale structures significantly into the yielding range, and because the response of structures that have been heavily damaged under the action of strong earthquake motion has not yet been recorded. Thus the desired full-scale, dynamic, confirmation of the approaches to the analysis of earthquake response of deteriorating hysteretic structures have not been obtained yet.

In many studies of nonlinear response to earthquake motions or other dynamic forces, the yielding properties of structurs have been modelled by the well-known elasto-plastic or bilinear force-deflection relations. References 1) and 2) are among the earliest works, and Reference 3) is one of the several studies presented at the fifth WCEE which used these relations. In addition to these simple yielding relations, trilinear[4] and smoother but more complex models of yielding behavior[5] have also been used in studies of earthquake response. Some of the most recent work in this area includes the development of models for the deteriorating hysteresis evidenced by structures that are weakened by excursions beyond the elastic limit.[6),7]

The occurrence of an earthquake can be viewed as a full-scale experiment and it is possible to learn much about the properties of

structures from examination of their response to strong shaking[8]. The largest collection of data of this type is from the recent San Fernando earthquake[9] in which responses of about 50 instrumented buildings in the Los Angeles area were obtained. None of the instrumented buildings was heavily damaged, but some did show evidence of nonlinear behavior in the form of lengthening of periods of the lower modes of vibration over those found from low-level vibration tests. A particular example of this occurred in the E-W response of the Millikan Library on the campus of the California Institute of Technology. The earthquake motion was measured at the basement and at the roof by two RFT-250 accelerographs which recorded the N-S, E-W and vertical components of the earthquake motion and building response. During the earthquake, the E-W motion at the roof reached a peak value of 340.5 cm/sec^2 (35%g), and clearly showed the fundamental period to be about one second, which is 50% greater than the value of 0.66 secs determined from forced vibration tests performed before the earthquake[10),11)]. (The N-S response showed about a 20% reduction in the fundamental natural frequency.) Visual examination of the E-W accelerogram and Fourier analysis of the record[12),13)] suggested that the library responded to the earthquake motion as a hysteretic structure to a degree that might make it an useful object of study.

The only observed effects in the building after the earthquake that might bear on the E-W response were small cracks at some floors in the interior plaster at the points of supports of the precast window wall panels. The exterior of the panels can be seen on the south face of the building in Fig.5.1. Because the building suffered no observable structural damage and because only the earthquake response at the top floor was available, it was not considered justified to make a detailed, nonlinear model of the structure of the library. It was decided instead to treat the response of the library in its fundamental mode as a single-degree-of-freedom (simple) hysteretic structure. The intent of this approach was to learn in a general way about the response of the building during the earthquake, and also to develop techniques of analysis that

may be useful when the response of damaged structures is obtained in the future. In particular, it was interested in finding out if the response of the library in its fundamental mode could be satisfactorily described by one of the simpler models for hysteretic behavior.

As described in this chapter, several methods were tried in the attempt to find simple descriptions for the nonlinear response of the building during the earthquake. First, the measured motion of the fundamental mode of the structure was examined to see if the hysteretic relation could be determined from the measured earthquake response. It was found that, with some care, the dynamic force-deflection relation of the fundamental mode could be recovered. Another portion of this analysis was concerned with the nonstationary characteristics of the response in terms of the parameters of equivalent fundamental frequency and equivalent viscous damping. The changes of these variables during the response guided the selection of nonlinear models of the structure. The second major portion of the study was devoted to a comparison of the recorded response of the fundamental mode with that predicted by analyses using various hysteretic models. The models included a stationary linear model with damping and frequency characteristics chosen to match the recorded response, a stationary bilinear model, and two nonstationary models. The nonstationary models were of two types, an equivalent linear model with damping and fundamental frequency that changed at selected times during the earthquake, and a nonstationary, bilinear hysteretic model whose properties also were changed during the response. A discussion is made for the accuracy of the proposed various methods to reproduce the recorded response of Millikan Library.

In the final portion of the study, a new simple method to represent deteriorating bilinear hysteretic structures was proposed. As a basic measure of structural deterioration, cumulative damage and residual strength derived from the theory of low-cycle fatigue were adopted. Then equivalent linear parameters of the hysteretic structures were controlled to degrade with decreasing residual strength of structures. Effects of

structural deterioration to earthquake response were examined by comparing nonstationary mean-square response of linear, conventional bilinear and proposed deteriorating bilinear structures.

5-2 Millikan Library and the Recorded Earthquake Response

5-2-1 Brief Description of Millikan Library

The Millikan Library at the California Institute of Technology is a nine-story, reinforced concrete building constructed in 1966[11]. The lateral load resistance in the N-S direction is provided by reinforced concrete shear walls and the resistance in the E-W direction is provided by a central elevator and stairwell core also of reinforced concrete. In addition, the structure possesses a reinforced concrete frame. The shear walls comprise the east and west faces of the building, whereas the north and south faces consist of precast concrete window-wall panels which are attached three per floor between reinforced concrete columns. It was determined from forced vibration tests of the structure during construction that these precast window-wall panels added appreciable stiffness to the structure for motions in the E-W direction. An exterior view of the building is shown in Fig.5.1 which also includes sketches of the foundation. More detailed information about the structure can be found in References 10) and 11).

5-2-2 Results of Vibration Tests of the Library

During the final stages of construction, the library was subjected to an extensive series of dynamic tests by P.C.Jennings and J.Kuroiwa[10),11)]. In these tests it was found that the fundamental period in the E-W direction was 0.66 secs. This value increased roughly 3% over the amplitude range of testing. The mode shape corresponding to this fundamental frequency was found from measurements taken at every other floor of the structure. In the vibration test the damping in the fundamental E-W mode varied between 0.7 and 1.5 percent of critical, increasing with the amplitude of response. Measurements of the foundation motions and

(a) General View

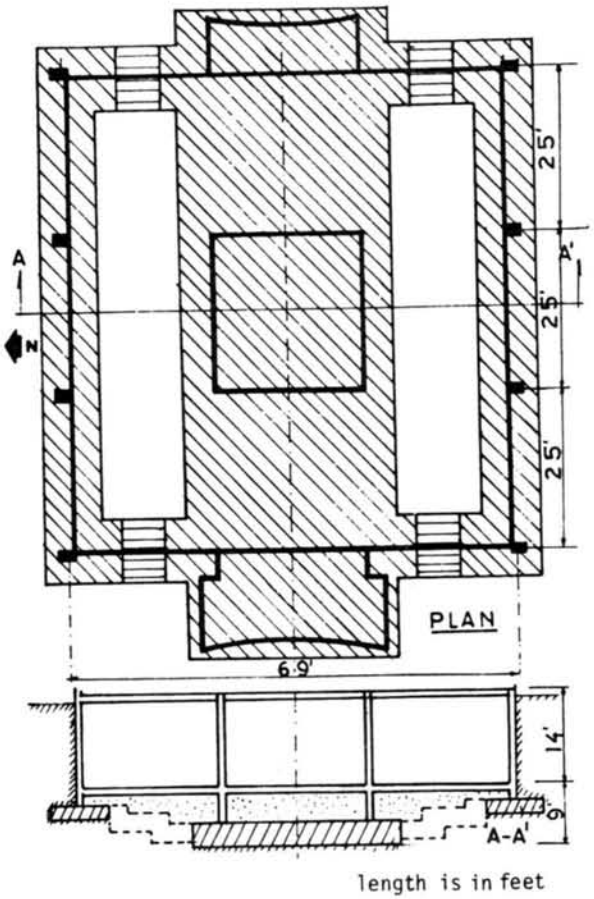

(b) Foundation and Framing Details

Fig.5.1 Millikan Library Building at the California Institute of Technology

motions on the nearby surface of the ground showed that the building responded nearly as if it were fixed at the foundation; rocking contributed less than one percent to the total roof motion of the structure, and foundation translation less than about two percent.

Within a few days after the earthquake an ambient vibration test was performed on the structure during which the fundamental E-W period was observed to be 0.80 secs[12),14)]. Hence, there appeared to be a permanent change in the fundamental period of small vibrations in the E-W direction. It has been found that since the post-earthquake test, the structure has partially recovered and it exhibited a fundamental period of 0.73 secs in the E-W direction in December, 1972[12)].

5-2-3 Accelerograms Recorded During the Earthquake

Two accelerograms, one at the basement and one at the roof, were obtained at the Millikan Library during the San Fernando earthquake. The accelerograms and the calculated velocities and displacements are shown in Figs.5.2 and 5.3[15),16)]. In these figures, 80 secs of motion is shown, but not all of this motion is important to the present study. The first 40 secs of the accelerogram at the basement may be separated for discussion into two parts. The first part of the accelerogram (from 0 to about 15 secs) has a high acceleration level with a relatively high predominant frequency, whereas the second part of the record (from 15 to 40 secs) shows a relatively low acceleration level, and a lower predominant frequency. Comparing Figs.5.2 and 5.3, it seems that the different character of the response in Fig.5.3 in the early and latter parts of the record may be due to the different types of excitation that arrived during these two portions of time[17)]; there appears to be a larger fraction of surface waves in the latter portion of the basement accelerogram. The first part (0-15 secs) of the accelerogram shown in Fig.5.3 consists of a mixture of the first and second modes of response. The period of the second mode in the E-W direction is approximately 0.17 sec. During the second portion of the response (15-40 secs) the motion consists almost exclusively of the fundamental mode. Comparing the levels of

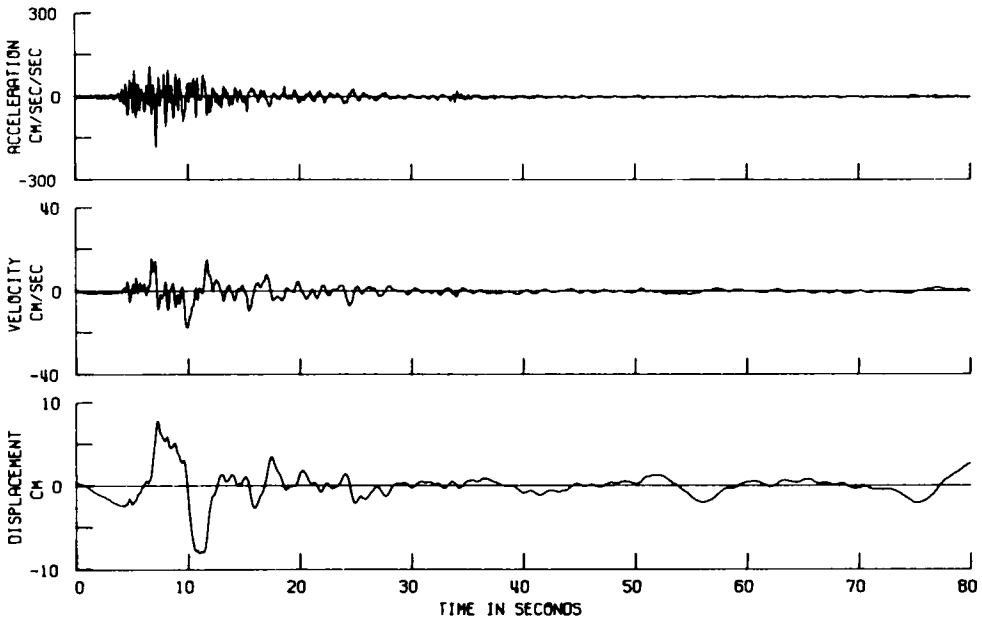

Fig.5.2 Recorded Acceleration, and Computed Velocity and Displacement for the Basement Motion, E-W Direction during the San Fernando Earthquake

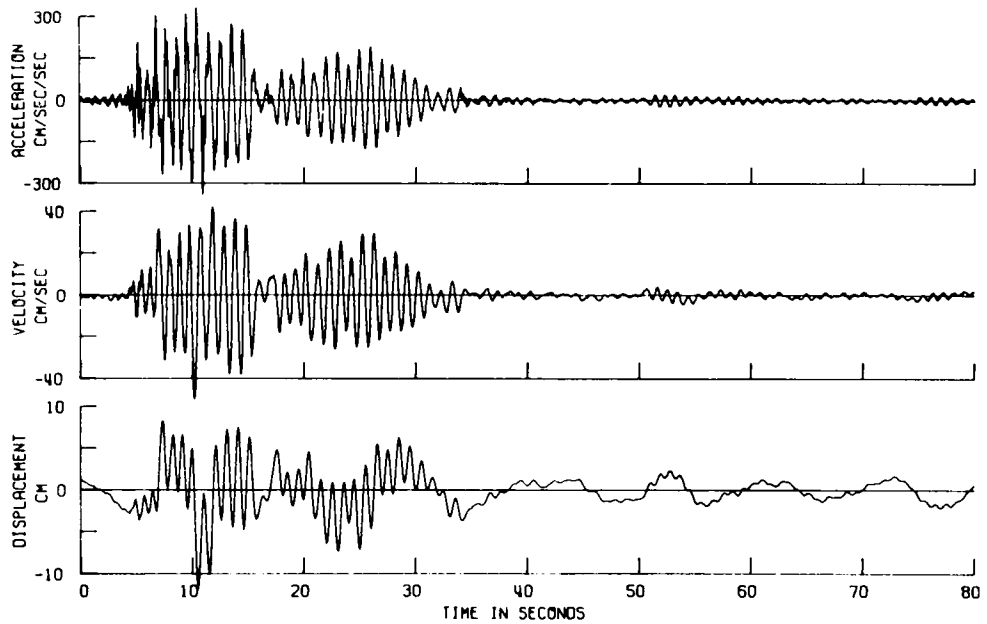

Fig.5.3 Recorded Acceleration, and Computed Velocity and Displacement for the Roof Motion, E-W Direction during the San Fernando Earthquake

measured acceleration at the base and at the roof, it appears that the ground motion was such as to excite the structure in a quasiresonant fashion during the latter part of the record.

The displacement record in Fig.5.3 consists of a short-period (about 1.0 sec) portion and fluctuations at longer periods. Since the acceleration at the roof records the absolute motion of the structure, it is considered that the displacement record shows a combination of the motion of the structure with respect to the base, which is the motion of shorter period, superimposed upon a longer-period motion which represents the displacement of the foundation seen in Fig.5.2.

There are two major characteristics of the motion which are most apparent from examination of the records of earthquake response. First, the fundamental period of the E-W vibration during the strong motion is about 50% longer than that measured at small amplitudes during vibration tests; it is clear from Fig.5.3 that the period of the E-W fundamental mode during the earthquake is near one second. Second, the records show that the library responded primarily in its fundamental mode in this direction. Although there is some vibration of the second mode apparent in the first part of the response, it is generally small with respect to the response of the fundamental mode. From these observations it was thought possible to consider the library to be a simple hysteretic structure responding to the earthquake, filtering or disregarding components of higher modes of response.

5-3 Analysis of Recorded Accelerograms

5-3-1 Calculation of Relative Velocity and Displacement

The calculation of relative velocity and displacement is required to determine the hysteretic character of the restoring force acting on the structure as a function of amplitude of response. Considering the library as a simple oscillator, the acceleration, velocity and displacement shown in Fig.5.3 may be considered as the absolute response of the oscillator, whereas those in Fig.5.2 may be considered as the base motion.

Therefore, if the two recorded accelerograms have an accurate time correspondence, the relative velocity and displacement of the oscillator can be obtained by subtracting the calculated ground velocity and displacement from the calculated values of velocity and displacement obtained from the record measured on the roof.

Fortunately, the two accelerograms were recording a common time signal and were, in fact, a part of a more extensive network[18] which included accelerographs at the Jet Propulsion Laboratory, Millikan Library and the Caltech Seismological Laboratory.

When the calculated values and displacement were subtracted from each other to obtain the relative motion, it was found in preliminary analyses that the relative displacement included long fluctuations with a period of about 11 secs. It was subsequently pointed out by T.C.Hanks that these were due to a processing error in the digitizing of some accelerograms, which has since been corrected. To eliminate this 11-second period motion from the records analyzed in this study, a low-pass filter proposed by Jennings, Housner and Tsai[19] was employed. The subtracted and corrected relative acceleration, velocity and displacement are plotted in Fig.5.4. Comparing Figs.5.3 and 5.4 (which are at different time scales) it is seen that the changes in the acceleration are slight, but the smoothing process of the integration, the subtraction of the long-period ground displacement, and the elimination of the digitizing error, have led to comparatively smooth curves for relative velocity and displacement. Some possible contributions of the second mode to the acceleration and relative velocity can be seen, but the relative displacement is essentially only that of the fundamental mode. It should be noted in Fig.5.4 that the motions beyond 40 secs have no longer been included in the analysis.

5-3-2 Natural Frequencies and Amplitudes From Relative Displacement

From the relative displacement shown in Fig.5.4 and replotted in Fig.5.5, it is easy to see that the period of the motion is much longer than the period of vibration exhibited at small amplitudes. To investigate

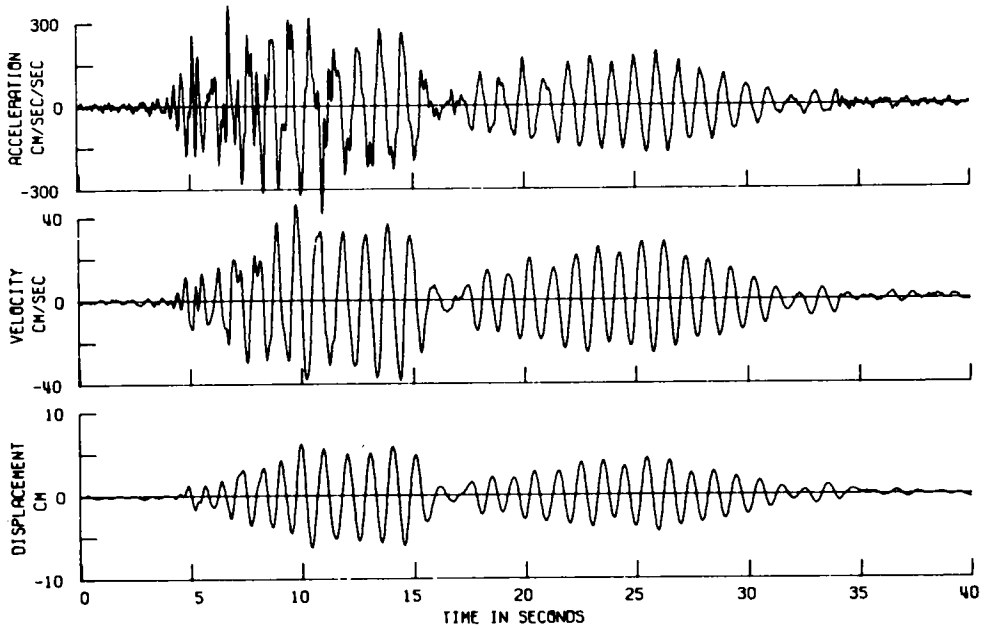

Fig.5.4 Relative Values of Acceleration, Velocity and Displacement of the Roof with Respect to the Basement

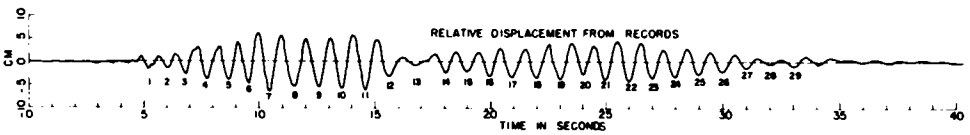

Fig.5.5 Relative Displacement of the Roof with Respect to the Basement.
(Numbers index cycles of the fundamental mode.)

the nature of the nonlinearity of the restoring force, the period and corresponding amplitude of each whole cycle of displacement were measured from Fig.5.5 and plotted in Fig.5.6. The number of each point in Fig.5.6 corresponds to the number of the cycle as indicated in Fig.5.5. The results obtained from the vibration tests before and after the earthquake are also plotted in Fig.5.6. The points in Fig.5.6 show considerable scatter, which is expected in a measure this crude, and it is hard to find clear relations in the figure. However, the points numbered 1 to 11 and the results of the tests before the earthquake suggest an approximately linear relation between the amplitude and period of vibration, with the larger amplitudes corresponding to the longer-period motion. The remaining points, numbers 12 to 29, are scattered about one second over a fairly wide range, but above the approximately linear band shown by points 1 to 11.

These results suggest that the library may have behaved like one hysteretic structure up until about 15 secs, and then changed to a different hysteretic structure. This is also consistent with the observed loss of structural stiffness indicated by the post-earthquake vibration test. To investigate this suggestion further, the measured periods of vibration are plotted on the time axis in Fig.5.7, which also includes, as lines, the results from the vibration tests before and after the earthquake. It is seen from this figure, which also shows considerable scatter, that the natural period tends to increase gradually until about 14 secs. Points number 12 and 13 show unusually long periods but these points may be subject to more error than others as the amplitude of response is quite small (Fig.5.5). After these points, most of the values fluctuate around one second. Similar trends were obtained by F.E,Udwadia and M.D.Trifunac from their analysis of the accelerograms using Fourier transform techniques[12),13)]. The results from their work confirm that the fundamental period of vibration in the E-W direction increased about 50% during the first part of the strong shaking, and remained at about one second for the rest of the first 40 secs of response, even though the amplitude of the response decreased. Their analysis also showed unusual behavior at about t=15 secs and, in the period of weak response from 40

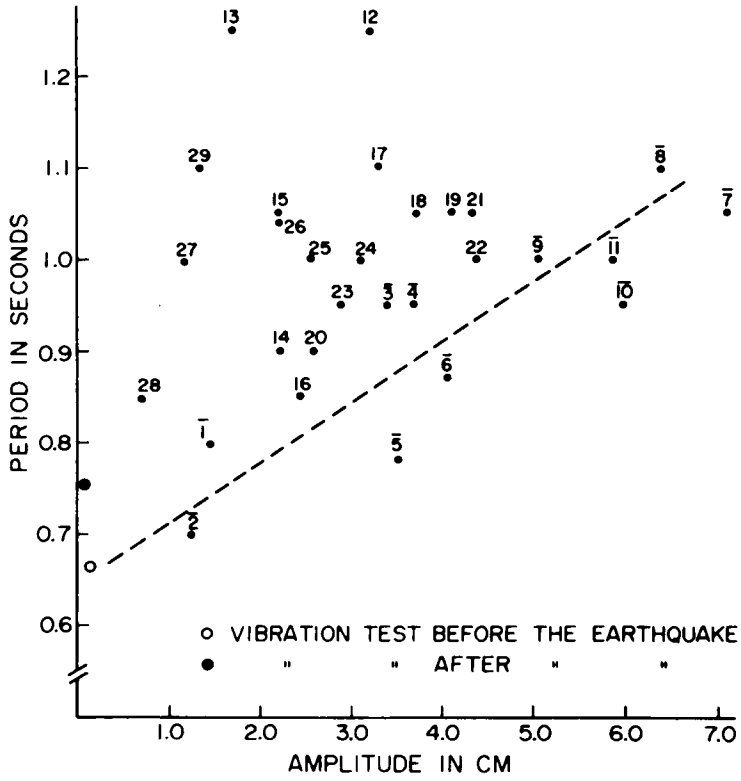

Fig.5.6 Plot of Period of Displacement Cycles vs. Amplitude of Motion (Numbers are indices shown in Fig.5.5.)

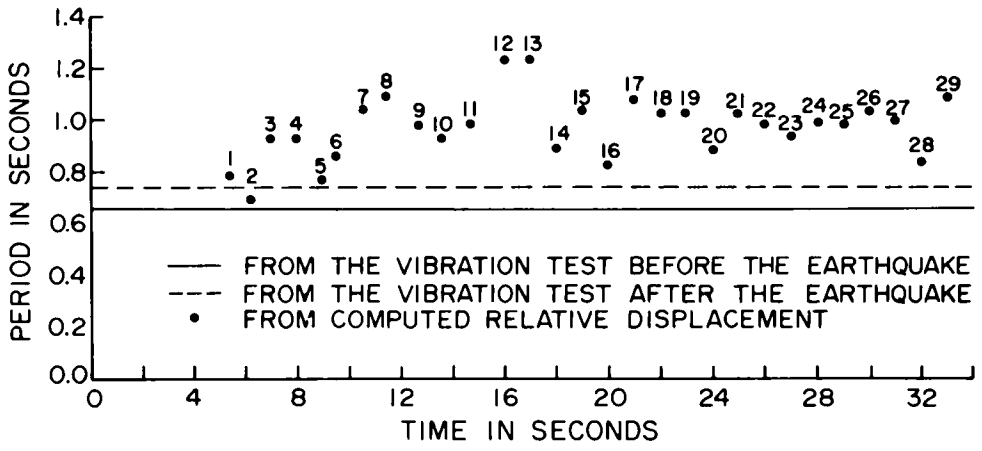

Fig.5.7 Plot of Period of Displacement Cycles vs. Time (Numbers are indices shown in Fig.5.5)

to 80 secs, a tendency for the period to shorten from 1.0 sec to values in the range of 0.8-0.9 secs.

5-3-3 Experimental Force-Deflection Relations of the First Mode

The analysis of the previous section identifies the nonlinearity of the restoring force as the reason for the lengthening fundamental period observed during the earthquake. In this section, the time-dependence of the hysteretic behavior of the library is studied by plotting the measured values of acceleration against the calculated values of relative displacement.

Consider the equation of motion of simple system excited by an earthquake:

$$F(x,\dot{x}) = -M(\ddot{x}+\ddot{z}) \tag{5-1}$$

in which $F(x,\dot{x})$ represents the nonlinear restoring force due to relative velocity $\dot{x}$ and displacement x ; M is the mass and $\ddot{z}$ is the ground acceleration. Eq.(5-1) shows that the total restoring force divided by the mass is the negative of the absolute acceleration. Using this relation, a preliminary version of the hysteretic response of the library was obtained by plotting the relative displacement shown in Fig.5.4 vs. the absolute acceleration shown in Fig.5.3. This trajectory, plotted every 0.02 secs, gave a reasobable estimate of the first-mode hysteresis of the library during the second portion of the response, because the first mode of the vibration predominates at this time. However, the first portion of the response (0 to 15 secs) showed marked fluctuations along the trajectory of the supposed first-mode hysteresis. This fluctuation was thought to be the result of the non-negligible contributions of the second mode of vibration of the library, which is discernible in this part of the acceleration records.

Because of the assumptions of the study it was considered appropiate to eliminate the effect of the second mode of vibration as well as any higher modes that may have participated in the response. If this

could be done, the desired trajectory between the absolute acceleration and the relative displacement of the fundamental mode would be obtained. The simple low-pass filter[19] mentioned above was again used to eliminate these higher mode responses from the absolute acceleration record and then the relative velocity and displacement were calculated. These curves are shown in Fig.5.8, which can be compared with the absolute acceleration in Fig.5.3 and the relative velocity and displacement in Fig.5.4. It can be seen from this comparison that the response of the higher modes has been greatly diminished, but not completely eliminated, especially in the region from about 5 to 8 secs. Using the results shown in Fig.5.8, the trajectory between the first mode absolute acceleration, which is proportional to the restoring force by Eq.(5-1), and the relative displacement was plotted every 0.02 secs and is given in Fig. 5.9. In plotting these trajectories it was found that there was a small phase error of about .04 to .06 secs between the absolute acceleration and the relative displacement. This phase error significantly affected the shape of the trajectories and, unless corrected, some of the trajectories indicated negative hysteretic damping. By close examination of the digitized data, the amount of this phase error was found to differ over the first 12 seconds of the response when compared to the part after 12 secs. The source of this small phase error could not be identified, but it is small enough that it is a possibility that it is a phase difference in the digitization, which cannot be expected to be much more accurate than about .04 to .06 secs. Other possibilities include instrument malfunction around t=12 secs or a small error in phase that might have been introduced because of the application of the filters to the record.

To adjust for the phase error, the time history of the relative displacement was shifted to match the peak value of the absolute acceleration during the two parts of the response. This was done because the maximum restoring force should occur at the same time as the maximum relative displacement for the small values of viscous damping associated

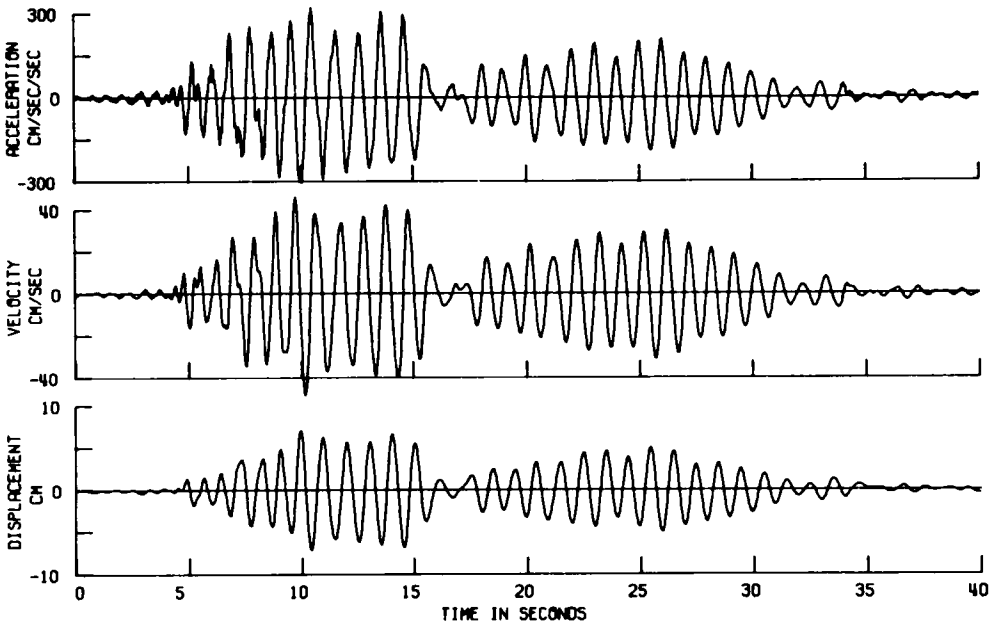

Fig.5.8 Absolute Acceleration, Relative Velocity and Relative Displacement, Filtered to Remove Response of Higher Modes

with the library. At the beginning of the response, from 0 to 4 secs as shown in Fig.5.9 (a), the hysteretic properties of the library are not clear because of the small amplitudes. As is well known, the tangent of the trajectory is equal to the square of the fundamental natural frequency for a structure that responds essentially in the linear range. The slope of the trajectory from 0 to 4 secs appears to be close to that of a linear structure with a natural period of 0.66 secs (for which the tangent value is $90/sec^2$), indicating that the library was vibrating at the beginning of the earthquake with the fundamental period found during the pre-earthquake vibration tests.

The slope of the trajectory is still steep from 4 to 6 secs as shown in Fig.5.9 (a). However, the plots show more hysteresis due to the high response levels. There is a large loop on the minus side of the trajectory and afterwards there is a sharp drop in the restoring force, perhaps indicating a sudden change in some structural elements due to the strong vibration. From 6 to 8 secs the slopes of the hysteresis loops have become less and the areas of the hysteresis loops have become larger. There are also some short-period fluctuations along the supposed first-mode hysteresis loops which are thought to be the results of the incomplete filtering of the absolute accelerogram as discussed above. It is also possible that these fluctuations represent small errors in the calculation, which appears to be a sensitive one. Fig.5.9 (b) shows the response from 8 to 10 secs, and it is seen that there are still some fluctuations and sudden changes in the restoring force but, in general, the loops are becoming smoother. The slopes of the hysteresis loops are clearly less than during the early part of the earthquake, and the area of the hysteresis loops is still large. As seen in the same figure, the slope of the hysteresis loops from 10 to 12 secs are almost as soft as the stiffness of the linear structure with a natural period of one sec. (a tangent value of $39/sec^2$). There is a suggestion, however, that the areas of the hysteresis loops during the period from 10 to 12 secs are less than those for 6 to 8, or 8 to 10 secs. There are still fluctuations in the trajectory which may be associated with the second mode of response.

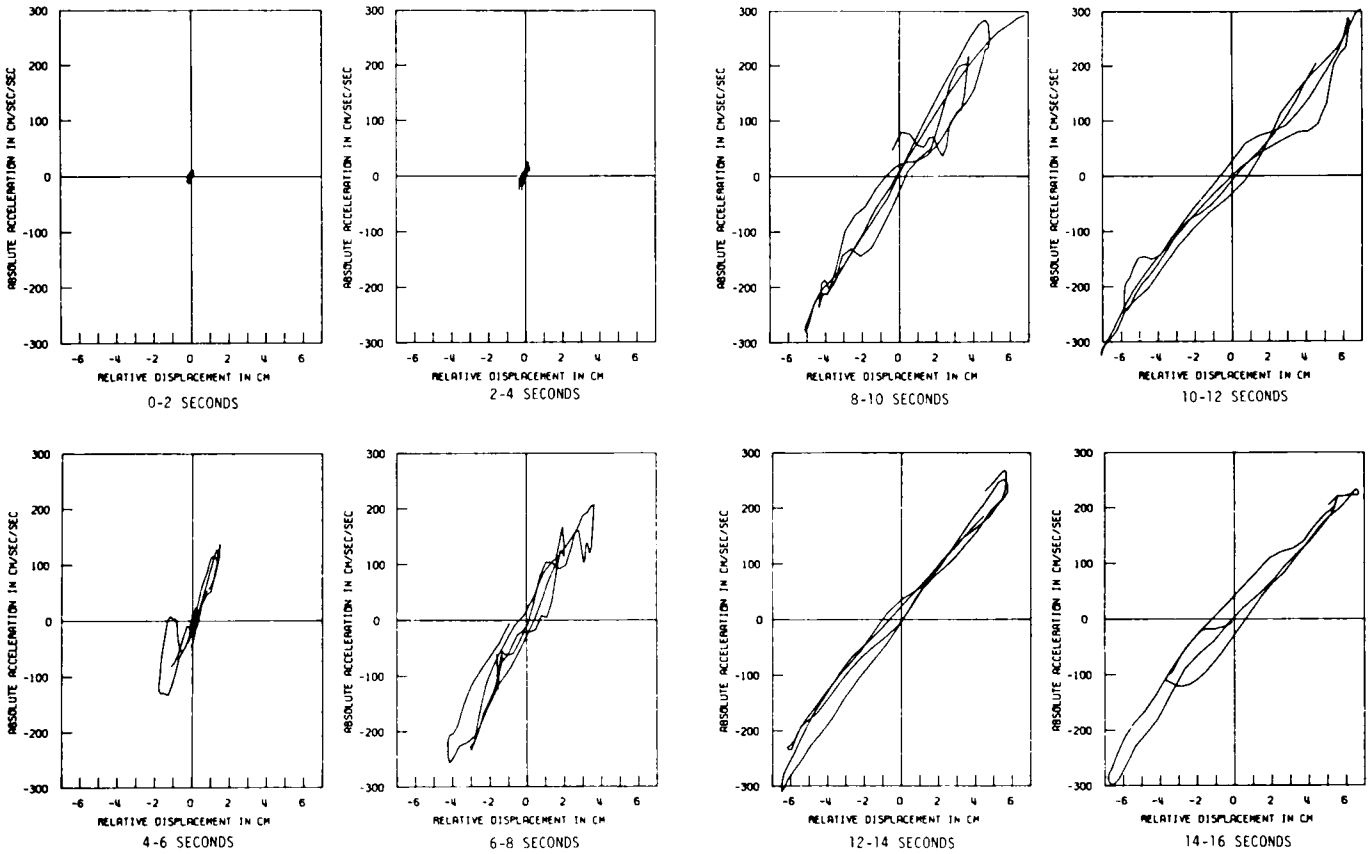

(a) 0-8 Seconds

(b) 8-16 Seconds

Fig.5.9 Hysteretic Response of Single-Degree-of-Freedom Oscillator Modelling Fundamental Mode, as Determined from Recorded Motions

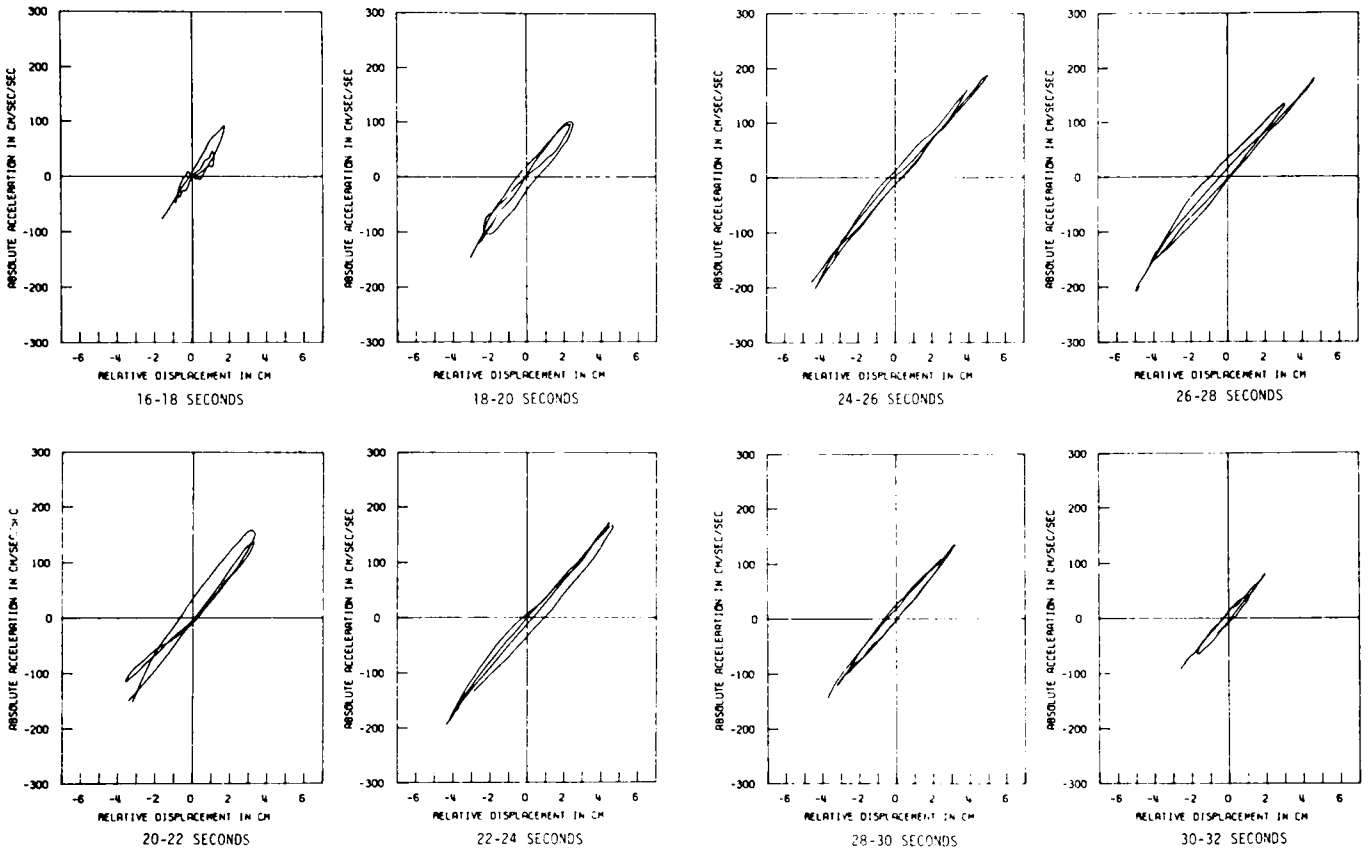

(c) 16-24 Seconds

(d) 24-32 Seconds

Fig.5.9 Hysteretic Response of Single-Degree-of-Freedom Oscillator Modelling Fundamental Mode, as Determined from Recorded Motions (Cont'd)

From 12 to 14 secs, the areas of the hysteresis loops have clearly become smaller, suggesting that the energy dissipation capacity of the library at this amplitude has decreased because of the previous vibrations. The hysteresis loops are also noticeably smoother, presumably due to the predominance of the fundamental mode of vibration. The remaining portion of the response, from 14 to 32 secs (Figs.9(b), (c), and (d) shows that the library continues to exhibit a softer restoring force with a relatively smaller energy dissipation capacity, when compared to the earlier response. This is true even though the response level is decreasing.

Comparing the responses between 4 to 6 secs and between 28 to 30 secs, which have about the same absolute acceleration level, it is seen that there has been a degradation of the stiffness of the structure. It is also seen, from comparing the two figures for the periods from 6 to 8 secs, and from 24 to 26 secs, that the energy absorbing capacity of the library has changed during the earthquake response.

The overall indication gained from Fig.5.9 is that the library lost not only some of its stiffness, but also some energy dissipation capacity due to the large amplitude response during the first part of the earthquake. This nonstationary characteristic of the hysteretic behavior of the library agrees, in principle, with those of simple theoretical models of deteriorating structures, although the details of the hysteretic behavior are somewhat different from the theoretical models so far suggested.

5-3-4 Nonstationary Equivalent Linear Parameters

It was thought desirable to estimate more precisely the loss of stiffness and energy absorbing capacity evidenced during the response. The stiffness of the library during each full cycle of relatively large amplitude has already been estimated and is shown in Fig.5.7. To make a similar study of the nonstationary behavior of the energy absorbing capacity, the hysteresis loops were used to estimate an equivalent viscous damping factor for each full cycle of response.

In this study the equivalent viscous damping factor h_{eq} was defined

by equating the energy dissipated by hysteresis to that dissipated by viscous damping.

$$\oint F(\mu,\dot{\mu})d\mu = \oint 2h_{eq}\omega_{eq}\dot{\mu}d\mu \tag{5-2}$$

in which $F(\mu,\dot{\mu})$ is the restoring force; μ, $\dot{\mu}$ are the relative displacement and velocity, respectively, and ω_{eq} is the equivalent natural frequency measured from that portion of the response. To evaluate the right-hand side of Eq.(5-2), it was assumed that over a cycle the amplitude of the response was a slowly varying sine wave, i.e.

$$\dot{\mu}(t) = -\omega_{eq}\mu_o(t)\sin\{\omega_{eq}t + \phi(t)\} \tag{5-3}$$

in which $\phi(t)$ is a slowly varying phase angle. (Appendix 2-A)

From Eqs.(5-2) and (5-3) the equivalent viscous damping factor h_{eq} is obtained as

$$h_{eq} = \frac{1}{2\pi\omega_{eq}^2\mu_o^2}\oint F(\mu,\dot{\mu})d\mu \tag{5-4}$$

in which μ_o is the measured amplitude of the relative displacement and $\oint F(\mu,\mu)d\mu$ is evaluated from the hysteresis loops given in Fig.5.9.

The equivalent viscous damping factors calculated this way are plotted for each full cycle in Fig.5.10. From the nature of the assumptions involved and the inherent errors, it is not expected that this would be a precise calculation. Fig.5.10 indicates that the library showed about 8 to 10% of critical damping from about 4 to 10 secs at which time the amplitude of the response reaches a maximum value. After 10 secs the energy absorbing capacity shows a reduction, which is consistent with the suggestion that a relatively sudden change in the energy absorbing capacity took place at about the time of maximum response. As pointed out above, the only observable earthquake effects on the structure were small cracking in the plaster in the vicinity of the mounts of the precast window wall panels. It is one possibility that the working loose of these mountings was the cause of the observed behavior.

5-4 Equivalent Linear and Hysteretic Modeling of the Library

5-4-1 Stationary Equivalent Linear Modeling

Before attempting to model the response by nonlinear hysteretic behavior, a simple linear model was tried, both to establish a base for further comparisons and to investigate the capabilities of this simplest possible approach. In order to model the first mode of the library as a simple oscillator it was necessary to calculate the participation factor of the fundamental mode. This was done using the experimentally determined values obtained in the vibration tests. As indicated in the Appendix 5-A, the input acceleration level to the equivalent linear oscillator was adjusted by the participation factor of the fundamental mode and by the weighting factor for the response of the roof.

The period of the equivalent linear model was taken as 1.0 sec in agreement with the second part of the response shown in Fig.5.7. The equivalent damping factor was chosen to be 5% of critical damping, a representative value taken from Fig.5.10. It might be noted that approximately 2% out of this 5% can be associated with viscous-like damping measured in the pre-earthquake vibration tests.

Using this simple linear model, the response of absolute acceleration was calculated and plotted in Fig.5.11. During the early part of the response, from 0 to 15 secs, the calculated response shown with a continuous line does not coincide with the measured first mode response shown with a broken line which is exactly same as that in Fig.5.8. The difference is particularly noticeable around 10 secs, where the calculated response is decreasing, whereas the measured response is growing and showing its maximum value. The reason for this discrepancy is that in the beginning of the vibration the library has a fundamental period of about 0.66 secs, whereas the simple linear model has a period of one second throughout the response. In addition, the assumed dissipation value of 5% is less than actually shown by the library during that early portion of the response. The coincidence of the calculated response and the measured first mode response is much better during the second

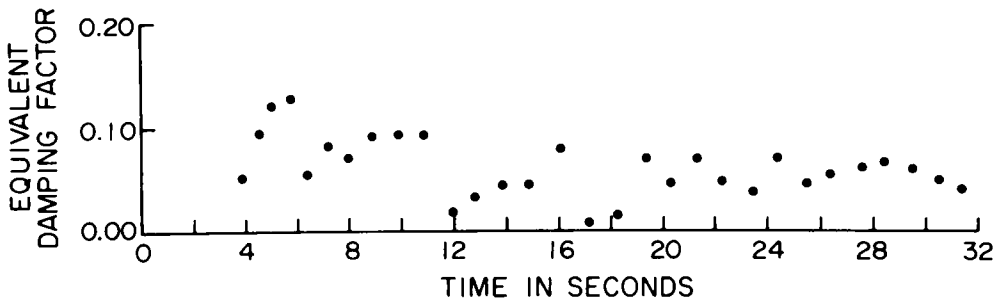

Fig.5.10 Equivalent Damping Factors Determined from Analysis of Measured Response

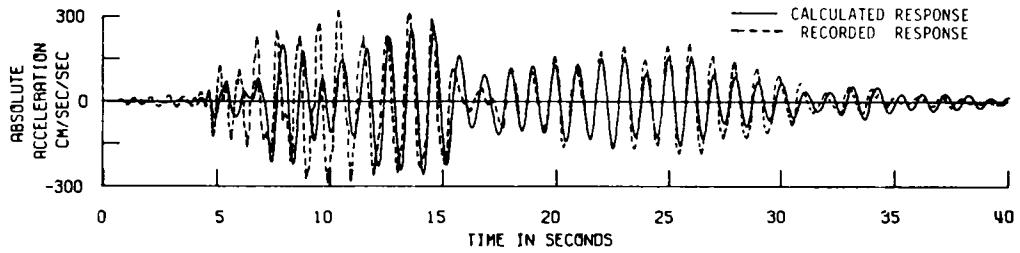

Fig.5.11 Absolute Acceleration Response of the Stationary Linear Model

part of the response, from 15 to 40 secs. In particular, the phase difference is very small. The simple linear model works well for this portion of the response, which is consistent with the smooth hysteresis loops shown in Fig.5.9, and the generally constant value of energy dissipation as indicated by Fig.5.10.

From these results it can be said that this simple linear model of the structure gives good agreement only for the portion of the response between 15 and 40 secs, the portion of the response over which structural parameters do not change significantly. The simple liear model does give a reasonably good estimate of the maximum response of the structure, and may therefore be useful from the point of view of design. From the point of view of research, however, it would seem that much better agreement could be obtained using a more detailed model of the hysteretic behavior.

5-4-2 Stationary Hysteretic Modeling

A stationary, bilinear hysteretic model was adopted in this section to represent the nonlinear hysteretic characteristics of the restoring force of the structure. Considering the shape of the hysteresis loops given in Fig.5.9, and the trends in the equivalent linear parameters shown in Figs.5.7 and 5.10, the bilinear model selected was chosen to have a small yield displacement with respect to the maximum response, and a relatively steep second slope. The yield level of this model was chosen to fit the observed behavior and does not indicate yielding in the structural frame of the library. A hysteretic model with these parameters will, for large deflections, show a small amount of energy dissipation and an equivalent natural frequency which is almost the same as that indicated by the second slope of the hysteretic diagram. The first slope of the bilinear hysteretic model was chosen to give a natural period of 0.66 secs, whereas the second slope was chosen to correspond to a linear restoring force for a structure with a natural period of 1.0 secs. The transition point between these two slopes was set at 0.25 cm, which is only slightly larger than the maximum

displacement during the vibration experiments. A typical hysteresis loop for a structure of this type is shown in Fig.5.12.

The calculated response of this bilinear hysteretic structure subjected to the recorded base acceleration is shown in Fig.5.13, which gives the absolute acceleration of the oscillator. The calculated hysteretic behavior comparable to Fig.5.9 is plotted in Fig.5.14. The response value plotted in Fig.5.13 shows very poor agreement with that from the measured first-mode response, Fig.5-8, except for the phase in the period from 12 to 17 secs. Comparing the hysteretic response from 4 to 6 secs, as shown in Figs.5-9 (a) and 5-14 (a), it is seen that the bilinear model gives a stiffness of the restoring force that is too low. Also it is seen from Figs.5.9 (b), (c) that the bilinear relation shows too much hysteretic damping from 8 to 24 secs. This is consistent with the calculated response being smaller than the measured response during this interval. These comparisons indicate that a satisfactory description of the response by a stationary hysteretic model is unlikely and that better agreement could be attained using a nonstationary model.

5-4-3 Nonstationary Equivalent Linear Modeling

It was seen previously that stationary models of the fundamental mode gave only limited agreement with response measured during the earthquake. In this section, a nonstationary, equivalent linear model, which changes its structural parameters at selected points during the response, was tried to see if the agreement could be improved. This was done both to check the accuracy of the equivalent linear parameters given in Figs. 5.7 and 5.10 and also to investigate the nonstationary characteristics of the response. The time-dependent equivalent natural frequency ω_{eq} and damping factor h_{eq} for the nonstationary model were selected from examination of the data, and are shown in Fig.5.15.

During the computation of the response, the changes of stiffness were implemented at times when the relative displacement was zero so as not to cause any permanent deformation. The calculated response of this oscillator, shown in Fig.5.16, agrees quite well with the measured response

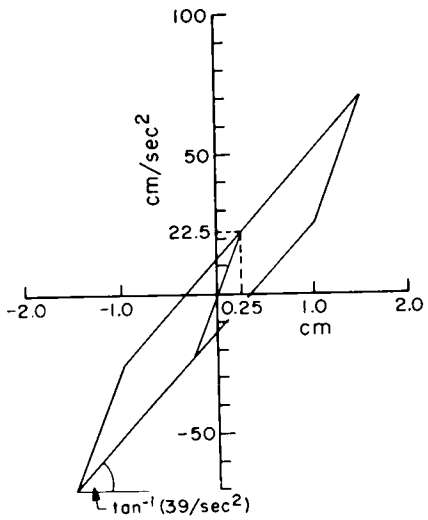

Fig.5.12 Typical Hysteresis Loop for the Stationary, Bilinear Hysteretic Model

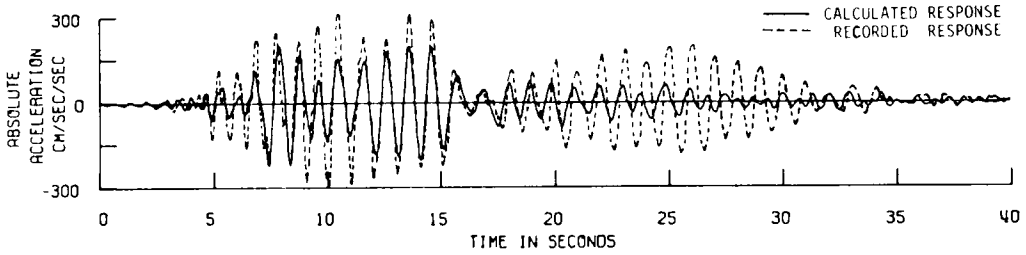

Fig.5.13 Absolute Acceleration Response of the Stationary, Bilinear Hysteretic Model

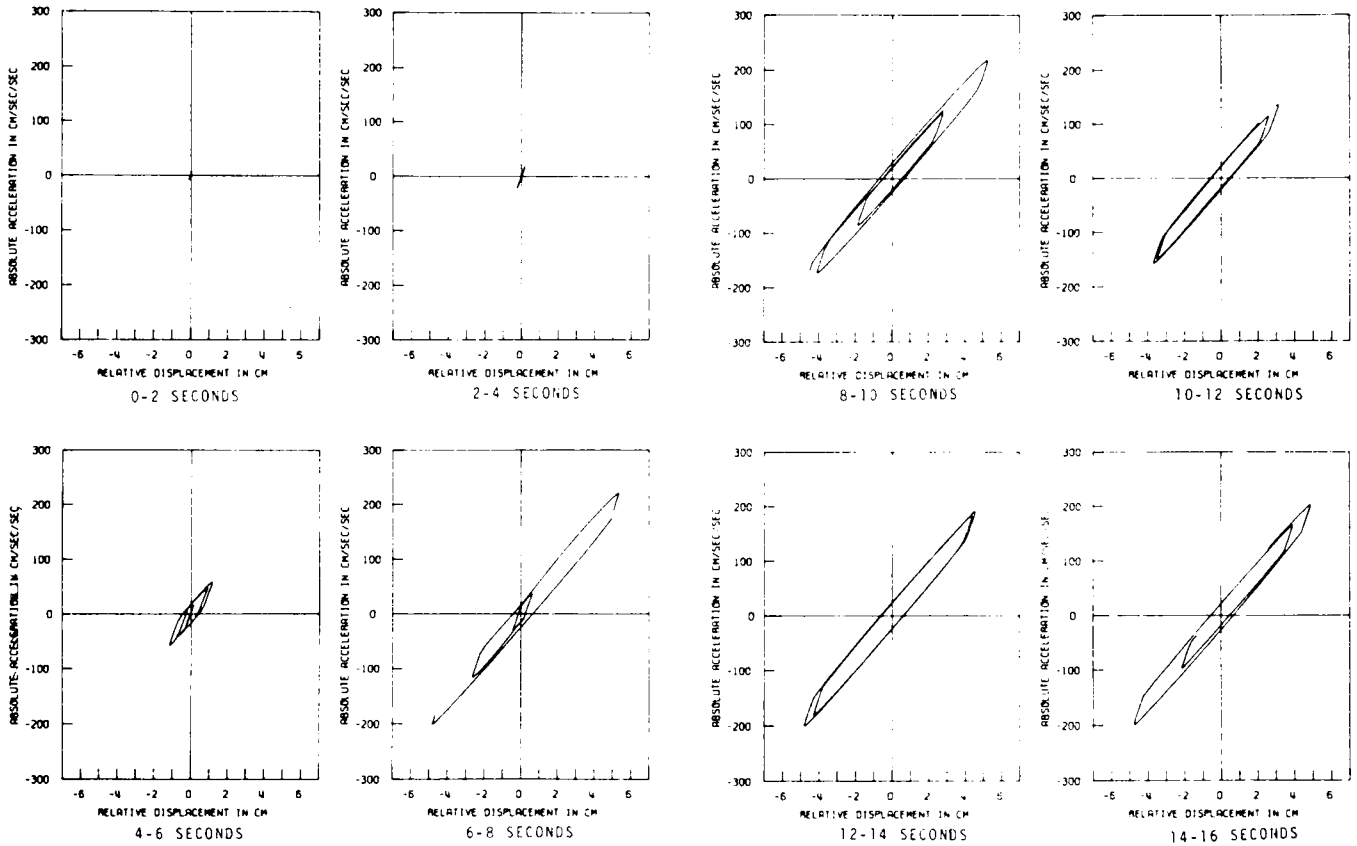

(a) 0-8 Seconds (b) 8-16 Seconds

Fig.5.14 Hysteretic Response of Stationary, Bilinear Hysteretic Model of Fundamental Mode

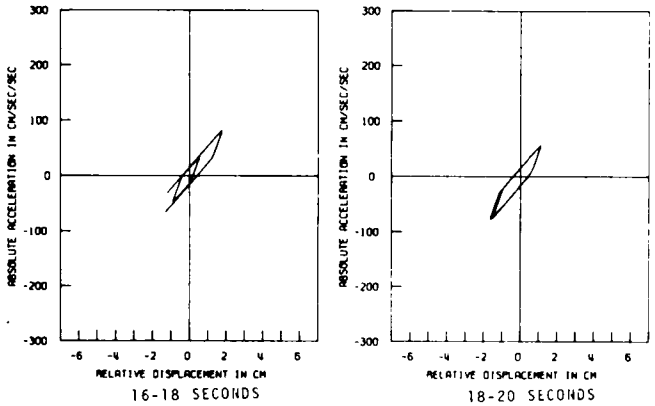

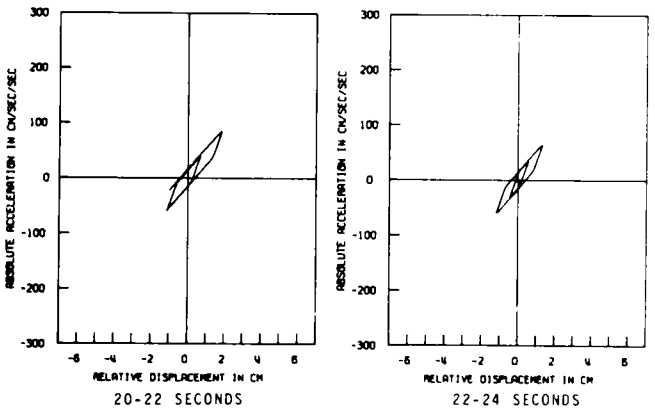

(c) 16-24 Seconds

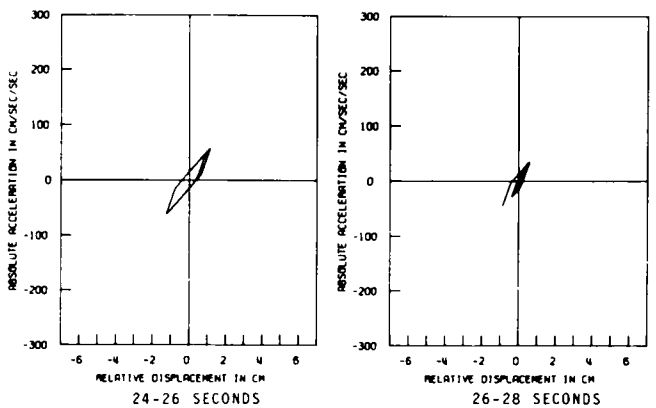

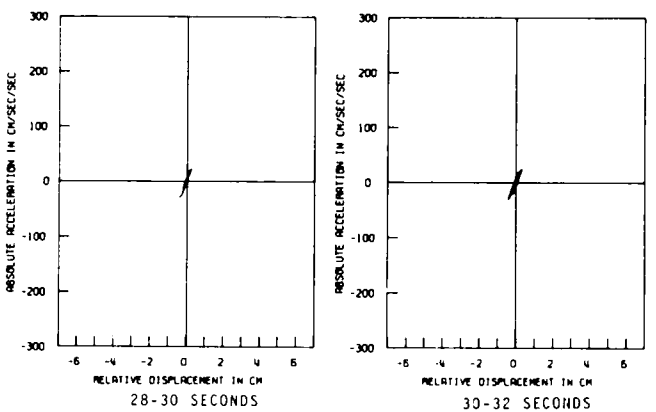

(d) 24-32 Seconds

Fig.5.14 Hysteretic Response of Stationary, Bilinear Hysteretic Model of Fundamental Mode (Cont'd)

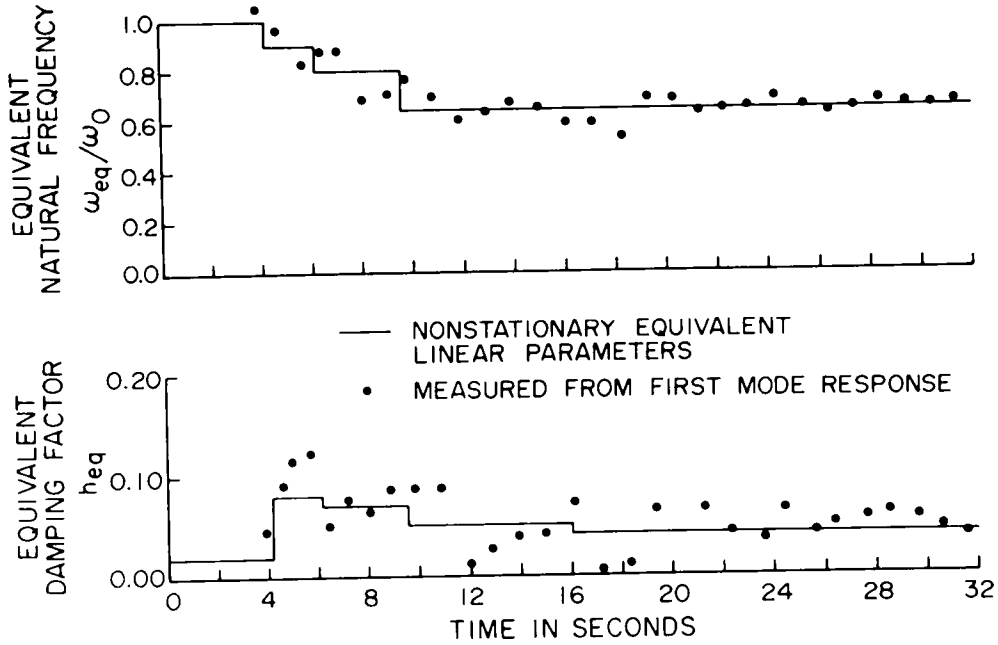

Fig.5.15 Equivalent Damping Factors and Natural Frequencies for Nonstationary, Equivalent Linear Model

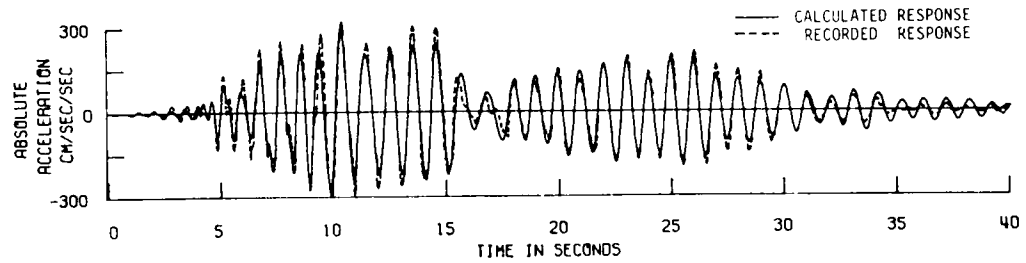

Fig.5.16 Absolute Acceleration Response of the Nonstationary Linear Model

of the first mode shown with a broken line. Thus, very good agreement with the observed behavior can be obtained by considering the structure to behave like a linear oscillator whose natural frequency and damping factor change during the course of the earthquake response. The good agreement suggests also that the analysis presented above can give sufficiently accurate nonstationary equivalent linear parameters. It is seen from Fig.5.15 that the stiffness of the equivalent linear system degrades to a constant value, whereas the equivalent damping factor of the system first increases and then decreases to a value somewhat lower than the peak response, but higher than the initial value.

5-4-4 Nonstationary Hysteretic Modeling

In this section, a nonstationary, deteriorating model of bilinear hysteresis is proposed to describe the response of the fundamental mode. The model chosen consists of four different bilinear hysteretic relations all having the same second slope. The time-dependent characteristics of the stiffness and energy dissipation capacity of the library are represented by changing the stiffness of the first slope and the yielding displacement. Guided by the results of previous analyses, the yielding displacement for the bilinear model was taken as large as 1.0 cm during the initial portion of the response; and for the latter portion of the response, a smaller value of 0.07 cm was used. The four different bilinear relations employed to model the nonstationary characteristics of the structure are consistent with the equivalent linear parameters shown in Fig.5.15, and hysteresis loops for these relations are shown in Fig.5.17. The loss of stiffness with time and the decreasing capacity for dissipating energy are apparent from Fig.5.17.

During the computations of response the transition from one hysteretic model to another was controlled to avoid jumps in the restoring force. The calculated values of absolute acceleration for the nonstationary bilinear hysteretic model is plotted in Fig.5.18. Fig.5.19 shows the calculated hysteretic behavior of the model, and is to be compared with Fig.5.9. Comparing the responses in Fig.5.18 with that of the

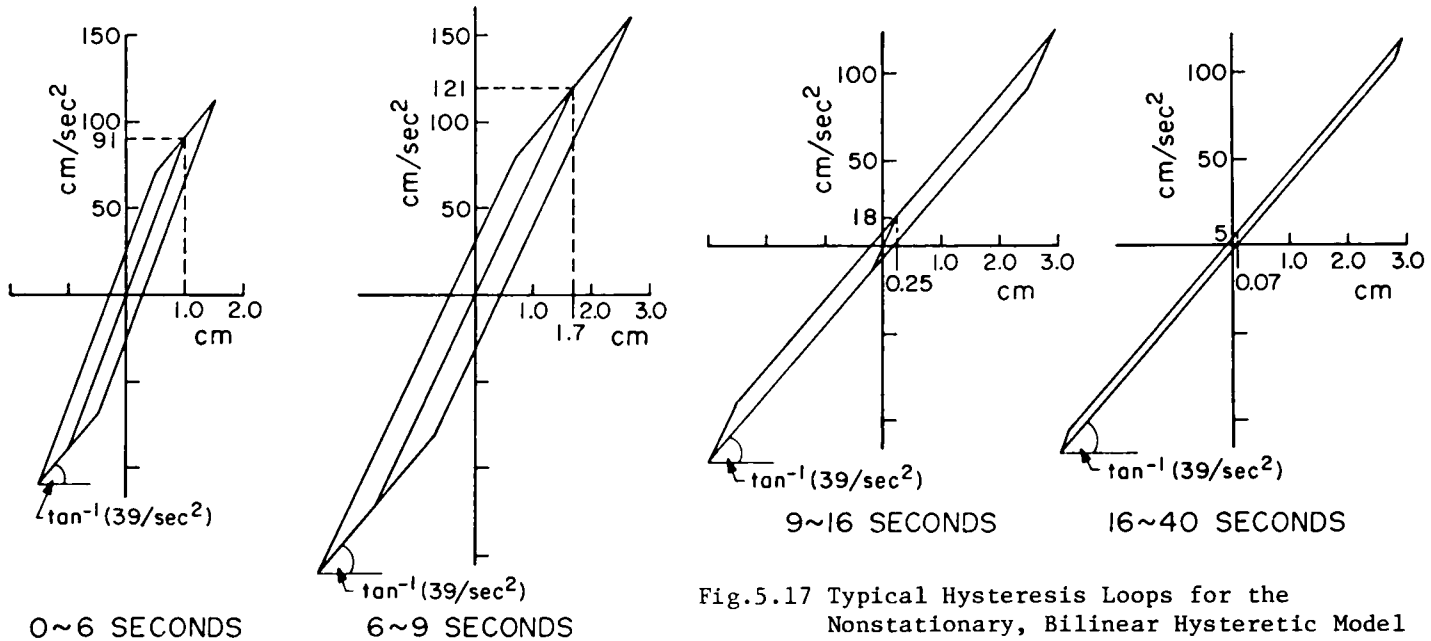

Fig.5.17 Typical Hysteresis Loops for the Nonstationary, Bilinear Hysteretic Model

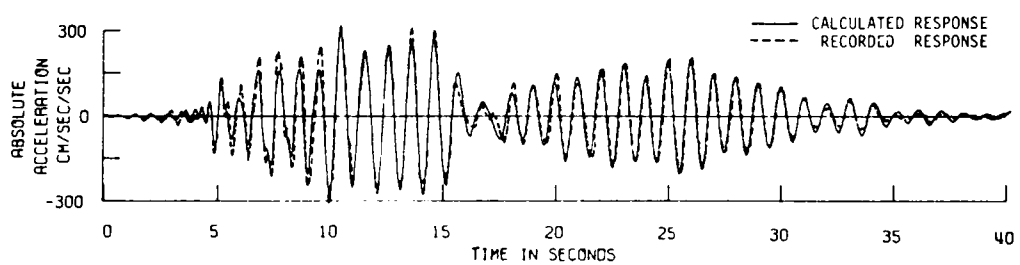

Fig.5.18 Absolute Acceleration Response of the Nonstationary Bilinear Hysteretic Model

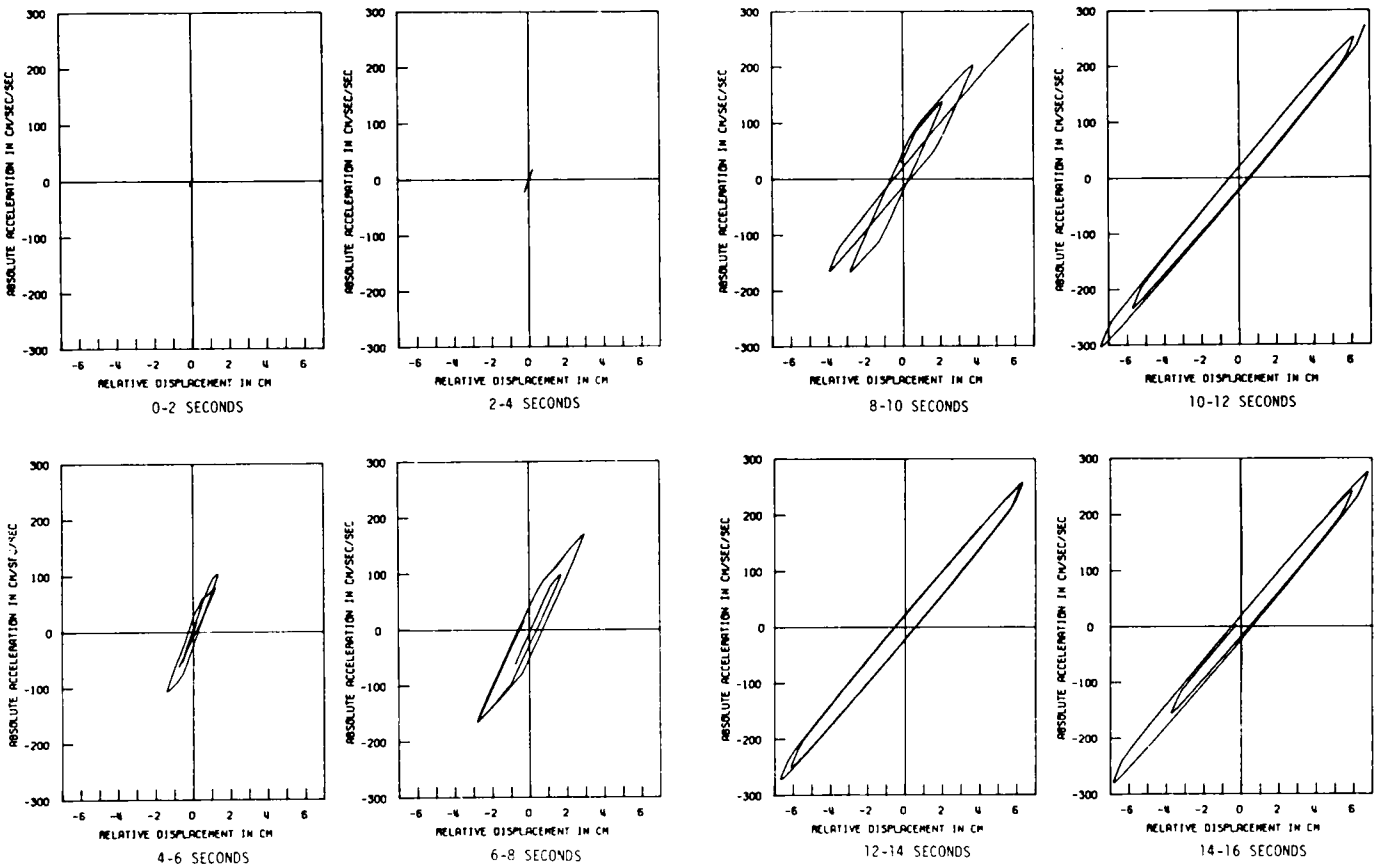

(a) 0-8 Seconds

(b) 8-16 Seconds

Fig.5.19 Hysteretic Response of the Nonstationary, Bilinear Hysteretic Model of Fundamental Mode

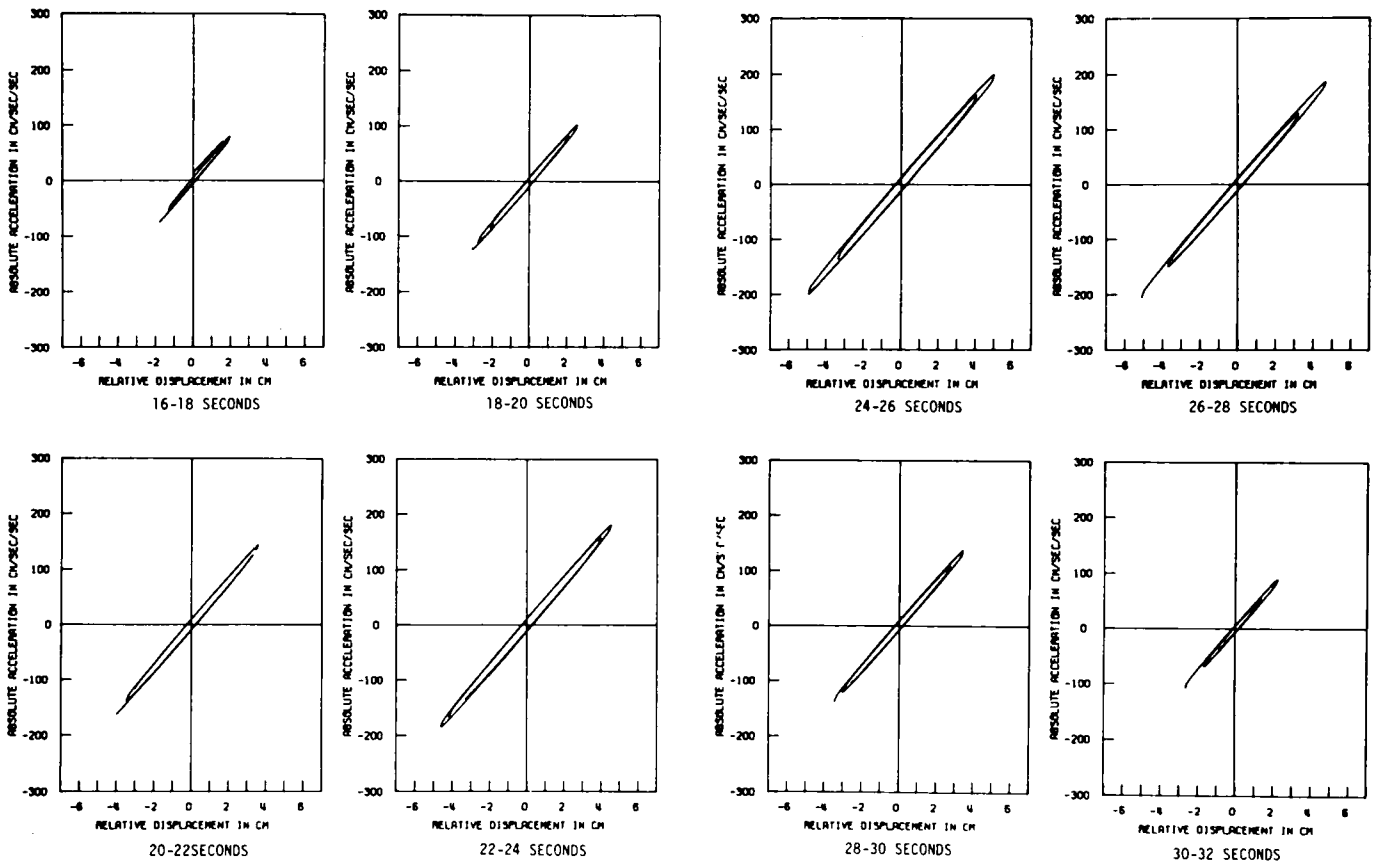

(c) 16-24 Seconds

(d) 24-32 Seconds

Fig.5.19 Hysteretic Response of the Nonstationary, Bilinear Hysteretic Model of Fundamental Mode (Cont'd)

measured first mode, it is seen that the two results agree very well except for a few peaks around 8 secs. Comparing the hysteretic diagrams in Figs.5.9 and 5.19, the calculated hysteretic behavior produced by the nonstationary bilinear model seems to represent the deteriorating characteristics of the restoring force of the structure fairly well. The agreement might be improved by the introduction of another, fifth model, or by changing the properties of the four used, but the main features of the hysteretic characteristics seem to be represented reasonably well by the nonstationary model used in the analysis.

5-5 A Model of Deteriorating Bilinear Hysteretic Structures

5-5-1 Comulative Damage and Residual Strength of Structures

From the investigations in the previous sections, it is clear that dynamic properties of the building deteriorated during the earthquake motion. Deterioration of reinforced concrete structures has also been suggested from laboratory experiments on restoring force characteristics of structural elements[20]. Examination of these data required to introduce a general deteriorating model to explain structural response and earthquake damages. For this purpose, a simple but general measure is needed to estimate the deterioration of hysteretic structures in random response.

In this section cumulative damage function defined in the theory of low-cycle fatigue[21] is adopted as a basic parameter to measure structural deterioration of stiffness and energy absorbing capacity with cyclic loading. Let us define the increment in cumulative damage D_i due to one cycle loading with amplitude of μ_i in ductility factor (D.F.) as:

$$\Delta D_i = 4(\mu_i/\mu_f)^{\alpha} \tag{5-5}$$

where μ_f: D.F. at failure under static loading, α: a parameter which determines the pattern of damage function. It is clear that α depends on material of structures. In this study, rounded value of 2.0 is used

for α because of lack of experimental data. Then, the accumulated damage $D(n)$ after n_i cycles of loading with amplitude of μ_i (i=1,2,.....) is written as

$$D(n) = \sum_i \Delta D_i = (4/\mu_f^{\alpha}) \sum_i n_i \mu_i^{\alpha} \tag{5-6}$$

When the loading is random as earthquake ground motions, it is desirable to define the cumulative damage with time t. Using R.W.Lardner's damage rate function[22], R.Minai[23] proposed the cumulative damage $D(t)$ over the time interval of (o,t) in the form of

$$D(t) = \int_0^t F(\mu)|\dot{\mu}|dt = (\alpha/\mu_f^{\alpha}) \int_0^t |\mu|^{\alpha-1}|\dot{\mu}|dt \tag{5-7}$$

The expected value of cumulative damage $E[D(t)]$ in nondeterministic response will be estimated when the joint probability density function $p(\mu,\dot{\mu},t)$ of D.F.μ and its rate $\dot{\mu}$ at time t' ($o \le t' \le t$) is known: i.e.,

$$E[D(t)] = (\alpha/\mu_f^2) \int_0^t \int_{-\infty}^{\infty} |\mu|^{\alpha-1} \int_{-\infty}^{\infty} |\dot{\mu}| p(\mu,\dot{\mu},t') d\dot{\mu} d\mu dt' \tag{5-8}$$

When the value of cumulative damage $D(n)$ or $E[D(t)]$ reaches to 1.0, it is regarded as complete failure of the structure. Therefore residual strength $R(n)$ or $E[R(t)]$ of structure is written as

$$R(n) = 1.0 - D(n) , \quad E[R(t)] = 1.0 - E[D(t)] \tag{5-9}$$

5-5-2 Equivalent Linear Parameters of Deteriorating Bilinear Structures

Although there would be many ways to describe deterioration effects of structures, it will be a simple and practical approach to measure the degraded capacity of structural strength in terms of the residual strength discussed in the previous section. In a proposed model, basic bilinear hysteretic restoring force shown in Fig.5.20 is firstly linearized with equivalent natural frequency ω_{eq} and equivalant damping co-

efficient β_{eq} as discussed in the sections of 4-2-2 and 4-2-3. Then it is assumed that the linearized stiffness (ω^2_{eq}) degrades proportional to the residual strength and that the linearized energy absorbing capacity (β_{eq}) degrades more rapidly in proportion to the square of the residual strength as shown in Fig.5.21. This is written as

$$\left.\begin{aligned} \omega^2_{eq}(\mu_i, R(n)) &= \omega^2_{eq}(\mu_i) R(n) \\ \beta_{eq}(\mu_i, R(n)) &= \beta_{eq}(\mu_i) R^2(n) \end{aligned}\right\} \qquad (5\text{-}10)$$

Where $\omega^2_{eq}(\mu_i)$ and $\beta_{eq}(\mu_i)$ are determined from Eq.(4-14). This assumption is made according to experimental results of reinforced concrete shear walls performed T.Shiga et al[20]. In their study, deterioration of the equivalent rigidity and the equivalent viscous damping under cyclic loading with constant amplitude is plotted against the number of loading cycles, which suggests that the present approach is appropriate in investigating the effects of structural deterioration.

Using Eq.(5-10), residual strength and deteriorated structural parameters of a model for sinusoidal cyclic loading are calculated and shown in Fig.5.22. Deterioration effects are shown for 1,5,10 cycles of loading. It is found that one cycle of loading with D.F. μ_i=12.5, five cycles of loading with D.F. μ_i=5.5 and ten cycles of loading with D.F. μ_i=3.9 lead to complete loss of residual strength. Consequently, the equivalent stiffness ω^2_{eq} and the equivalent energy absorbing capacity β_{eq} are reduced to zero. In this figure, no deterioration means equivalent linear parameters of a conventional bilinear hysteretic model.

When loading is random but deterministic like structural response subjected to recorded earthquake motions, structural damage is calculated at every half cycle of vibration from Eq.(5-5). According as increasing damage, deteriorated structural parameters are estimated from Eq.(5-10) and they are adjusted also at every half cycle of vibration when relative displacement is zero not to cause any plastic deformation. Fig.5.23

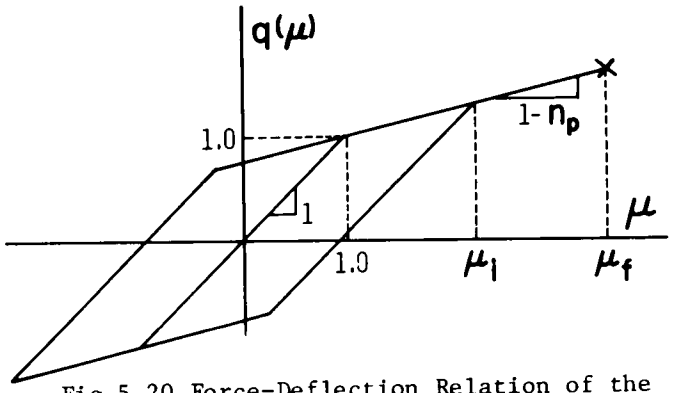

Fig.5.20 Force-Deflection Relation of the Deteriorating Bilinear Model

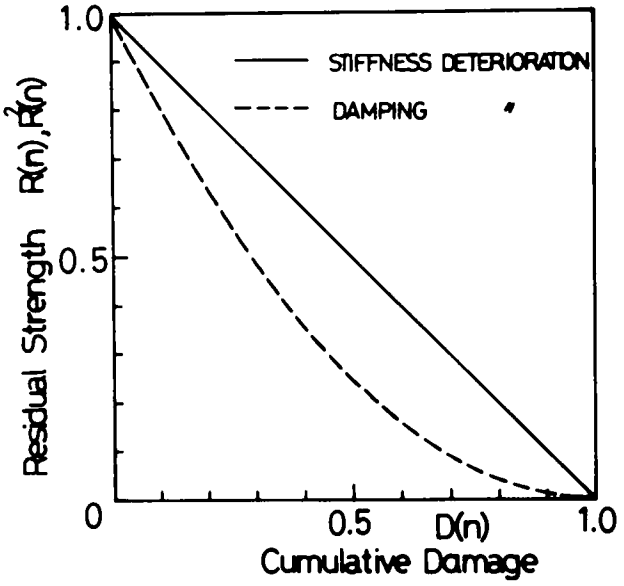

Fig.5.21 Deterioration Model of Structural Stiffness and Damping Capacity

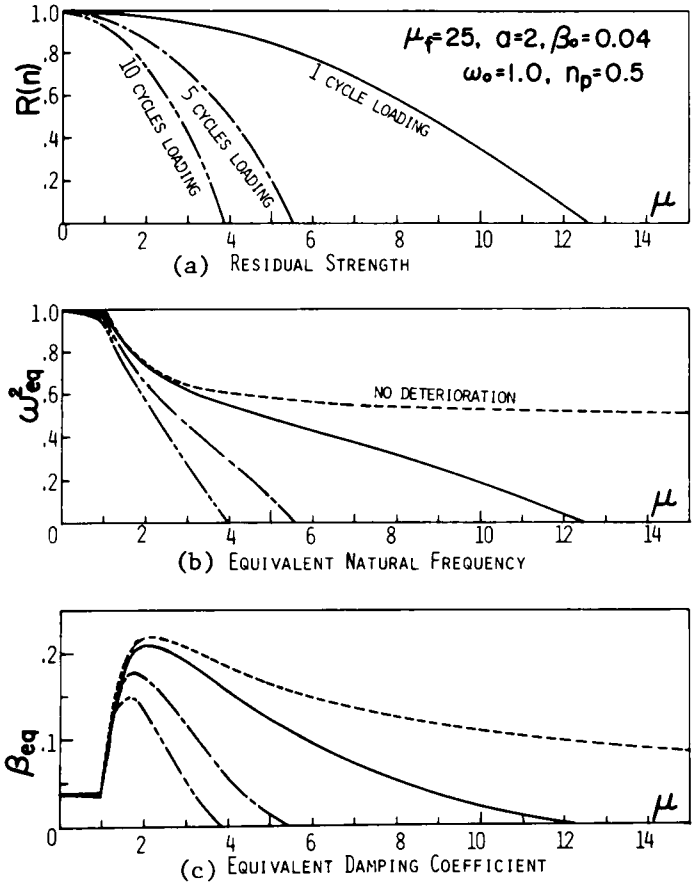

Fig.5.22 Residual Strength and Equivalent Linear Parameters Subjected to Sinusoidal Excitation

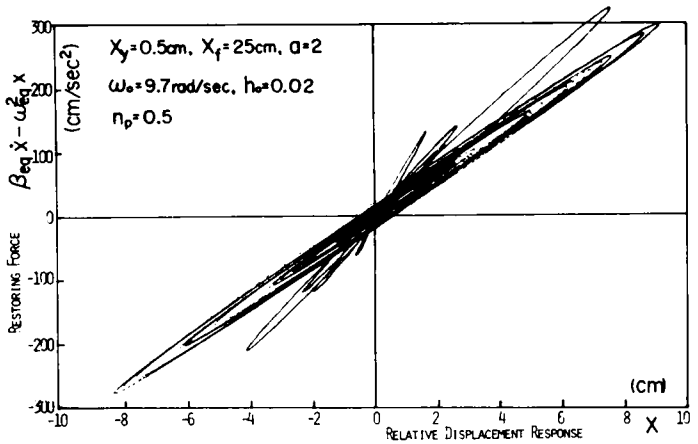

Fig.5.23 Hysteretic Response of a Deteriorating Bilinear Model Subjected to the Recorded Earthquake Motion

shows the numerically calculated response of a proposed deteriorating model subjected to the recorded acceleration at Millikan Library during the San Fernando earthquake shown in Fig.5.2. Structural parameters of a model indicated in Fig.5.23 agree with those obtained from pre-earthquake vibration test of the library when no damage is considered. The total restoring force ($\beta_{eq}\dot{x} + \omega^2_{eq}x$) is plotted against the relative displacement response x to reproduce deteriorating hysteretic loops. Although some discrepancy is found between Figs.5.9 and 5.23, general trends of deterioration of slopes and area of hysteresis loops agree well to suggest usefullness of the proposed model.

5-5-3 Nonstationary Mean-Square Response of Deteriorating Bilinear Structures

Nonstationary mean-square response of a proposed deteriorating bilinear model subjected to earthquake-type random excitation is predicted by the step-by-step linearization technique discussed in the section of 4-5-1. The equivalent linear parameters of the model are estimated from the covariances of response σ_μ, $\rho_{\mu\dot{\mu}}$, $\sigma_{\dot{\mu}}$ and the expected residual strength $E[R(t)]$ following almost the same idea discussed in Eq.(5-10). This procedure is expressed as

$$\left.\begin{aligned} \omega^2_{eq}(\sigma_\mu, \rho_{\mu\dot{\mu}}, \sigma_{\dot{\mu}}, E[R(t)]) &= \omega^2_{eq}(\sigma_\mu, \rho_{\mu\dot{\mu}}, \sigma_{\dot{\mu}}) E[R(t)] \\ \beta_{eq}(\sigma_\mu, \rho_{\mu\dot{\mu}}, \sigma_{\dot{\mu}}, E[R(t)]) &= \beta_{eq}(\sigma_\mu, \rho_{\mu\dot{\mu}}, \sigma_{\dot{\mu}}) E^2[R(t)] \end{aligned}\right\} \quad (5\text{-}11)$$

Where $\omega^2_{eq}(\sigma_\mu, \rho_{\mu\dot{\mu}}, \sigma_{\dot{\mu}})$ and $\beta_{eq}(\sigma_\mu, \rho_{\mu\dot{\mu}}, \sigma_{\dot{\mu}})$ are determined from Eq.(4-18). Another procedure to estimate the covariances of nonstationary response of equivalent linear structures is exactly the same as one used in the section of 4-5-1.

Deterioration effects of structural stiffness and energy absorbing capacity during earthquake response are examined by comparing nonstationary mean-square response of linear, conventional bilinear and proposed deteriorating bilinear structures. Calculated results for three models subjected to moderate and strong excitations are shown in Figs.5.25 and

5.26. The nonstationary excitation $\alpha_f \psi(t) f(\omega_f, h_f, t)$ is represented by the product of nonstationary envelope function $\psi(t)$ shown in Fig.5.24 and stationary random process $f(\omega_f, h_f, t)$ discussed in the previous chapter.

In Fig.5.25 (a), a linear structure shows large value of mean-square response in D.F. with large time-lag between the peaks of response and excitation. This is due to small value of damping factor $h_o (=\beta_o/(2\omega_o)=$ 0.02). The maximum mean square response of the conventional bilinear structure is found less than 50% of the linear structure and there is almost no time-lag between the peaks of response and excitation because of the energy absorbing effects of hysteresis loops. The deteriorating bilinear structure shows, except at the beginning of response, larger response than that of conventional bilinear structures due to structural damage. The cumulative damage shows comparatively rapid growth when the response attains its maximum value (t/T_o=4.0) and then gradually increases up to 50% of the complete failure value (E[$D(t)$]=1.0). Equivalent linear parameters of conventional bilinear structures depending only on response amplitude recover their initial values at the end of vibration. On the contrary, those of proposed deteriorating bilinear model calculated from Eq.(5-10) loses their capacity according as the increasing damage and does not recover their initial values. Deterioration of ω_{eq} in this figure is found very similar to that in Fig.5.15 to suggest that the propose model can reasonably explain the deterioration of structural parameters by the measure of residual strength.

In Fig.5.26, square of an intensity parameter α_f of the nonstationary excitation is increased from 0.75 used in Fig.5.25 up to 1.0 to represent strong earthquake motions. Other parameters are exactly the same as those used in Fig.5.25. It is a natural result that linear response in Fig.5-26 is 133% of that in Fig.5-25 from the theory of linearity between excitation and response. Conventional bilinear response in Fig.5-26 shows the rate of increase as almost the same as the linear structure because of a little change between equivalent linear parameters in Figs.5.25 and 5.26. In contrast, response of the deterio-

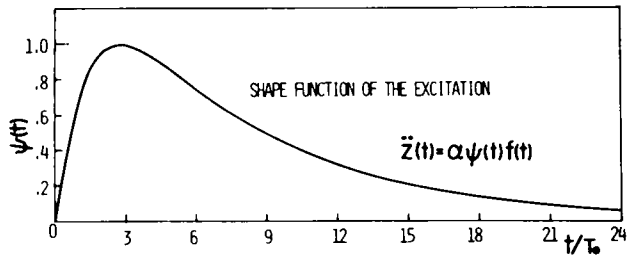

Fig.5.24 Nonstationary Envelope Function of the Excitation

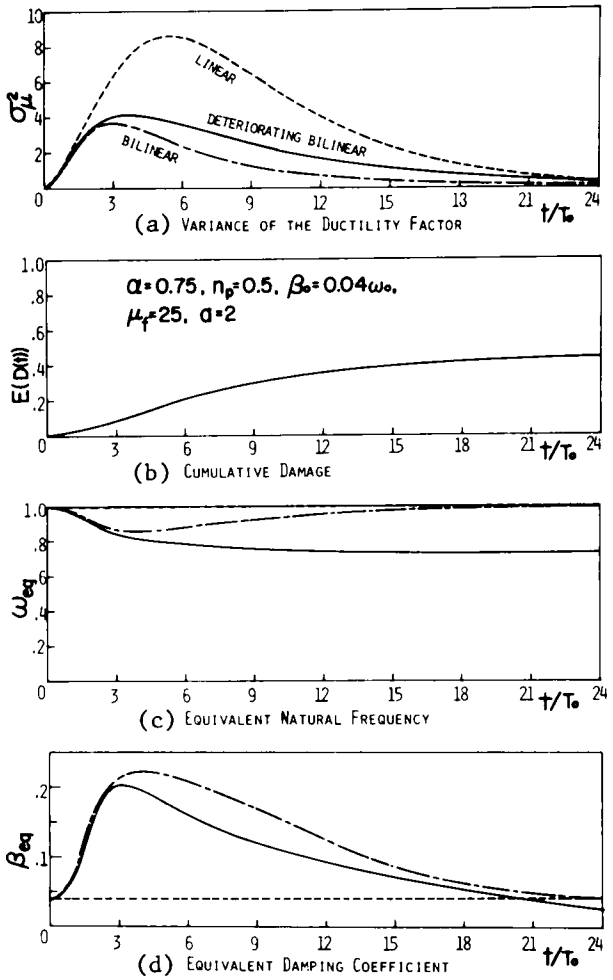

Fig.5.25 Nonstationary Response of Linear, Bilinear and Deteriorating Bilinear Structures Subjected to Moderate Excitation

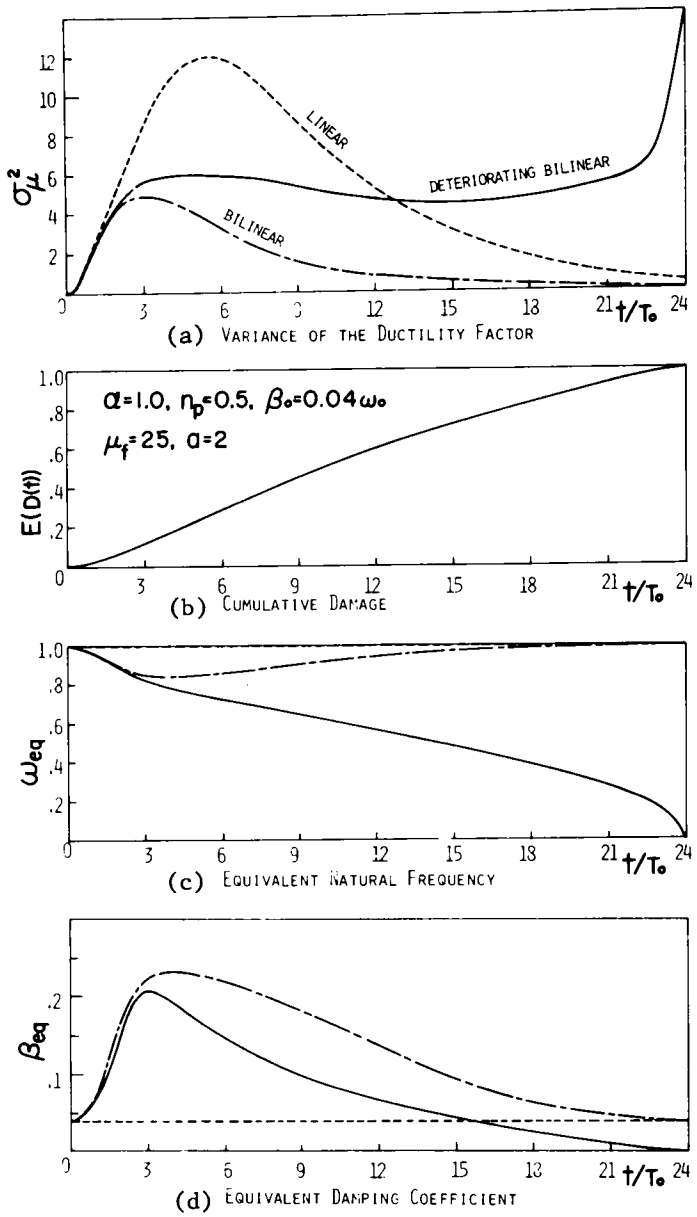

Fig.5.26 Nonstationary Response of Linear, Bilinear and Deteriorating Bilinear Structures Subjected to Strong Excitation

rating bilinear model decreases only slightly after its peak value at t/T_o=5 inspite of rapid decrease in excitation level. After t/T_o=13, the response becomes larger than that of a linear structure and finally shows very rapid growth at t/T_o=24. This is the effects of deterioration of structural stiffness and energy absorbing capacity with increasing cumulative damage. Extreme loss of structural capacity results in rapid growth of response to cause the collapse; i.e., E[$D(t)$]=1.0.

For the purpose of measuring deterioration of structural capacities and investigating their effects on earthquake response, the proposed method is much simpler than conventional methods of controlling every process of deteriorating hysteresis loops. The proposed method can also cover wide range of deteriorating structures by choosing a suitable value for the parameter α in Eq.5-5 and by defining appropriate relation between cumulative damage and equivalent linear parameters. Hence, the proposed method seems promissing for practical use in earthquake response analysis of deteriorating hysteretic structures.

5-6 Conclusions

In this chapter, deterioration of dynamic parameters of the Millikan Library on the campus of California Institute of Techonology during the San Fernando earthquake is detected from the examination of recorded seismograms. Calculated response of four simple models are compared with the recorded motion to see whether they could describe the response of the fundamental mode of the Library. The study also proposes a new simple model to represent general deteriorating hysteretic structures. Main results obtained are as follows.

(1) The simultaneous measurement of the ninth floor and basement motions allowed the calculation of the relative response which, in this case, could be used to construct an experimental estimate of the hysteretic response of an oscillator modelling the fundamental mode of the structure. To this extent it was possible to study the actual hysteretic behavior of the library and thereby to judge the type of hysteresis that best described the response. The

method used in this report appears to be a promising one for studying earthquake response of hysteretic structures, even though some difficulties exist in obtaining hysteretic trajectories from the response. To study the hysteretic behavior in more detail, in particular to determine where in the structure the hysteresis might be concentrated, would require more instrumentation than is present in the library. It is concluded that one instrument per floor, all with a common timing signal, would be the minimum requirement to give the information needed.

(2) The results of the analysis, and study of the observed E-W response of the library, clearly indicate a significant decrease in the stiffness and energy dissipation capability of the building during the course of the earthquake response. This is perhaps most easily seen in Fig.5.15. It is not possible to relate the changes, with confidence, to any observed damage to the building, nor is it possible to ascertain whether the changes were sudden or gradual. It seems quite possible, however, that the observed behavior is at least partly a consequence of the behavior of the precast concrete panels that contain the windows, and it seems that relatively rapid or sudden changes in properties are more likely to have occurred than gradual ones.

(3) Of the four simple models used to describe the E-W response of the fundamental mode of the library during the San Fernando earthquake, the best agreement was achieved by the use of the two nonstationary oscillators. The two stationary models, an equivalent linear model and a bilinear hysteretic model, also with constant properties, were not capable of duplicating the earthquake response nearly so well as the nonstationary oscillators. The simpler, stationary models did give maximum responses close to that observed in the earthquake, however, so that their use would have produced valid information in an analysis intended for design.

(4) The two nonstationary models that gave good agreement were an

equivalent linear model with properties that were changed at four times during the earthquake, and a bilinear hysteretic model that also changed properties four times during the response. Equally good agreement was obtained with either model, and it is concluded that any of the more common hysteretic models giving the general trend of equivalent natural frequency and equivalent damping factor shown in Fig.5.15 probably could be made to give good agreement between observed and calculated responses. In doing any such analyses, however, it does appear necessary to change the properties of the model during the course of the response; it seems doubtful that any of the simple, nondegrading hysteretic models could be capable of giving the degree of agreement shown by the nonstationary models.

(5) Another new simple model is proposed to represent dynamic properties of deteriorating hysteretic structures. As a basic measure of structural deterioration, cumulative damage and residual strength derived from the theory of low-cycle fatigue were adopted. Then equivalent stiffness and energy absorbing capacity of hysteretic structures were controlled to degrade with decreasing residual strength of structures. The proposed method appears to be much simpler for practical use than conventional methods of controlling every process of deteriorating hysteresis loops.

(6) Effects of structural deterioration to earthquake response were examined by comparing nonstationary mean-square response of linear, conventional bilinear and proposed deteriorating bilinear structures subjected to artificial earthquake motions with different intensity. When excitation level is moderate, deteriorating bilinear structures show slightly larger response than bilinear response. At the end of excitation, response level asymptotically approaches to zero, although structural stiffness and energy absorbing capacity have permanent damages. When excitation level becomes strong, extreme loss of structural capacity results in rapid growth of response to cause the collapse of structures.

References for Chapter 5

1) R. Tanabashi: Studies on the Nonlinear Vibrations of Structures Subjected to Destructive Earthquakes, Proc. of the first WCEE, 1956, pp. 6-1∿16.
2) G.V. Berg and D.A. Da Deppo: Dynamic Analysis of Elasto-Plastic Structures, Journal of the EM Division, Proc. of ASCE, Vol. 86, No. EM2, April, 1960, pp. 35∿58.
3) H. Goto and H. Iemura: Earthquake Response of Single-Degree-of-Freedom Hysteretic Structures, Proc. of the fifth WCEE, Vol. 2, June, 1973, pp. 2132∿2135.
4) H. Umemura, A. Aoyama and H. Takizawa: Analysis of the Behavior of Reinforced Concrete Structures During Strong Earthquakes Based on Empirical Estimation of Inelastic Restoring Force Characteristics of Members, Proc. of the fifth WCEE, Vol. 2, June, 1973, pp. 2201∿2210.
5) P.C. Jennings: Earthquake Response of a Yielding Structure, Journal of the EM, Proc. of ASCE, Vol. 91, EM4, August, 1965, pp. 41∿68.
6) R.W. Clough and S.B. Johnston: Effect of Stiffness Degradation on Earthquake Ductility Requirements, Proc. of the JEES, October, 1966, pp. 227∿232.
7) W.D. Iwan: A Model for the Dynamic Analysis of Deteriorating Structures, Proc. of the fifth WCEE, Vol. 2, June, 1973, pp. 1782∿1791.
8) D.E. Hudson: Dynamic Properties of Full-Scale Structures Determined from Natural Excitations, Dynamic Response of Structures, Edited by G. Herrman and N. Perrone, Pergamon Press, 1972, pp. 159∿177.
9) P.C. Jennings, Ed.: Engineering Features of the San Fernando Earthquake, EERL Report, No. EERL 71-02, Cal Tech, June, 1971.
10) P.C. Jennings and H. Kuroiwa: Vibration and Soil-Structure Interaction Tests of a Nine-Story Reinforced Concrete Building, Bulletin of the SSA, Vol. 58, No. 3, June, 1968, pp. 891∿916.

11) H. Kuroiwa: Vibration Test of a Multistory Building, EERL Report, Cal Tech, June, 1967.

12) F.E. Udwadia and M.D. Trifunac: Time and Amplitude Dependent Response of Structures, EERL Report, October, 1973.

13) F.E. Udwadia and M.D. Trifunac: Ambient Vibration Tests of Full-Scale Structures, Proc. of the fifth WCEE, Vol. 2, June, 1973, pp. 1430∿1439.

14) V.P. McLamore: Post Earthquake Vibration Measurements, Millikan Library, 1970, (unpublished report).

15) Strong-Motion Earthquake Accelerograms, Uncorrected Data, Vol. I, Part G, EERL Report, No. EERL 72-20, Cal Tech, June, 1972.

16) Strong-Motion Earthquake Accelerograms, Corrected Accelerograms and Integrated Ground Velocity and Displacement Curves, Vol. II, Part G, EERL Report, No. EERL 73-52, Cal Tech, Nov., 1973.

17) M.D. Trifunac: Stress Estimates for the San Fernando, California, Earthquake of February 9, 1971: Main Event and Thirteen Aftershocks, Bulletin of the SSA, Vol. 62, No. 3, June, 1972, pp. 721∿750.

18) W.O. Keightley: A Strong-Motion Accelerograph Array with Telephone Line Interconnections, EERL Report, No. EERL 70-05, Cal Tech, Sept., 1970.

19) P.C. Jennings, G.W. Housner and N.C. Tsai: Simulated Earthquake Motions, EERL Report, Cal Tech, April, 1968.

20) T. Shiga et al: Experimental Study on Dynamic Properties of Reinforced Concrete Shear Walls, Proc. of the fifth WCEE, Vol. 1, June, 1973, pp. 1157∿1166.

21) M.A. Miner: Cumulative Damage in Fatigue, Journal of Applied Mechanics, the Proc. of ASME, 1945, pp. A1-159∿164.

22) R.W. Lardner: A Theory of Random Fatigue, Journal of Mech. Phys. Solids, Vol. 15, 1967, pp. 205∿221.

23) R. Minai: On the Aseismic Safety of Building Structures, Annuals of DPRI, Kyoto Univ., Vol. 13, 1970, pp. 5∿22.

APPENDIX 5-A

Calculation of the Participation Factor and the Weighting Factor

This appendix describes the calculation of the participation factor of the fundamental mode and the weighting factor for the first mode for response as measured on the roof. These factors are required to scale the measured response on the roof to the response of the simple oscillator that models the fundamental mode of the building.

The equation of motion for earthquake response of a n degree-of-freedom system such as the library can be written as

$$M\{\ddot{x}\} + C\{\dot{x}\} + K\{x\} = -M\{1\}\ddot{z}(t) \qquad (5\text{-A-}1)$$

in which M, C and K are the nxn mass, damping and stiffness matrices, respectively. The vector $\{x\}$, ($\{x\}^T=\{x_1,x_2,\ldots\ldots,x_n\}$) denotes the relative displacement, $\{1\}$ symbolizes the vector $\{1\}^T=\{1,1,\ldots,1\}$, and $\ddot{z}(t)$ is the acceleration of the base of the structure.

The matrix of mode shapes Φ is defined by

$$\Phi = [\{\phi_1\},\{\phi_2\},\ldots\ldots,\{\phi_n\}] \qquad (5\text{-A-}2)$$

in which the column vectors are the individual mode shapes, i.e., $\{\phi_i\}^T=(\phi_{1i},\phi_{2i},\ldots\ldots,\phi_{ni})$ defines the i^{th} mode.

Letting

$$\{x\} = \Phi\{\xi\} \qquad (5\text{-A-}3)$$

and substituting into Eq.(5-A-1), and multiplying by Φ^T gives

$$\Phi^T M\Phi\{\ddot{\xi}\} + \Phi^T C\Phi\{\dot{\xi}\} + \Phi^T K\Phi\{\xi\} = -\Phi^T M\{1\}\ddot{z}(t) \qquad (5\text{-A-}4)$$

Under the assumption that the damping matrix C can be diagonalized by the same transformation Φ which diagonalizes M and K, the individual equation in matrix equation (5-A-4) will be uncoupled. A tipical equation will have the form

$$\ddot{\xi}_i + \frac{\{\phi_i\}^T C\{\phi_i\}}{\{\phi_i\}^T M\{\phi_i\}}\dot{\xi}_i + \frac{\{\phi_i\}^T K\{\phi_i\}}{\{\phi_i\}^T M\{\phi_i\}}\xi_i = -\frac{\{\phi_i\}^T M\{1\}}{\{\phi_i\}^T M\{\phi_i\}}\ddot{z}(t) \qquad (5\text{-A-5})$$

The coefficient of $\ddot{z}(t)$ is the participation factor, a_i, for the i^{th} mode, and in paticular

$$a_1 = \frac{\{\phi_1\}^T M\{1\}}{\{\phi_1\}^T M\{\phi_1\}} \qquad (5\text{-A-6})$$

Assuming that the solutions to Eq.(5-A-5) are known, the response of each of the n masses can be found by use of Eq.(5-A-3). If an index of 1 corresponds to the roof, the roof displacement is

$$x_1 = \phi_{11}\xi_1 + \phi_{12}\xi_2 + \cdots\cdots + \phi_{1n}\xi_n \qquad (5\text{-A-7})$$

The modal ordinate ϕ_{11} is herein called the weighting factor.

From the test data[10], the first mode of the nine-story library was found as

$$\{\phi_1\}^T = \{1.00, 0.87, 0.74, 0.62, 0.51, 0.40, 0.28, 0.20, 0.11, 0.04\} \qquad (5\text{-A-8})$$

where values for intermediate floors have been interpolated from the measurements. The mass matrix is given in the same reference as

$$M = \frac{2600\text{kips}}{g}\begin{bmatrix} 1.0 & & & & & & & & & \\ & 0.75 & & & & & & & & \\ & & 0.75 & & & & & & & \\ & & & 0.75 & & & & & & \\ & & & & 0.75 & & & & & \\ & & & & & 0.75 & & & & \\ & & & & & & 0.75 & & & \\ & & & & & & & 0.94 & & \\ & & & & & & & & 0.88 & \end{bmatrix} \qquad (5\text{-A-9})$$

Evaluating Eq.(5-A-6), it is found that

$$\alpha_1 = 1.44 \tag{5-A-10}$$

and from Eq.(5-A-8)

$$\phi_{11} = 1.00 \tag{5-A-11}$$

The product of these two factors, 1.44, is the desired ratio, i.e., the response of an oscillator subjected to the recorded base acceleration should be multiplied by 1.44 before comparison with the fundamental mode response, as measured on the roof. For the calculation in this report, the rounded value of 1.4 has been used.

6. CONCLUDING REMARKS

This dissertation has presented the results of investigation on earthquake response properties of stationary and deteriorating simple hysteretic structures through theoretical analyses, numerical simulations and examinations of recorded seismograms. In this conclusive chapter, the objectives of this study and the main results of foregoing chapters will be reviewed comprehensively to discuss commonly related conclusions with proposals for earthquake engineers and also in relation to the prospect for future studies to be continued.

It would be the most reasonable way of earthquake resistant designing to build a structure capable of responding to moderate shaking without damage, and capable of resisting the unlikely event of very strong shaking without seriously endangering the occupants. In the latter case which is the most significant point in earthquake engineering, it is indispensable for structural response analyses to take account of the nonlinear hysteretic properties in dynamic force-deflection relations over yielding limit and also of the randomness found in earthquake ground motions. Hence, probabilistic evaluation of random response of hysteretic structures has been strongly needed in order to estimate the reliability of structures in the occasions of strong earthquakes.

A large number of studies aiming to achieve this goal have been devoted to earthquake response analyses of nonlinear hysteretic structures as reviewed in Chapter 1. However following three crucial issues which are the main topics of this dissertation are considered not to have been investigated satisfactory both in experimental and analytical sense.

(1) Effects of types and shapes of hysteresis loops to random response of yielding structures especially to plastic deformation in search of dynamic failure mechanisms of structures caused by strong earthquake.

(2) General understanding of probabilistic response of nonlinear hysteretic structures subjected to nonstationary random excitation, in concern with establishment of a new aseismic designing code to

reflect the results of hysteretic response analyses.

(3) Detection and modeling of time and amplitude dependent force-deflection relations of existing structures in large amplitude for accurate estimation of their dynamic response due to strong ground shaking.

In this dissertation, Chapter 2 and 3 are aimed to contribute to the first issue through simulational and analytical techniques.

Simulated plastic deformation in Chapter 2 is found to increase rapidly when the stiffness after yielding becomes close to zero. When the stiffness in the plastic range is greater than one quarter of that in the elastic region, plastic deformation is noticed to grow little. Hence it is recommended to earthquake engineers to try to increase the stiffness of structural members in the plastic range for the purposes not to cause permanent damages due to plastic deformation and consequently to guarantee hysteretic energy absorption during earthquake response.

When the stiffness in the plastic range can be anticipated, reliability of hysteretic structures will be discussed from the probability approach developed in Chapter 4. Otherwise, the accumulated plastic deformation which is proportional to the total energy dissipated by hysteresis loops would become one of the important parameters which represent the degree of structural damages due to severe ground motion. An improved linearization technique proposed in Chapter 3 can be applied to predict the expected amount of accumulated plastic deformation during earthquake response.

Chapter 4 has been devoted to development of the second issue with the aid of linearization techniques which are found powerful to predict probabilistic response of hysteretic structures except with strong nonlinearity in comparison with simulated results. From examinations of simulated and predicted results, it should be noted that effects of hysteresis loops with softening spring let random response of the relatively short-period structures grow larger than corresponding linear structures. On the contrary, that of the relatively long-period

structures is found to be suppressed due to hysteretic effects.

When it is required to estimate accurate reliability of structures in plastic range due to strong ground motions, proposed probability distribution of maximum response of hysteretic structures can be used as the distribution of dynamic loads to structural elements. From this approach, a new designing code which is based on allowable ductility factor with a specified probability may be developed instead of the current elastic-designing code. More intensive studies in near future are of course needed to achieve the goal of a new designing code.

In Chapter 5, the third issue has been discussed from the examinations of recorded seismograms. The proposed method to construct an experimental estimate of hysteretic response of the structure during strong earthquakes can be applied to more complex structures if sufficient number of instruments are installed at the suitable places with a common timing signal.

Detected deterioration of stiffness and energy absorbing capacity of a reinforced concrete structure is found to have significant effects on the earthquake response. Suggested from this results, a new simple model of which structural parameters degrade with the decreasing residual strength is proposed to represent general yielding structures. Statistical response analyses developed in Chapter 4 are applied to the proposed model to find general effects of structural deterioration. Although relation between the degree of structural deterioration and the defined residual strength of a structure should be examined through future experimental studies, the proposed method of modeling is promissing for practical use by earthquake engineers because of its simplicity.

Throughout this dissertation, structures are modeled by simple systems with nonlinear hysteretic restoring force and their fundamental characteristics of random response are intensively investigated. However it is evident that existing structures are not simple but complex systems having many-degree-of-freedom. Hence, future studies should be devoted to earthquakes response analyses of multi-degree-of-freedom structures with nonlinear hysteretic restoring forces.